Hot Mix Asphalt Permeability: Tester Size Effects and Anisotropy

Christopher H. Harris

Thesis submitted to the faculty of the
Virginia Polytechnic Institute and State University
in partial fulfillment of the requirements
for the degree

Masters of Science
in
Civil and Environmental Engineering

Dr. Linbing Wang, Chair
Dr. Geraldo Flintsch
Dr. George Filz

November 14, 2007
Blacksburg, VA

Keywords: Permeability, Anisotropy, Hot Mix Asphalt

Hot Mix Asphalt Permeability:
Tester Size Effects and Anisotropy

Christopher H. Harris

(ABSTRACT)

Permeability of hot mix asphalt (HMA) is a property that is important to the pavement's durability. Measuring permeability along with density will give a better indication of a pavement's durability than density alone. The presence of water for extended periods of time in the pavement is directly linked to early deterioration.

The first goal of this research is to study the anisotropic nature of hot mix asphalt permeability within the lab, which required the development of a horizontal permeameter. This method is inexpensive and suitable for a lab technician to use and analyze. A series of samples with different air void contents were used to observe how the ratio of vertical to horizontal permeability changes with air void content.

The second goal was to develop a modified field permeameter to study the water-pavement contact area effect on field permeability. A reliable sealing system was created that is consistent and is not detrimental to the pavement surface. The results of the study show that larger contact areas yield increasing influence of vertical flow, which represents the one dimensional assumption of Darcy's Law falling head method.

The third goal was to validate the results by simulating the field permeability test with a finite element model. A number of simulations with different permeability values and anisotropic permeability ratios were conducted. The horizontal and vertical flows were observed within the test area to analyze the flow pattern and influence of the directional permeability. The results matched the trends found in the field permeability study.

Dedication

I would like to dedicate this thesis to my father Col. Richard H. Harris, Jr. He set an unsurpassed example of excellence every day of his life. His exemplary work in the area of transportation guided me in my academic career and instilled within me a great sense of character. His wisdom and encouragement made me the person and engineer that I am today. I am forever grateful for the sacrifices that he made to ensure that I was successful in any path that I might choose in life.

Acknowledgments

I would like to express my deepest gratitude to my advisor Dr. Linbing Wang for his guidance and support in completing this project. I would also like to thank Dr. Geraldo Flintsch and Dr. George Filz for serving on my advisory committee, as well as offering their generous advice.

This project was also facilitated by the students and staff at the Virginia Tech Transportation Institute. The entire infrastructure group has provided advice, support and encouragement throughout this project. I would like to specifically thank Billy Hobbs and Dong Wang for making this project run smoothly. I would also like to thank the Virginia Department of Transportation Salem Materials Division for their help in obtaining materials and testing results.

Finally, I would like to thank my friends and family for their support throughout the years. Everyone I have met in Blacksburg has been an outstanding friend and colleague who I will miss dearly. I extend my profound appreciation to my parents who have given me love, support and encouragement through the most challenging times of my life.

Table of Contents

LIST OF FIGURES

LIST OF TABLES

Chapter 1
Introduction

1.1 Background

Permeability of hot mix asphalt (HMA) is a property that is important to the pavement's durability. Measuring permeability along with density will give a better indication of a pavement's durability than density alone. The presence of water for extended periods of time in the pavement is directly linked to early deterioration. Permeability or the hydraulic conductivity of the pavement, defined as the rate of flow of a fluid through a material under a unit head, is usually based on Darcy's Law. Kovacs further refined the method to include the properties of the transported fluid.

There are two schools of thought when addressing permeability in hot mix asphalt. The first is that the pavement's surface layer should be impermeable, thus protecting the structure from any surface infiltration. The other theory is that some permeability is needed to help release fluid that infiltrates the structure from the side and bottom surfaces. When applied to either theory, the measure of permeability is essential in providing quality assurance that the design criteria has been met.

Due to the acceptance and use of the SuperPave mix design, pavements are now coarser than in previous years. Pavements with high permeability values will rapidly deteriorate due to water and air infiltration that cause stripping and oxidation. Research has shown that coarse SuperPave mixes become overly permeable when the air voids reach eight percent (Hainin, et al. 2003). Since there is high variability of interconnected voids in the pavement and many questionable assumptions are being used to measure permeability, continuing research is necessary in the field of permeability.

The testing devices that are used for obtaining both field and lab permeability have their limitations. The field testing device that was developed by the National Center for Asphalt Technology (NCAT) has shown problems in the sealing method. Also, data is available only for a 3.5" diameter fluid-pavement contact area. A modification of this device can address these problems to ensure more reliable data can be acquired. The lab

permeability testing device that was developed by the Florida Department of Transportation (FDOT) only considers the vertical flow through a specimen and neglects the effects of horizontal permeability. Directional permeability has been addressed by researchers, but the method used incorporated an expensive and complex X-Ray Computed Tomography imaging system coupled with numerical simulations of fluid flow. A series of tests needs to be developed that can address the directional flow or anisotropy of HMA in a simple and inexpensive manner.

1.2 Research Goals and Approach

The objectives of this research can be broken into three associated foci: 1) evaluation of anisotropic effects on permeability in lab testing; 2) investigate water-pavement contact area effect on field permeability; and 3) development of a numerical model to interpret field data and present a better understanding of the directional permeability of hot mix asphalt.

Studying the anisotropic nature of hot mix asphalt permeability within the lab required the development of a horizontal permeameter. A new method was found that is inexpensive and suitable for a lab technician to use and analyze. A series of samples with different air void contents were be used to observe how the ratio of vertical to horizontal permeability changes with air void content.

In order to find the contact area effect on field permeability, a new field permeameter was developed. This device was able to accommodate multiple contact areas. Also, a more reliable sealing system was created that is consistent and is not detrimental to the pavement surface.

A finite element model provided information that was useful for understanding the anisotropic nature of HMA permeability and simulating the field permeability test. By running a number of simulations with different permeability values and anisotropic permeability ratios, the horizontal and vertical flows were observed within the test area to analyze the flow pattern and influence of the directional permeability. Two extreme cases were modeled, one with a permeable lower boundary and one with an impermeable boundary representing an effective tack coat.

1.3 Thesis Outline

This thesis is organized into five chapters. Chapter 2 provides a literature review of subjects related to this study. The literature review covers permeability theory, lab and field testing, directional permeability, factors influencing permeability, critical permeability values and problems with current methods. Chapter 3 discusses the methods used for developing the lab and field tests along with describing the finite element analysis model. Chapter 4 provides the test results and discussion of the relevance of these results. Chapter 5 concludes the analysis and provides the limitations of the study along with recommendations for further study.

Chapter 2
Literature Review

2.1 Introduction

Permeability in HMA has traditionally been calculated using Darcy's Law. More recently, the Kozeny-Carman equation has been utilized in conjunction with the use of X-Ray CT imaging. These techniques are coupled with the many field and lab testing devices available. For field testing, there are five designs that have been used in published research. They all calculate the coefficient of permeability using Darcy's Law. There are two methods of calculating permeability in the lab, one using the device developed by the Florida Department of Transportation (FDOT), the other uses the Corelok device. The FDOT device also uses Darcy's Law, while the Corelok device uses a volumetric approach to calculated permeability. There have been recent studies on directional permeability that use X-Ray CT imaging to develop a computer model of an HMA core sample. A numerical fluid flow model based on the Kozeny-Carman equation is then used to simulate and analyze the fluid flow within the sample. These methods are not perfect, and there are some problems with collecting and analyzing the permeability data.

There are many factors that can affect the in place permeability of a pavement structure. The two major areas that control permeability are the pavement design and the field compaction techniques.

2.2 Darcy's Law

Darcy established the fundamental ideas of permeability in 1856 when he was developing a sand filter for water purification. He study focused on a term called the coefficient of permeability (Wisconsin 2004). This term is used to determine the fluid flow through a material. This principle is applicable when the flow through the material is laminar. This creates a linear relationship between specific discharge and hydraulic

gradient. When turbulent flow is exhibited, the flow paths become more complex and create a non-linear relationship between specific discharge and hydraulic gradient. Several other assumptions must be true for Darcy's Law to be valid. These assumptions are a homogenous material, steady-state flow, laminar flow, incompressible fluid, and one-dimensional flow (Cooley 1999).

Darcy's Law can be written as: $$Q = k \cdot i \cdot A = k \cdot \frac{\Delta H}{L} \cdot A \qquad \text{(Eq. 2.1)}$$

where: Q = rate of flow
k = coefficient of permeability
i = hydraulic gradient
A = cross sectional area of specimen perpendicular to the direction of flow
ΔH = head loss across the specimen
L = length of the specimen

In order to determine the coefficient of permeability according to Darcy's Law, two methods can be used. The first is a constant head method, where the rate of flow is measured while sustaining a constant head of water. The coefficient of permeability can be represented as $$k = \frac{Q \cdot L}{h \cdot A \cdot t} \qquad \text{(Eq. 2.2)}$$

where: k = coefficient of permeability
Q = rate of flow
L = length of specimen
h = pressure head
A = cross sectional area of specimen
t = time during which Q is measured

The second method for measuring permeability is the falling head test. This method measures the head loss over time. The coefficient of permeability can be represented as:

$$k = \frac{a \cdot L}{A \cdot \Delta t} \cdot \ln\left(\frac{h1}{h2}\right) \qquad \text{(Eq. 2.3)}$$

where: k = coefficient of permeability
a = area of standpipe
L = length of specimen
h1 = water head at beginning of test
h2 = water head at end of test
A = cross sectional area of specimen
Δt = time between reading h1 and h2

The constant head method is more appropriate for highly permeable materials with k values greater than 10^{-3} cm/s. The falling head method is preferred for materials with low permeability coefficients; k values less than 10^{-3} cm/s. Asphalt concrete generally has a k value between 10^{-3} cm/s and 10^{-5} cm/s, making the falling head method the best choice (Wisconsin 2004).

2.3 Kozeny-Carman Equation

Another method has been proposed for estimating permeability by Al-Omari (2004), using a simplified version of the Kozeny-Carman equation. This equation shows that the effective air voids are proportionally related total air voids, specific surface area and tortuosity. These properties are most easily acquired through the use of X-Ray CT imaging. The equation is represented as follows:

$$k = \frac{n^3}{c.T^2.S^2}\frac{\gamma}{\mu} \qquad \text{(Eq. 2.4)}$$

Where: k = coefficient of permeability (m/s)
n = the percent total air voids
γ = 9.79 kN/m^3 is the unit weight of water at 20° C
c = 3 is a constant
T = tortuosity
S = the average specific surface area of given gradation and NMAS
μ = 10^{-3} kg/(m sec) is the water viscosity

Table 2.1 – Average Specific Surface Area for Given Gradation and NMAS

Gradation	Average Specific Surface Area (1/mm)
9.5-BRZ	0.229
12.5-ARZ	0.352
12.5-BRZ	0.182
19.0-ARZ	0.18
12.0-BRZ	0.161

(BRZ = Gradation below restricted zone, ARZ = Gradation above restricted zone)

2.4 Lab Permeability

2.4.1 FDOT Permeameter

For laboratory test procedures, the general method that is used was developed by the Florida Department of Transportation (FDOT), and slightly modified by Carol-Warner, Inc. This test method has been adopted as the standard lab test and the procedure is outlined in ASTM PS 129-01, Permeability of Bituminous Materials. The main difference between the FDOT and modified test is that the FDOT test used an epoxy resin to seal the sidewalls of the core, and the modified test uses a flexible latex membrane. This test can use a sample cut from the field, or loose mix from the plant can be formed into a core for testing (Allen, et al. 2001).

The permeameter consists of a vertical standpipe, two expandable pressure rings, a six inch aluminum containment cylinder, a latex membrane, a water release valve, and a manual air pump with a pressure gauge.

After the test specimen has been prepared, it is saturated in a deaeration chamber under 26 inches of Hg for 15 minuets. Next the sample is placed in the chamber where the latex membrane is pressurized to prevent water passing through the sides of the sample. To create a better seal, petroleum jelly can be placed on the sidewalls of the sample. The standpipe is then filled with water and the valve is released. The time is then recorded for the water level to move from the initial head value to the final head value.

The information from the test and dimensions of the core are entered into Darcy's Law to obtain the coefficient of permeability.

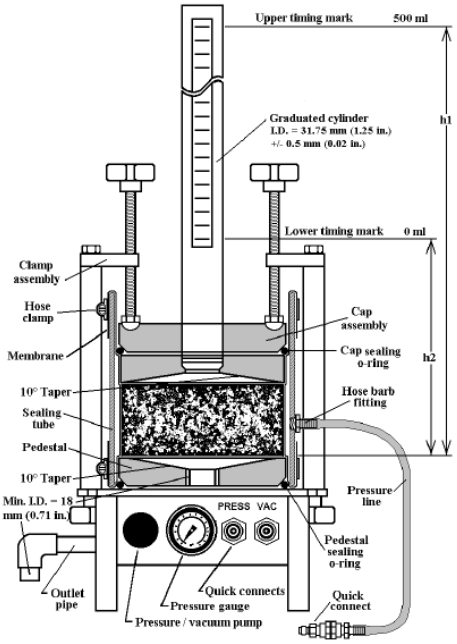

Figure 2.1 – FDOT Lab Equipment

The constant head device that is used to test the permeability of soils can also be used to test asphalt concrete samples. A 152 cm sample is enclosed in a rubber membrane, and porous aggregate is placed above and beneath the sample. A confining pressure is applied using water with the specimen placed inside a cell. The inlet and outlet pressures are adjusted to keep a constant head as the water flows through the sample. It was found that low differential pressure is optimal to resist turbulent flow throughout the sample (Maupin 2000).

2.4.2 CoreLok Device

Another device, the CoreLok machine, has been developed by InstroTek Incorporated and can be used to determine permeability through measuring percent porosity. This method recognizes that measuring the percent air voids is an acceptable for design and quality control for fine graded mixes, but percent porosity is more adequate and meaningful for use with open graded mixtures. Percent porosity expresses the

amount of voids that are accessible to water, thus it is closely related to the permeability of the sample. This method is better for determining permeability because two samples with the same percent porosity will have the same permeability. This is not true for two samples with the same percent air voids.

Figure 2.2 – CoreLok Device

To determine the percent porosity, the bulk specific gravity and apparent maximum gravity of a compacted sample are used. This method completely relies on the specific mixture of the tested sample instead of the Gmm value that does not always represent the gradation of a randomly selected coarse graded compacted sample. The test takes approximately 7 minuets, which is much shorter than standard testing procedures. This test is not based on a number of assumptions that can not be proven physically or theoretically as in the standard tests.

The CoreLok machine determines a fundamental parameter without using any assumptions. The sample is placed in a vacuum-sealed bag and a sealed density, $\rho 1$ is calculated. The bag containing the same sample is opened while under water and a second density $\rho 2$ is calculated. This second density will yield an apparent density since the sample was in a complete vacuum prior to opening the bag under water. The density $\rho 2$ includes the volume due to inaccessible air voids. To calculate the percent porosity (also known as the Corelok Infiltration Coefficient), the following equation can be used:

$$\% \text{ Porosity} = \left(\frac{\rho 2 - \rho 1}{\rho 2} \right) \bullet 100 \qquad \text{(Eq. 2.5)}$$

where: ρ1 = the CoreLok vacuum sealed density of compacted sample

ρ2 = Density of the vacuum sealed sample after opening under water

NCAT has performed testing to find the relationship between the percent porosity obtained from the CoreLok machine with field and laboratory permeability testing. A fairly good relationship was found with the three types of testing. The closest relationship was between the CoreLok machine and laboratory testing ($R^2 = 0.7137$). This is due to the water only flowing in a vertical direction. In field testing, pores can be interconnected horizontally and flow outside the area of the permeameter ($R^2 = 0.5436$) (Cooley et al. 2002).

2.5 Field Permeability

There are five basic designs for lab permeameters, two being commercially manufactured and three were designed by NCAT or modified versions of this device. Four of these devices are detailed in Cooley (1999), *Permeability of SuperPave Mixtures: Evaluation of Field Permeameters*. The main difference in these devices is the sealant used to attach the permeameter to the pavement. Each device used the falling head method and made the following assumptions: sample thickness is equal to the immediate underlying HMA course thickness, the area of the tested sample was equal to the area of the permeameter from which water was allowed to penetrate into the HMA, one dimensional fluid flow, steady-state flow, and laminar fluid flow.

2.5.1 NCAT Field Permeameter

The device that was build by NCAT utilizes a three tier standpipe. Each standpipe has a different diameter, the largest being at the bottom and the smallest at the top. This configuration is designed so that the device can be sensitive to all levels of permeability. For pavements with low permeability, the water level will move slowly down in the first,

small diameter standpipe. For pavements that have a larger permeability, the water will flow quickly through the first standpipe and then move slowly through either the second or third standpipe. This allows the head levels to be easily measured for all level of permeability.

A flexible rubber base is placed under a metal base plate to help seal the device to the pavement. Because the rubber base is flexible, it will help push the sealant into the surface voids of the pavement. Silicon-rubber caulking is applied between the rubber base and the metal base plate and between the rubber base and the pavement. The permeameter is then pushed onto the surface to distribute the sealant as evenly as possible. If there are large voids in the surface of the pavement, sealant can be directly applied to help fill these voids. A square weight is then placed on top of the base plate to keep a good seal when water is placed into the device.

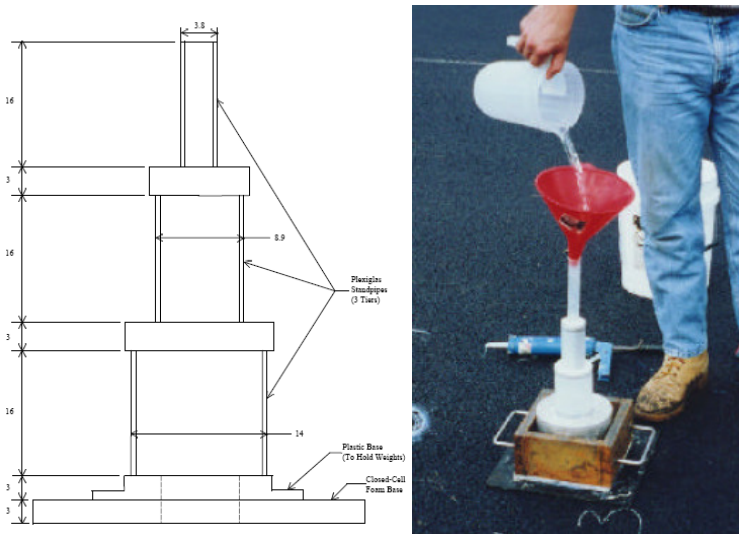

Figure 2.3 – NCAT Permeameter (Cooley, et al. 1999) used with permission

2.5.2 WPI Modified NCAT Permeameter

A modified version of the NCAT permeameter was developed by Worcester Polytechnic Institute, as given in Mallick, et al. (2003). The design is essentially the same except for the sealing mechanism. A closed-cell sponge rubber base was used because it is non-absorptive and molds to the macrotexture of the pavement. Donut shaped weights

totaling 110 lbs. are placed over the base plate to seal it to the pavement. This allowed cores to be cut for laboratory study at the exact spot the field test was run because no liquid sealant contaminated the test site.

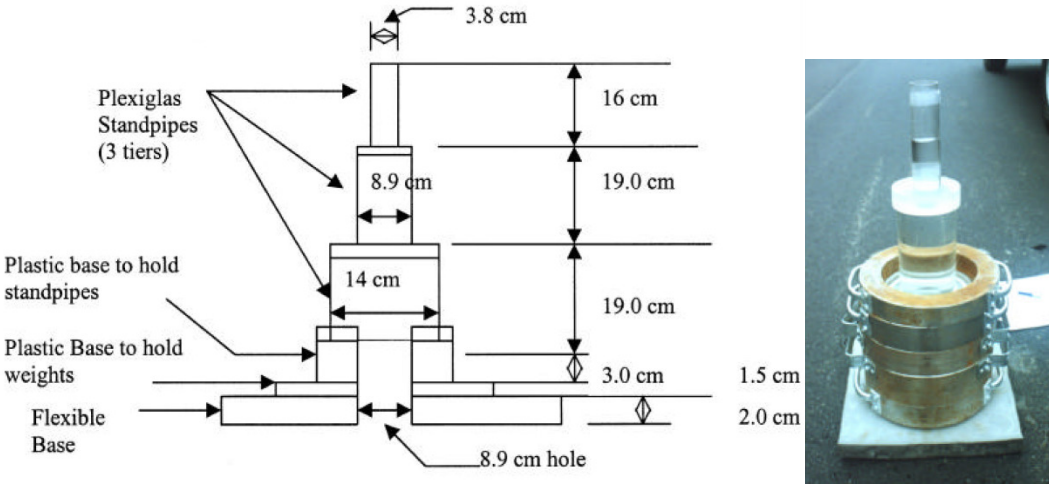

Figure 2.4 – Modified NCAT Permeameter 3 Tier (Mallick, et al. 2001) used with permission

2.5.3 Modified NCAT Permeameter – Single Standpipe

Another slightly modified NCAT permeameter has been developed. This device has a single standpipe attached to a base plate. The modification from the original NCAT design was increasing the diameter of the base plate to create a better seal between the base and the pavement. A similar technique to the previous NCAT permeameter is used to seal the device to the testing location. Silicone-rubber caulk is placed on the base plate, and the base is pressed into the pavement. If the seal is not adequate, caulk can be placed directly on the pavement. A circular weight is then placed on the base plate to keep the device from lifting after water has been placed in the standpipe.

Figure 2.5 – Modified NCAT Permeameter 1 Tier (Cooley, et al. 1999) used with permission

2.5.4 Marshall Mold Permeameter - Paraffin Seal

The next permeameter is supplied by a commercial supplier. This device consists of a six inch Marshall mold with a plastic cap attached to the top of the mold. There is a hold drilled into the plastic cap to fit the end of a single standpipe into. A ring that is approximately 50 mm larger in diameter than the Marshall mold is used for the sealing process. Heated paraffin is poured in between the Marshall mold and the ring. The liquid paraffin will flow into the surface voids and upon hardening it would seal the permeameter to the pavement. This method is labor intensive and special attention must be paid to the paraffin. If the paraffin was not allowed to cool before pouring, it would flow beneath the edges of the permeameter and close flow paths. If the paraffin cooled too much, it would harden quickly and would not seal the device properly.

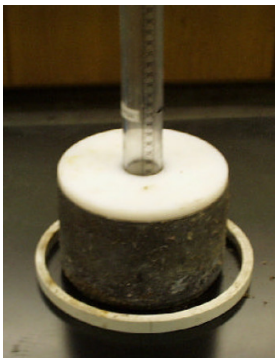

Figure 2.6 – Marshall Mold Permeameter Paraffin Seal (Cooley, et al. 1999) used with permission

2.5.5 Marshall Mold Permeameter - Silicon Seal

The last permeameter is similar to the previous device except for the sealing technique. This device also uses a Marshall mold with a plastic cap and a singe standpipe. There is no base plate on this model, so this model must be sealed at the mold. Silicon-rubber caulk is used to seal this device. For best results, sealant must be applied on the inside and outside of the mold. To seal the inside, the plastic cap can be removed for easy access to the center of the mold. Due to sealant being placed on the inside of the mold, the cross sectional area of the specimen is slightly reduced.

Figure 2.7 – Marshall Mold Permeameter Silicon Seal (Cooley, et al. 1999) used with permission

2.5.6 Field Permeameter Evaluation

Cooley (1999) conducted a study to evaluate four of the five permeameters that are described in this paper (the Mallick permeameter is excluded). Field tests were conducted in Mississippi, Virginia and South Carolina. A total of 20 tests were performed with each permeameter in all of the states. Five cores were cut from each state to test in the laboratory for comparison. The field permeameters were ranked by ease of use, repeatability and accuracy as compared to lab testing. The best permeameter according to

this study is the three tiered, NCAT permeameter. There was no significant change between the lab tests and the field tests, it was simple to use, and consistent.

2.6 Directional Permeability

The measure of directional permeability is an issue that has been investigated in recent years. Mainly these studies acquire the coefficient of permeability in two directions, vertical and horizontal. This data is necessary due to the anisotropic and heterogeneous distribution of air voids within HMA. Al-Omari (2004) used the finite difference method to model fluid flow within the pore structure of HMA. Kutay, et al. (2007) based the fluid flow model on the lattice Boltzmann technique. Both studies have employed the use of X-Ray CT imaging to acquire a three dimensional representation of an asphalt core to analyze with a numerical simulation for fluid flow. These studies modeled fluid flow in many lab and field specimens and concluded that horizontal permeability is much larger than vertical permeability. Generally the horizontal/vertical permeability ratio was between 1 and 10, but some specimens were larger than 30. Accurate data was obtained for the fluid flow characteristics and the distribution of air voids within HMA specimens.

Kutay, et al. (2007) developed a method to estimate directional permeability using the CoreLok device. A specimen was cut into three sections: upper (0-20mm), middle (20-80mm), and lower (80-100mm). The percent porosity was higher in the upper and lower sections of the samples. The values determined are shown in table 2.2. It was found that the horizontal permeability was well correlated with the average porosity in the upper and lower section and the vertical permeability was well correlated with the middle section. Masad, et al. (2004) proposed a modified version of the Kozeny-Carman equation (Eq. 2.6) to easily predict permeability. This equation is applied to the upper and lower section to estimate horizontal permeability and to the middle section to estimate vertical permeability. The lab tested results were then compared to the numerical simulation with good results. The results of this comparison are given in Figure 2.8.

Table 2.2 – Air Void Distribution for HMA Samples (Kutay, et al. 2006) used with permission

Specimen ID	n_{top} (%)	n_{middle} (%)	n_{bottom} (%)
9.5C25	9.1	4.6	8.8
12.5C25	4.9	1.4	4.5
19C25	13.6	4.8	4.2
19C50	8.2	2.7	11.5
19C75	9.9	5.2	8.1
25C25	11.4	9.8	15.6
25C50	12.7	6.5	4.8
25C75	14.4	3.1	3.3
9.5SMA-A1	23.2	12.7	20.8
9.5SMA-A2	18.1	11.8	17.8
9.5SMA-B1	24.9	20.5	22.1
9.5SMA-B2	19.4	10.8	20.9
12.5SMA-A1	19.9	11.8	17.7
12.5SMA-A2	22	20	29.6
12.5SMA-B1	12.4	8.1	12.9
12.5SMA-B2	15	10.6	12.9
19SMA-A1	9.7	8.3	18.2
19SMA-A2	15.3	9.4	16.3
19SMA-B1	11.2	5.4	13.2
19SMA-B2	16.8	8.6	12.1
L2	15.1	9.8	10.2
L4	7.0	4.7	9.1
F-24	10.8	9.4	10.3
F-23	4.7	5.3	7.8
OG-SGC-04	27.8	15.3	24.2
OG-SGC-07	13.7	10.4	11.9
OG-MAR-08	13.1	15.6	20.3
OG-MAR-10	13.8	7.1	8.5

$$k = \frac{\overline{C} n^3}{(1-n)^2} \left[D_s \left(1 + \frac{G_{sb}\left(P_b - P_{ba}\left(1-P_b\right)\right)}{G_b\left(1-P_b\right)} \right)^{\frac{1}{3}} \right]^2 \frac{\gamma}{\mu} \qquad \text{(Eq. 2.6)}$$

Where: k = coefficient of permeability
C = an empirical constant
n = the porosity
D_s = the average particle size
G_b = the binder specific gravity
P_{ba} = the percent of absorbed binder by weight of aggregate
P_b = the percent of asphalt content by total weight of the mix
G_{sb} = the bulk specific gravity of the aggregate

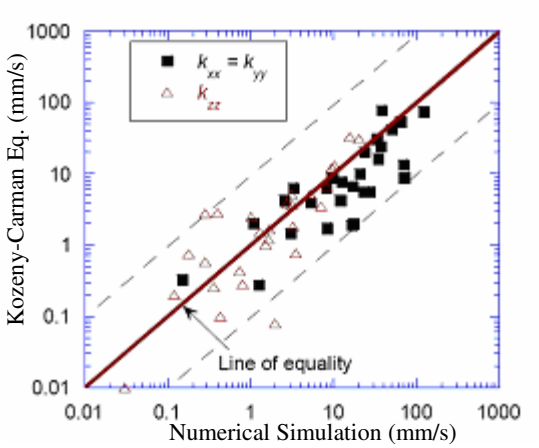

Figure 2.8 – Comparison of Kozeny-Carman and Numerical Simulation Results (Kutay, et al. 2006) used with permission

2.7 Factors Affecting Permeability

The most important factor that affects HMA permeability is in-place density. Higher percentages of air voids yield a higher permeability due to more interconnected voids in the pavement (Mallick, et al. 1999). Testing has shown that permeability is very low at air void contents less than 6 percent. Between 6 and 7 percent air voids, permeability increases significantly. Pavements become excessively permeable between 8 and 8.5 percent air voids (Hainin, et al. 2003).

Nominal maximum aggregate size (NMAS) also has a large effect on permeability. As NMAS increases, a pavement can become excessively permeable with lower in place air voids. This is due to the creation of larger individual air voids with larger aggregate sizes (Choubane, et al. 1998). The potential for more interconnected voids is increased with larger individual void size.

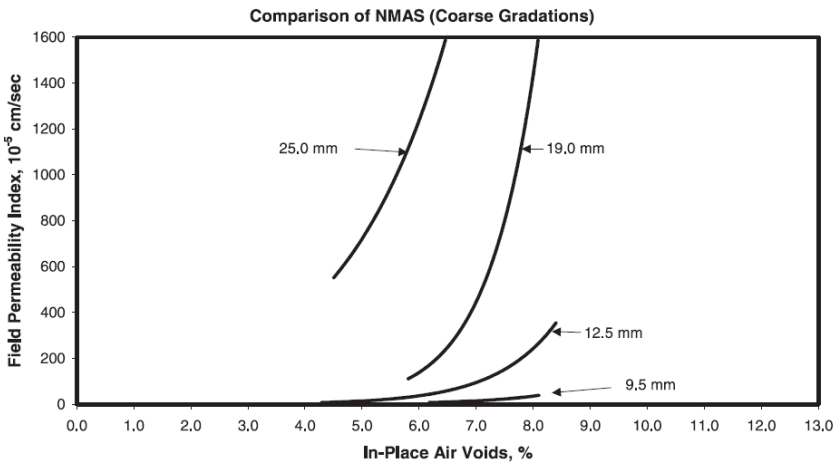

Figure 2.9 – Effect of Nominal Maximum Aggregate Size on Field Permeability (Cooley, et al. 2002) used with permission

The gradation shape and NMAS have similar affects on HMA permeability. Gradations that are considered fine-coarse mixes have lower permeability as compared to coarse graded mixes. The gradation shape affects the size of the individual void sizes within the pavement (Mallick, et al. 1999). Fine particles create small voids that are less likely to become interconnected voids for water to flow through. Coarse graded mixes create larger air voids that are more likely to be interconnected and create a more permeable pavement.

Due to the fact that NMAS and gradation shape both affect permeability, by controlling the amount of fine aggregates in a mix, the permeability characteristics can also be controlled. By adding fine aggregates, the individual air void size can be decreased. This will create less possibility of interconnected air voids (Cooley, et al. 2001).

Another factor that affects permeability is lift thickness during construction of the pavement. As lift thickness increases, the permeability will usually decrease (Mallick, et al. 1999). This is due to easier compaction of thicker lifts that can retain internal heat for longer periods of time and allow proper orientation of aggregates. This will result in a higher density pavement, and leave fewer voids that can transport water. Also, when using dense graded mixtures the potential for voids to be interconnected decreases as lift thickness increases. These factors show that using a thinner lift will create higher permeability.

A study conducted at Hainin, et al. (2003) investigates the effects of the majority of the aforementioned factors on permeability. The study encompassed 42 SuperPave projects with 39 of these projects having a NMAS of 9.5 or 12.5mm. The other three projects had a NMAS of 19mm. A stepwise statistical regression was performed and it was concluded that the following factors impacted the natural log of permeability by significance in this order: the natural log of air voids from the CoreLok machine, the coarse aggregate ratio, percent passing 12.5 mm sieve, percent passing 1.18 mm sieve, the N_{des}, and the average sample thickness. The following regression equation was given for this relationship:

$$\text{Ln}(k) = -19.2 + 5.96\text{Ln}(CL) + 1.47(\text{CA Ratio}) + 0.078(P12.5) + 0.0485(P1.18) + 0.00928(N_{des}) - 0.0124(\text{Ave. Thickness}) \quad \text{(Eq. 2.7)}$$

where: k = coefficient of permeability (cm/s)
CL = air voids from CoreLok machine
CA Ratio = coarse aggregate ratio
P12.5 = percent passing 12.5mm sieve
P1.18 = percent passing 1.18mm sieve
N_{des} = design number of gyrations

2.8 Critical Permeability Value

Cooley, et al. (2001) conducted a study to relate in-place pavement density with a critical value for permeability. A total of 11 ongoing construction projects were studied to collect data. The projects consisted of 9.5, 12.5, 19.0, and 25.0 mm nominal maximum aggregate sizes. Field permeability tests were run using the NCAT field permeameter, and cores were taken at the testing locations to obtain density information.

In order to determine the critical value, a regression line from field data was plotted. The area in the plot is divided into three regions corresponding to the interconnectivity of the voids. With a low value of air voids, it is less likely that the voids are connected. A high value of in place air voids will create a larger amount of interconnected air voids. The critical point falls in between these regions, specifically where the ratio of interconnected and non-interconnected air voids are equal. To determine this point, a line tangent to the regression line in the low air voids is placed. Next, a tangent line to the regression line in the high air voids section is placed. The point

at which a bisecting line drawn from the intersection of the two tangent lines meets the regression line provides the critical permeability and percent air voids.

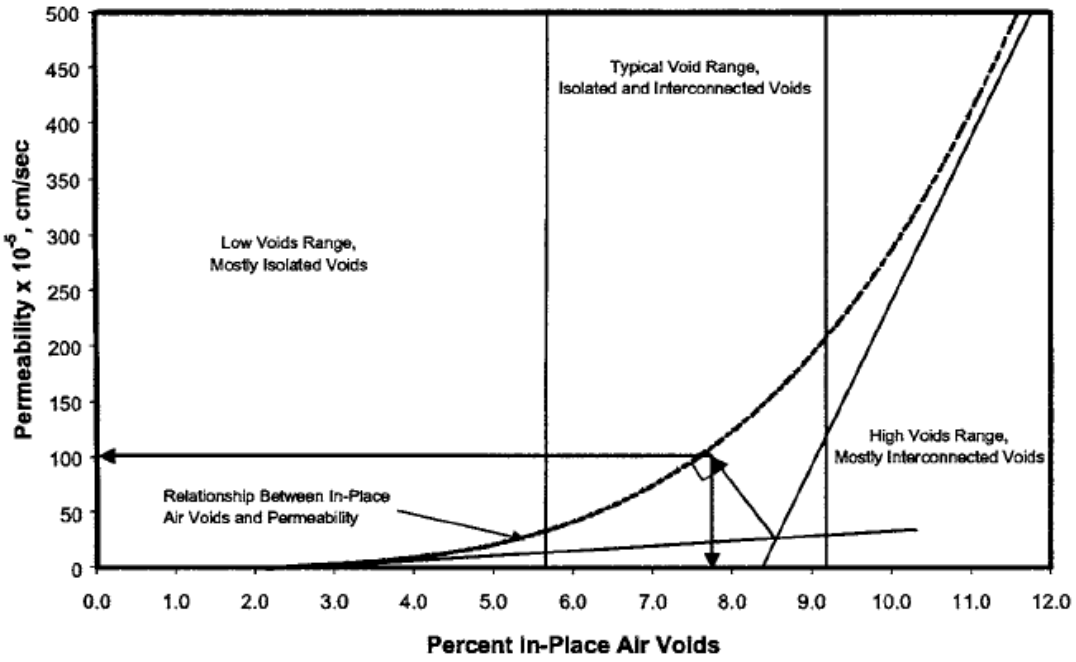

Figure 2.10 – Method for selecting critical permeability and air voids value (Cooley, et al. 2001) used with permission

The study found a strong correlation between in place air voids and field permeability for the subject projects. There was also a strong relationship between NMAS and in place permeability. Both of these observations agree with previous research that has been done in HMA permeability. The results of the testing show that the 9.5 and 12.5 mm NMAS mixes has similar permeability characteristics. The pavements became excessively permeability at 7.7 percent in place air voids with a coefficient of permeability of 100 x 10^{-5} cm/s. The 19.0 mm NMAS mix became excessively permeable at 5.5 percent air voids with a coefficient of permeability of 120 x 10^{-5} cm/s. The 25.0 mm NMAS mix became excessively permeable at 4.4 percent air voids with a coefficient of permeability of 150 x 10^{-5} cm/s. It was recommended that field permeability be used in conjunction with density testing to obtain an accurate estimate of the durability of HMA pavements.

2.9 Problems

Darcy's law is used to calculate the permeability in both lab and field tests. This becomes a problem in the field tests because the falling head methodology of Darcy's Law is based on the assumption of one dimensional flow. In the field test, there are no effective side boundaries allowing for two dimensional (vertical and horizontal) flow (Cooley 1999). This makes it difficult to compare or correlate test results from the laboratory and field testing. This method of data analysis will not be completely valid for field testing due to the lack of "ideal" conditions. However, this method still provides a good estimation of the permeability and a basis for comparison between other field tests (Mallick, et al. 2001).

Also, there is a boundary condition problem with the potential of water flow through pavement layers. Without taking a core, there is no way of knowing whether or not this is occurring (Mohammad, et al. 2003). Due to horizontal permeability the specimen cross-section area cannot be accurately represented.

Another potential problem with field testing is the assumption of saturation in the sample. In the laboratory, this condition can be achieved fairly easily but in the field it cannot be measured. In the field it was observed that the drop in water level during the first test usually took less time than following tests at the same location. An explanation for this is that during the first test the water fills up the voids, including some that are not interconnected; and additional suction force before wetting. During the second and third tests the water cannot travel through these unconnected voids and only flows through the interconnected voids (Mohammad, et al. 2003).

During lab tests the sample dimensions can be conveniently determined. For field testing a core must be taken to measure the exact dimensions. Without a core, the sample thickness must be estimated along with the effective area of the pavement through which the flow takes place. In addition, it is difficult to assess the boundary conditions at the bottom of the HMA layer of which the field permeability is being estimated. When water is introduced into the standpipe it flows into the pavement. The water can flow in any direction and most likely flows outside the area of the standpipe (Cooley 1999). Water

can also flow through pavement layers (Gogula, et al. 2003) if the tack coat wasn't applied evenly or there is some deterioration of the tack coat.

NCAT experienced a problem while conducting the NCHRP study "Designing Stone Matrix Asphalt Mixtures". The problem was that they could not seal the permeameter to the surface of the pavement due to the rough texture of this mixture. This makes the test unable to be repeated and not an accurate estimate of permeability. The sealing technique includes using a silicon rubber caulking which is very difficult to remove from the surface of the pavement, leaving semi permanent residue at each testing location.

Chapter 3
Methods

3.1 Introduction

There are many methods available to measure permeability both in the lab and in the field, but there are issues that have not been resolved with these methods. Studies have shown that hot mix asphalt permeability has anisotropic properties. The main method for evaluating the directional properties of core samples involves the use of an expensive X-Ray CT imaging device. The data must then be entered into a numerical model and analyzed. This chapter presents a simple falling head method for evaluating horizontal permeability in HMA core samples. This method is inexpensive and simple to analyze. It is coupled with ASTM PS 129-01 to measure the vertical permeability, giving an overall picture of the directional flow within the sample.

The NCAT field testing device has issues with creating a seal between the base and the pavement. Also, only one diameter of water-pavement contact area has been evaluated. This section addresses these problems by creating a device that uses pressure to seal the base to the pavement and incorporates multiple base plates for various water-pavement contact areas.

A finite element model was used to validate the experimental data obtained from the field test. A parametric study encompassing total permeability, anisotropic permeability ratio, applied pressure head length (representation of contact area), and permeable and impermeable lower boundary were studied. The horizontal and vertical flow rates were compared below the applied pressure head to observe the flow characteristics of each scenario.

3.2 Laboratory Investigation of Anisotropy

The laboratory tests were used to determine the horizontal and vertical coefficients of permeability. This test used gyratory compacted samples from loose HMA

mix. A 7 inch tall, 6 inch diameter cylindrical sample were compacted to specified air void contents between 4 and 8 percent. One end of the compacted sample was saw cut to 1.5" tall. The remaining sample was used for the horizontal permeability test. A vertical core was removed from the center of the sample to insert fluid for measuring horizontal permeability.

3.2.1 Vertical Permeability

The device used to test the vertical permeability was the FDOT lab permeability tester as per ASTM Standard PS 129-01. The permeameter consists of a vertical standpipe, two expandable pressure rings, a six inch aluminum containment cylinder, a latex membrane, a water release valve, and a manual air pump with a pressure gauge. The sample is 1.5 inches in height with a 6 inch diameter, giving 9π square inches of contact area as shown in Figure 3.1.

` After the test specimen has been prepared, it is saturated in a deaeration chamber under 26 inches of Hg for 15 minutes. The testing device and deaeration chamber are shown in Figure 3.2. Next the sample was placed in the chamber where the latex membrane was pressurized to prevent water passing through the sides of the sample. To create a better seal, petroleum jelly can be placed on the sidewalls of the sample. The standpipe was then filled with water and the valve was released. The time was then recorded for the water level to move from the initial head value to the final head value. The information from the test and dimensions of the core sample are entered into Darcy's Law to obtain the coefficient of permeability.

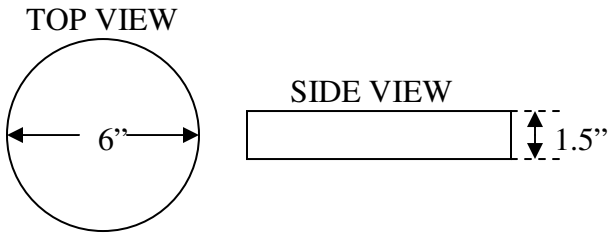

Figure 3.1 – Vertical Permeability Sample Dimensions

Figure 3.2 – FDOT Lab Permeameter/Pycnometer photographed by author

3.2.2 Horizontal Permeability Initial Design

For horizontal permeability, the bottom of the sample was saw cut and coated in asphalt binder. Then a one inch core was removed from the remainder of the sample so that the horizontal voids can be accessed throughout the length of the sample. These two pieces are then reattached using the binder for adhesion, thus sealing the bottom of the sample and preventing vertical flow. The device built to test horizontal permeability consisted of a 2 inch clear PVC pipe glued to a 2 inch to 4 inch PVC adapter. A 4 inch sample can be placed on the opposing end of the adapter and silicon rubber caulking is used to prevent fluid flow along the interface. This method, shown in Figure 3.3, proved to be inconsistent in providing an adequate seal along with an extensive preparation time.

Figure 3.3 – Horizontal Permeameter Initial Design photographed by author

3.2.3 Horizontal Permeability Final Design

A new system was developed that would be similar to the previous device except it seals in the inner portion of the bored hole. It will consist of a standpipe with an adapter and is shown in Figure 3.5. On this adapter will be two o-rings to seal the adapter to the sample. The sample is dipped in melted paraffin wax to prevent flow through the top and bottom of the sample. This ensures that the flow of the fluid is directed in the horizontal direction. This will decrease the preparation time immensely and make the system easier for the user to operate. Also, multiple samples can be prepared at one time, independent of the testing equipment. First, a one inch core was taken from the center of the sample. This core will be 4 inches in depth, thus leaving 1.5 inches in tact at the bottom of the sample. The fluid-asphalt contact area is 3π square inches and the width from the inner to outer diameter is 2.5 inches. Next, a 2.5 inch core was taken from the same sample to achieve a closer contact area and thickness to the vertical lab test sample. This sample has 7.5π square inches of contact area and 1.75 inches from inner to outer diameter.

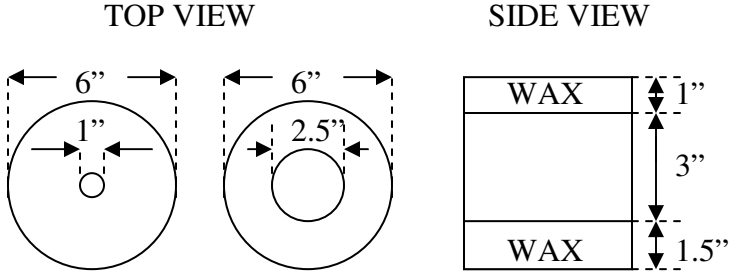

Figure 3.4 – Horizontal Permeability Sample Dimensions

Figure 3.5 – Horizontal Permeameter Final Design photographed by author

3.2.4 Experimental Design

Loose mix is placed into the gyratory compactor and compacted to obtain the desired air void percentage for a 7 inch tall, 6 inch diameter cylindrical sample. The mix design is a 9.5mm nominal maximum aggregate size with PG 70-22 binder at 5.7%. The target air void contents were 4, 5, 6, 7, and 8 percent. Two samples were compacted for each of the air void contents. Once the sample cooled, a 1.5 inch tall specimen was saw cut from the top of the sample. This specimen was cleaned, and then prepared for vertical permeability testing. The appropriate diameter core was taken from the remainder of the sample. The sample is drilled with 1.5" inches remaining solid at the bottom of the sample. The core is then broken off and removed. This sample is dipped in paraffin wax to seal the top and bottom to prevent leakages. The wax covers the bottom 1.5" and top 1" to ensure water flows only from the 3" that are exposed to fluid from the inner core.

The samples prepared for the vertical permeability test were placed underwater and had air vacuumed out of the sample for 15 mins under 26mm of Hg. The horizontal samples were too large to fit in the vacuum container, so they were immersed in water for

24 hours before testing began. Each sample was tested three times to establish an average permeability coefficient.

3.2.5 Analysis Techniques

The results from the vertical and horizontal tests will be plotted against the actual air void content. The vertical permeability will be evaluated using Darcy's Law falling head method as represented in equation 2.3. The horizontal permeability is calculated by the following derived equation:

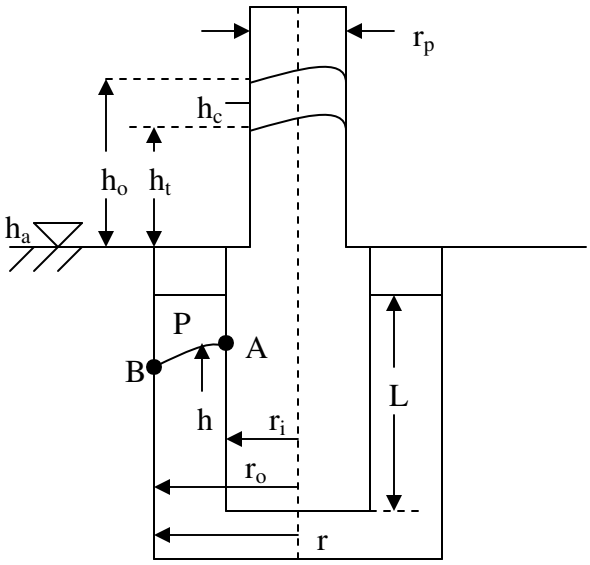

Figure 3.6 – Horizontal Permeability Diagram

From point A to B, the head will drop from h_c to h_a. For any point on the head curve, P, its corresponding head is h and its location is r. If the pressure at h_o and h_a are held constant, the total flow can be represented as $Q = k \cdot \frac{dh}{dr} \cdot 2 \cdot \pi \cdot r \cdot L \cdot t$ where Q is constant. Where k is the coefficient of permeability, the hydraulic gradient is $i = \frac{dh}{dr}$ and the area is 2πrL. The flow rate can be shown as $q = k \cdot \frac{dh}{dr} \cdot 2 \cdot \pi \cdot r \cdot L$. Rearranging this equation, the following is formed $2 \cdot \pi \cdot L \cdot dh = \frac{q}{r} \cdot dr$. The equation can then be

integrated from the upper to lower head level and the inner to outer radius, $\int_{hc}^{h_a} 2 \cdot \pi \cdot L \cdot k \cdot dh = \int_{r_i}^{r_o} \frac{q}{r} \cdot dr$. The integration yields $2 \cdot \pi \cdot L \cdot k \cdot (h_c - h_a) = q \cdot \ln\left(\frac{r_o}{r_i}\right)$.

Solving for the coefficient of permeability, k, gives $k = \frac{q \cdot \ln\left(\frac{r_o}{r_i}\right)}{2 \cdot \pi \cdot L \cdot (h_c - h_a)}$. For the falling head test the flow rate, q, can be shown as $q = \frac{(h_o - h_t) \cdot \pi \cdot r_p^2}{t}$. The value of h_c is the average of initial and final head levels $h_c = \frac{h_o + h_t}{2}$ and the value of h_a equals zero because it is at atmospheric conditions. Combining and simplifying these equations yields equation 3.1.

$$k_h = \frac{\left(\frac{r_p{}^2 (h_o - h_t)}{t}\right) \ln\left(\frac{r_o}{r_i}\right)}{L \cdot (h_o + h_t)} \qquad \text{(Eq. 3.1)}$$

Where:
r_p = radius of standpipe
r_o = Outer radius of sample, cm
r_i = inner radius of sample, cm
h_o = initial head, cm
h_t = final head, cm
t = time, sec.
L = length of sample, cm

3.3 Field Permeability Various Tester Size

Current field permeability testing is mostly accomplished with the NCAT field permeameter. The water-pavement contact area is 3.5" and the permeameter uses a silicon-rubber sealant to adhere the device to the pavement. A replication with base plates that accommodate multiple contact areas was built. The effect of water-pavement contact area was performed with a modified version of the NCAT permeameter on the Smart Road in Blacksburg, VA.

3.3.1 Field Permeability Initial Design

The permeameter used for this study, as shown in Figure 3.7, was based on the three tier NCAT design that is available commercially. The dimensions have been changed due to availability of materials, cost efficiency and suitability for this particular study. There are three tiers on the permeameter, with the top two used for water level measurements. The top two tiers are constructed of clear PVC pipe. For pavements with low permeability, the top tier of 2" diameter pipe is used to read the water level. For pavements with higher permeability, the second tier of 4" diameter pipe was used for measurement. The third tier is a 14" inner diameter box constructed of grey PVC sheeting. This tier is used to apply water to the largest contact area of 14" in diameter. A box was used instead of a 14" diameter pipe due to cost efficiency. Each tier is 6.5" tall as per the NCAT design.

The base of the permeameter is 24" by 24" to allow the placement of weights for sealing the device to the pavement. To facilitate the multiple contact area sizes for this test, base plates were constructed to constrict the flow of water. Each base plate was cut to the desired diameter contact area and attached to the base of the permeameter. The base plate consists of a 24" by 24" grey PVC sheet and 24" by 24" sheet of closed cell rubber. The rubber sheet assists in the sealing of the permeameter to the pavement. Contact areas of 14", 10", 6" and 3.5" diameter circles were selected for this study.

To seal the permeameter to the pavement, silicon-rubber caulking was applied to the rubber sheet on the bottom of the permeameter. The permeameter was then placed on the selected testing location. Metal bars weighing a total of 120lbs were then placed on the base of the permeameter. The rubber sheet pushes the caulking into the voids between the permeameter and the pavement to create a seal.

This device was found to create an inconsistent seal along with leaving residue on the pavement at the testing location. When a seal could be accomplished, the removal of the device would damage the closed-cell rubber.

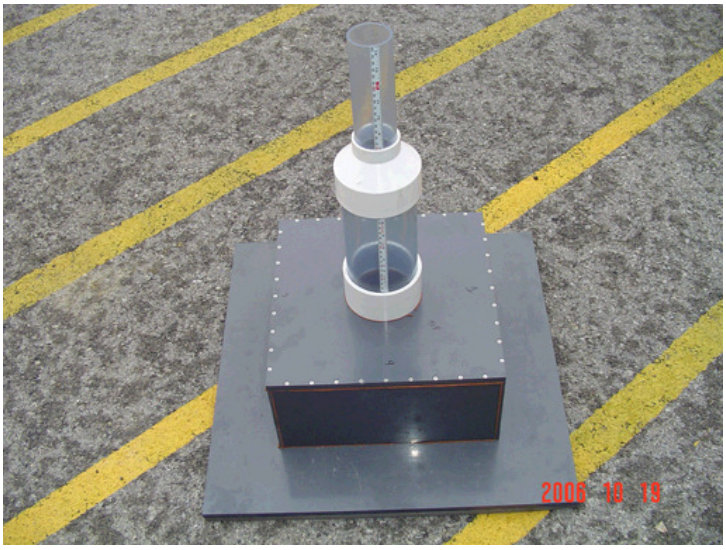

Figure 3.7 – Initial Field Permeameter photographed by author

3.3.2 Field Permeability Final Design

A more consistent and easy to use device, as shown in Figure 3.8, was designed for field testing. There are two clear PVC pipes with an attached measuring tape to read the head level. The top pipe has an inner diameter of 2" to read less permeable pavements, and the bottom pipe has an inner diameter of 4" to read higher permeable pavements. The major modification in the device is the sealing mechanism. The designed device utilizes pressure instead of a sealing agent. The lower standpipe is connected to a steel box with a receiver ring on the top. A hitch mounted jack with an inverted ball is used to lift the vehicle and transfer its weight to the steel box. On the base of the box, a PVC plate with the desired diameter hole is attached to the device. The PVC plate has a rubber gasket on the top, and a neoprene foam rubber layer on the bottom. As pressure is applied, the neoprene molds to the surface texture of the pavement to create a seal surrounding the test location. A large water tank on the vehicle equipped with a hose will provide the water necessary for running the tests.

Figure 3.8 – Final Field Permeameter photographed by author

3.3.3 Experimental Design

The Smart Road at the Virginia Tech Transportation Institute was utilized for field testing. The modified field permeameter that was developed for this research was used to run all field tests. Three sections of the Smart Road were chosen for permeability measurements. Each of the three sections has a surface mix with a nominal maximum aggregate size of 9.5mm. Within each of the three sections, three locations will be tested for permeability for a total of nine testing locations. It was previously determined through field testing that achieving a fully saturated state is impractical due to the amount of water needed and the amount of time to achieve steady state. Due to this finding, each testing location was subjected to four permeability readings. The coefficient of permeability decreased as the pavement becomes increasingly saturated. Each test was conducted with the same protocol, and similar amounts of water to achieve comparable states of saturation for each set of tests.

Since the saturation level has a significant effect on the permeability estimation, only one contact area configuration can be tested in one day. To ensure accurate results, testing periods were chosen by the same criteria. The testing days had to be mild in temperature to ensure the water temperature does not fluctuate. Also, the pavement must

stay dry for one full day prior to testing. During the day of tests, one contact area plate is selected. This contact area is then tested at each of the three locations in each section.

The pavement sections chosen were sections B, C, and I on the Smart Road and are represented in Figure 3.9. Sections B and C were the same structure, but used a different aggregate type on the surface mix. The structure consists of SM-9.5, BM-25.0, open graded drainage layer, 21A cement stabilized base, and 21B sub-base. Section B used a SM-9.5D and section C used a SM-9.5E. Section I consists of SM-9.5A with a reinforcing mesh, BM-25.0, SM-9.5A, open graded drainage layer, 21A cement stabilized base, and 21B sub-base.

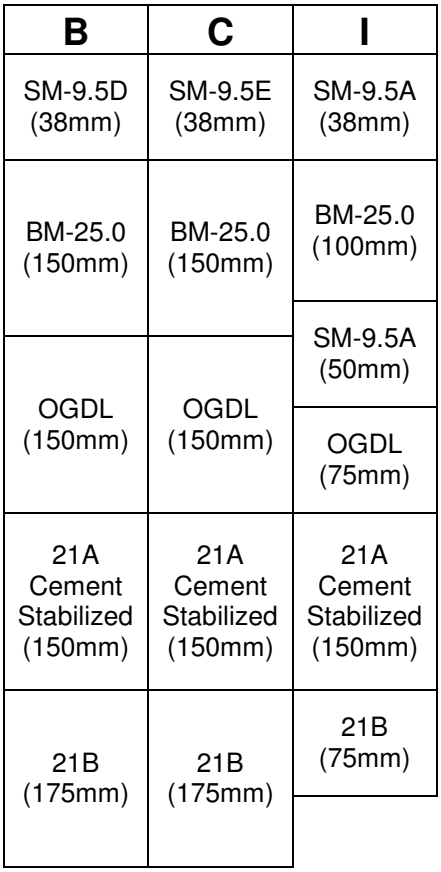

Figure 3.9 – Smart Road Layers

The field test devices include the permeameter, base plate of desired contact diameter, polymer screws to attach base plate, hitch mounted jack, water tank with hose, and stop watch. The vehicle was parked in the desired test location. Next, the hitch

mounted jack was secured, and the permeameter was placed centered underneath the jack. The jack handle was rotated, applying force to the permeameter until the jack was fully extended or a significant amount of resistance was observed. If multiple tests were conducted within close proximity, chains were secured to the jack with cotter pins so that the jack could be used to lift the permeameter off the ground without completely disassembling the device. The hose was placed in the top standpipe and water was released from the tank. The permeameter was filled to the desired head level and testing can begin when the water stabilizes. Observations were made of the starting and ending head levels, also the time elapsed between the two head levels. For this study, readings were generally taken when the head dropped 10 cm or 5 minuets have elapsed.

3.3.4 Analysis Techniques

The field permeability test data is analyzed using Darcy's Law falling head method (Eq. 2.3). The coefficient of permeability in cm/s was calculated using the dimensions of the pavement sample along with the head and time data collected in the field.

In order to evaluate the significance of contact area on field permeability estimations, Fisher's least significant difference test was employed. This test determines which means amongst a set of means differs from the rest. A one-way analysis of variance was used to evaluate whether there is any evidence that the means of the populations differ. This test assumes that the data form a normal distribution and have constant variance. An exact overall Type I error rate is achieved based on normality. Fisher's LSD concludes a pairwise difference is significant when equation 3.3 holds true.

$$\left|\bar{y}_i - \bar{y}_j\right| > t_{\alpha/2, df_{Error}} \sqrt{MSE\left(\frac{1}{n_i} + \frac{1}{n_j}\right)} \qquad \text{(Eq.3.3)}$$

This test was performed by Minitab statistical software. The output was analyzed to determine if there is a significant difference between the different contact areas for permeability in the same location. The test was run by pavement section (B,C,I) and individual locations.

3.4 Finite Element Analysis of Field Permeability

In order to validate the data obtained from the field permeability data, a finite element analysis was utilized. The model simulated the field test that was used previously in this study. Two scenarios were simulated, one with a permeable lower boundary and a base layer with a higher permeability, the other with an impermeable lower boundary representing an effective tack coat. The directional flow in the specimen cross sectional area was evaluated. This provided information on the true nature of directional flow for the falling head permeability testing method. Also, the flow data was used to calculate the Darcy's Law vertical permeability that was observed in the field as compared to the actual vertical permeability prescribed in the model.

3.4.1 Model Boundaries and Initial Conditions

The structure of the Smart Road sections that were tested for field permeability were represented in the finite element model. The surface layer is 1.5 inches thick and the width of the section modeled was 48 inches. The model containing a permeable base layer has a depth of 6 inches. The upper boundary had an applied total pressure head of 0.75 m which corresponds to the average head during the field test. This pressure was applied at the center of the pavement layer for a length analogous to the diameter of the water-pavement contact area. A zero total pressure head boundary condition was applied to the upper boundary from the extreme horizontal points to 12 inches towards the center. This condition was used to simulate the boundary that is exposed to atmospheric pressure past the extents of the testing device. The remaining section between the zero pressure head and .75 m pressure head is a no flow condition. This represents the extents of the base plate that seals the permeameter to the pavement to prevent surface flow.

3.4.2 Permeable Lower Boundary

The first scenario consists of analyzing two pavement layers with a permeable boundary separating them. This configuration represents a surface layer placed on top of a base layer with an uneven tack coat application or a deteriorated tack coat. The model is shown in Figure 3.10. Three variables were used in this simulation that included applied head length (contact area), total permeability and horizontal to vertical permeability ratio. The applied head lengths correspond to the diameter of contact area used in the field testing. The applied head lengths include 3.5, 6, 10 and 14 inches. The total permeability values are a representation of the values obtained from the field testing. The coefficients of total permeability used were $5x10^{-3}$, $5x10^{-4}$ and $5x10^{-5}$ cm/s. Total permeability is represented as:

$$k_t = \sqrt{k_v^2 + k_h^2} \qquad \text{(Eq. 3.4)}$$

where: k_t = coefficient of total permeability (cm/s)
k_v = coefficient of vertical permeability (cm/s)
k_h = coefficient of horizontal permeability (cm/s)

The horizontal to vertical permeability ratios were based of the lab tests developed for this study and also from the results of Kutay et. al. The values used were k_h/k_v = 1, 3 and 5. By combining all of the possible scenarios, there were a total of 36 simulations performed. The initial mesh consisted of approximately 11,000 elements. The mesh was then refined beneath the applied pressure head in the surface layer increasing the elements up to 20,000 depending on applied pressure head length. The horizontal discharge lines were placed at the two boundaries of the applied pressure head to establish an average. The vertical discharge line was placed below the applied pressure head at the lower boundary of the surface layer. The ratio of vertical flow to horizontal flow was calculated.

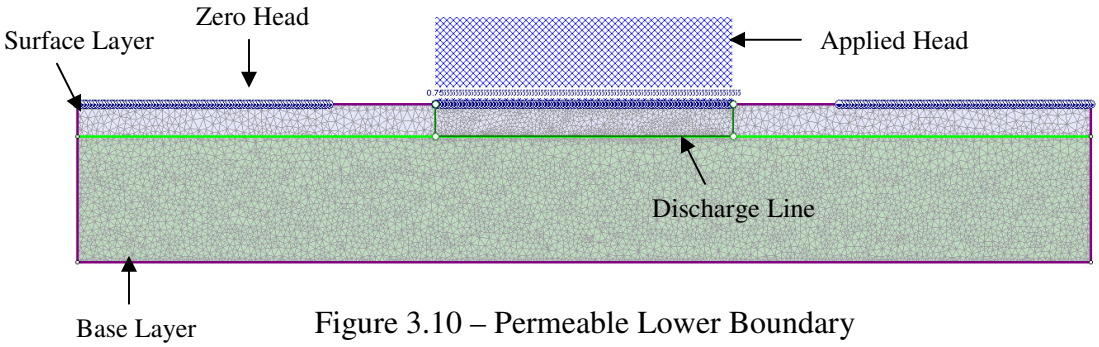

Figure 3.10 – Permeable Lower Boundary

3.4.3 Impermeable Lower Boundary

The second scenario consists of analyzing a single pavement layer with an impermeable lower boundary. This configuration represents a pavement layer with an even tack coat applied to the base layer before surface layer placement. The model is shown in Figure 3.11. The same variables and values from the previous simulation were used in this simulation. The initial mesh consisted on approximately 5,500 elements. The element density was increased in the area beneath the applied pressure head. The number of elements increased up to a total of 18,000 depending on the applied pressure head length. Three discharge lines were placed within the pavement layer that reports the flow rate through the given section. The flow rates were measured at the center of the pavement layer because there is no flow at the lower boundary. The horizontal flow rate at the boundaries of the applied pressure head were measured and averaged. The flow rate in the vertical direction was measured under the applied pressure head, between the horizontal discharge lines. The ratio of vertical flow to horizontal flow was calculated.

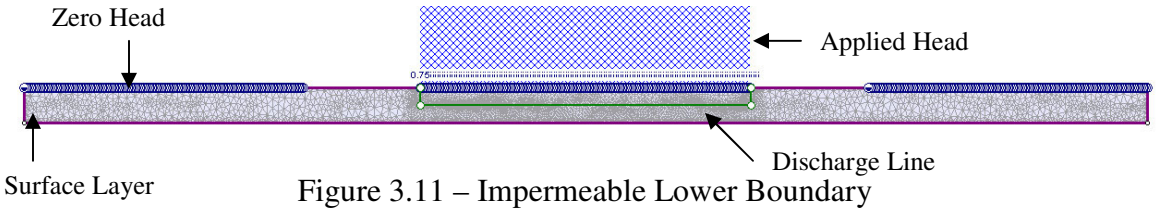

Figure 3.11 – Impermeable Lower Boundary

Chapter 4
Results and Discussion

4.1 Introduction

This chapter presents the results and analysis of the anisotropic laboratory testing, effects of contact area on field permeability, and finite element simulation of field permeability testing. The laboratory testing provides insight into the ratio of horizontal to vertical permeability in lab compacted samples. The field permeability testing presents results of the impact of water-pavement contact area on the overall permeability value obtained. The finite element model is used to validate the field permeability testing by investigating the influence of horizontal and vertical flow on the calculated results from the field.

4.2 Laboratory Investigation of Anisotropy

In order to investigate the anisotropy of laboratory compacted samples, both the vertical and horizontal permeability must be measured. To measure the vertical permeability ASTM PS 129-01 was followed. A new device was designed to easily measure horizontal permeability. This section will present the results from both types of testing.

4.2.1 Vertical Permeability Testing

Ten 1.5 inch tall samples were used to conduct vertical permeability testing. The samples were cut from the larger 7 inch tall sample. Three tests were conducted for each sample to establish an average. The water-pavement contact area was 9π in.^{2}. It was found that as the air void content increased, the permeability also increased. This is due to the greater amount of voids, and the larger probability that they are interconnected. The results from the vertical permeability testing can be found in Figure 4.1.

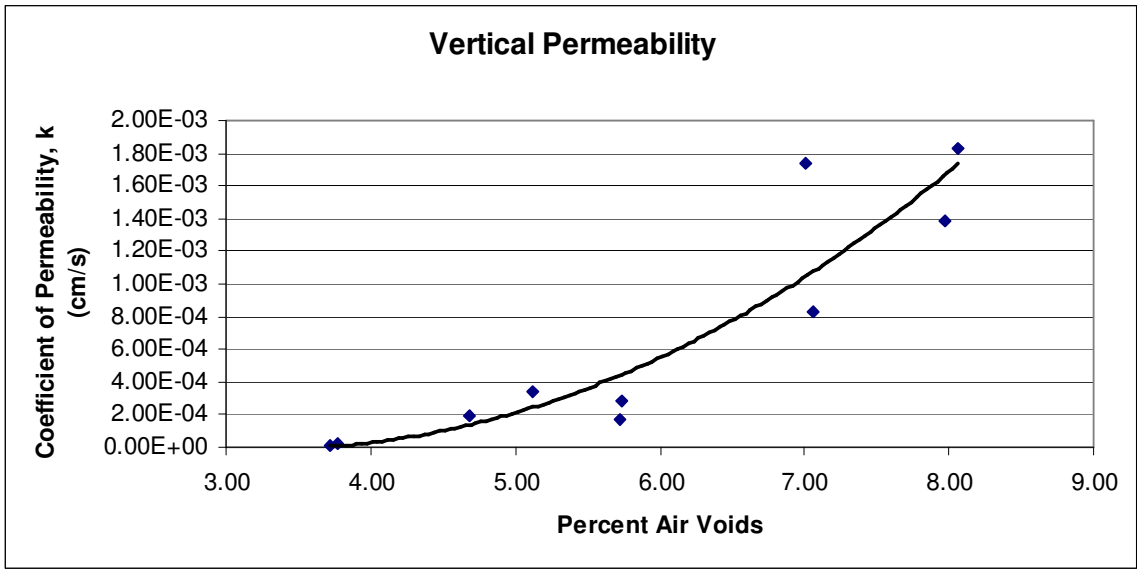

Figure 4.1 – Vertical Permeability Testing Results

4.2.2 Horizontal Permeability Testing – 1 Inch Core

The remaining laboratory sample was used to calculate the horizontal permeability of the specimen. A 1 inch diameter core was taken from the center of the sample, leaving a width of 2.5 inches from the inner to outer diameter of the specimen. There was a contact area of 3π in.^{2}. It was found that as the percent air voids increase, the horizontal permeability also increased. The results from the horizontal permeability testing can be found in Figure 4.2.

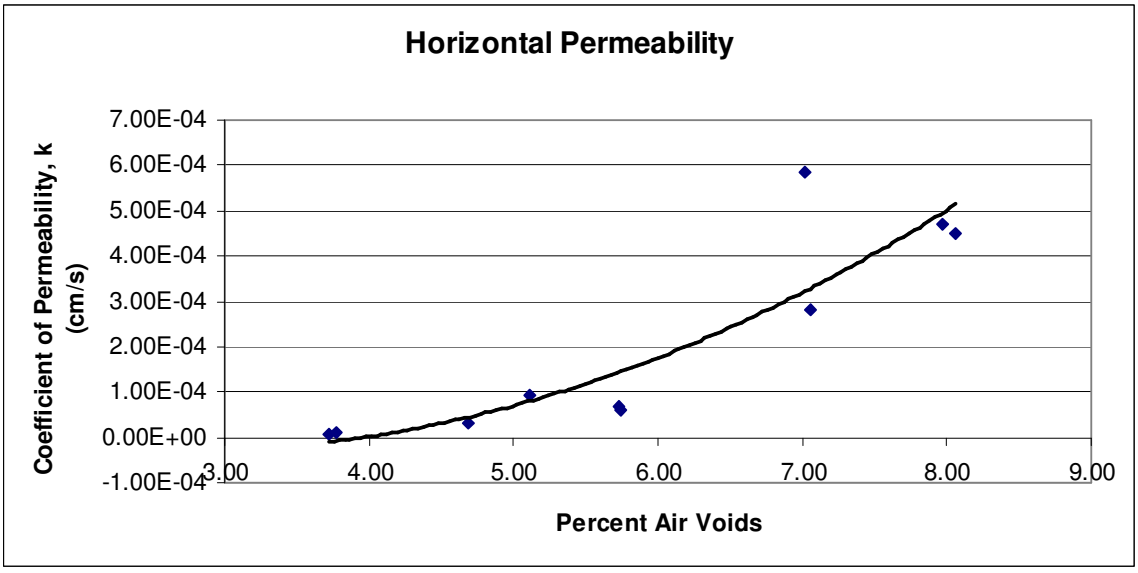

Figure 4.2 – Horizontal (1 Inch Core) Permeability Testing Results

4.2.3 Horizontal Permeability Testing – 2.5 Inch Core

Due to the large difference in specimen width and water-pavement contact area between the vertical permeability test and the one inch core horizontal permeability test, a second horizontal permeability test was conducted using a 2.5 inch core. This provided 7.5π in.^{2} inches water-pavement contact area and a specimen width of 1.75 inches. The results had the same increasing trend with air voids but the permeability values were larger than previous horizontal testing. This is due to the fact that HMA is a heterogeneous material and there is a non-uniform distribution of air voids. The results from the horizontal permeability testing can be found in Figure 4.3.

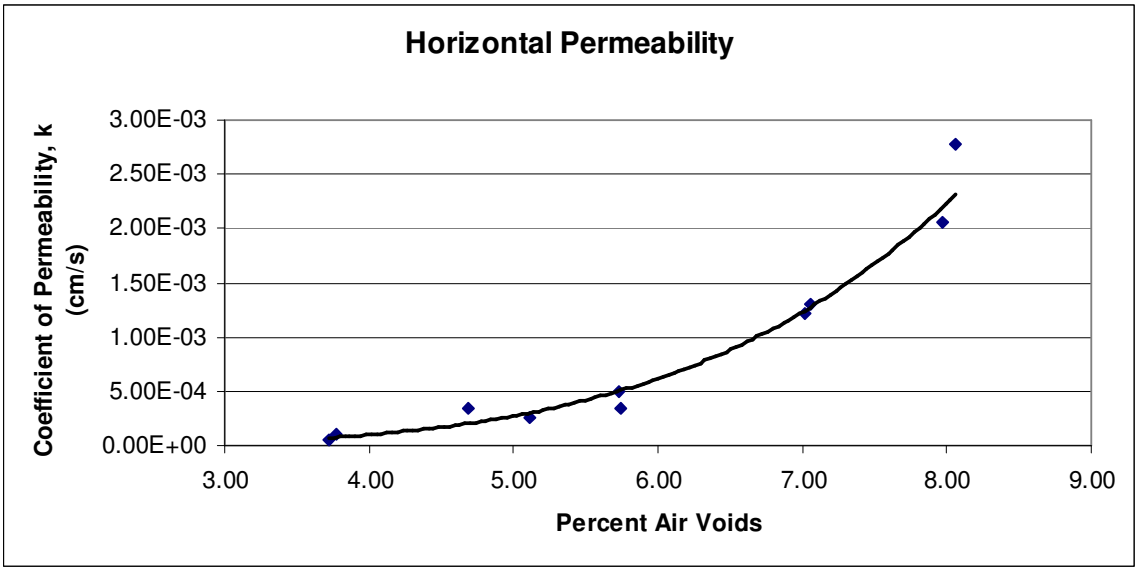

Figure 4.3 – Horizontal (2.5 Inch Core) Permeability Results

The horizontal permeability increased significantly when the thickness of the sample was decreased. This is due to both the variability in compaction within the sample and the connectivity throughout the length of the sample. The gyratory compaction method doesn't allow the exterior of the sample to be compacted as dense as the center of the sample. This is due to the friction of the aggregate with the mold, not allowing the aggregates to properly align. This friction is not present at the center of the sample, allowing for a denser compaction. The permeability will be larger in the exterior regions of the sample because of this higher air void content.

The overall connectivity of air voids decreases as the sample thickness increases. This was shown by compacting a sample to 5% air voids, and measuring the permeability at different thicknesses. The top and bottom of the sample was removed due to the higher variation in air void content at those locations. One of the removed sections was also tested for comparison. The results are shown in Table 4.1.

Table 4.1 – Variable Thickness Permeability Measurements

Thickness	Permeability (cm/s)
4"	0.00E+00
3"	2.08E-05
2"	9.52E-05
1"	2.31E-04
1"-Top	2.24E-03

4.2.4 Comparison of Vertical and Horizontal Permeability

The horizontal and vertical permeability values were compared to get an overall picture of the directional fluid flow characteristics within the HMA specimen. The ratio of horizontal permeability to vertical permeability was plotted against the percent air voids to identify any trends that may be present.

The values obtained from the samples with the 1 inch core showed that vertical permeability was larger than horizontal permeability. This information was contradictory to previous research that was described in section 2.6 which showed that horizontal permeability is generally 1 to 10 times larger than vertical. This difference was due to the larger difference in specimen width and water-pavement contact area. The horizontal specimens were 80% thicker and had 33% of the contact area of the vertical permeability test. Due to the fact that the air void structure is variable within the lab compacted sample, this led to less exposure to interconnected voids that travel from the inner core to the outer surface of the specimen. No significant trend is apparent in the data between the air voids and ratio of horizontal to vertical permeability. The results from the horizontal to vertical permeability testing can be found in Figure 4.4.

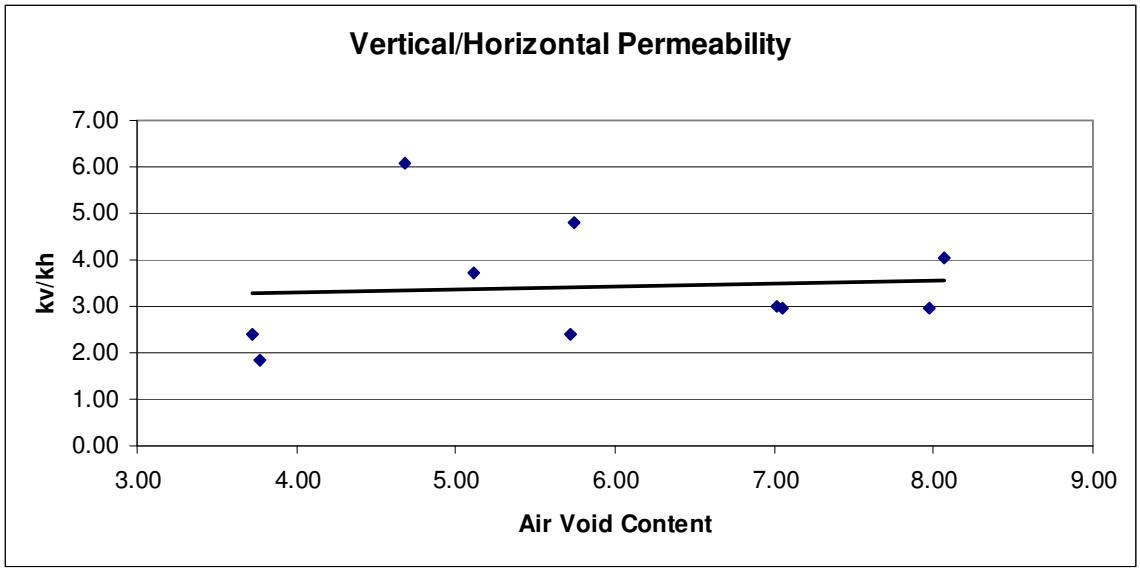

Figure 4.4 – Vertical/Horizontal Permeability Ratio 1 Inch Core

The values obtained from the horizontal testing using a 2.5" core from the HMA specimen yielded typical results as compared with previous research. The horizontal permeability was larger than the vertical permeability in all but two comparisons. The ratio of horizontal to vertical permeability ranged from 0.70 to 5.19. This test provided similar conditions to the vertical permeability test with a 17% larger thickness and 17% lower contact area. There is a decreasing trend apparent when comparing air voids to ratio of horizontal to vertical permeability. The data is from this comparison is presented in Figure 4.5.

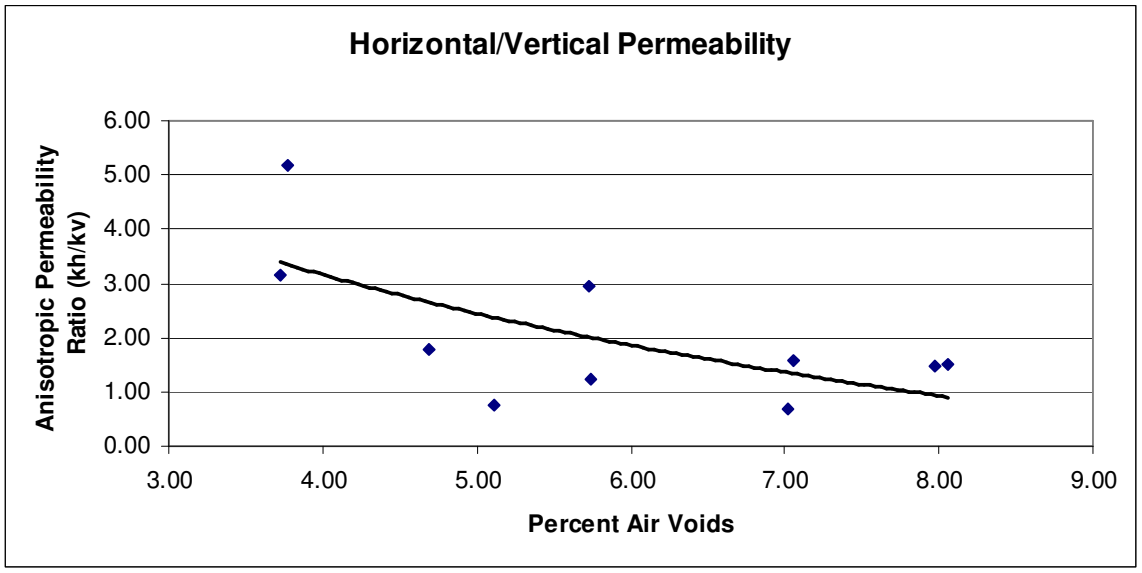

Figure 4.5 – Horizontal/Vertical Permeability Ratio 2.5 Inch Core

A stronger relationship was exhibited between air void content and percent air voids in the sample with the 2.5 inch core. This test using also yielded results that correspond with previous research. The thickness and water-pavement contact area are comparable in this scenario.

4.3 Field Permeability Tester Size

Data collected at the Smart Road in Blacksburg, VA was analyzed in the following section. Darcy's Law using the falling head method to compute permeability

was the technique used to determine the coefficient of permeability. The permeability values were then analyzed to find the effects of saturation on field testing. Also, the effects of water-pavement contact area were found using Fischer's Least Significant Difference method. This section will present the results from the field permeability testing along with the statistical analysis of the data.

4.3.1 Effect of Saturation

A total of 9 locations were tested for field permeability and 4 readings were taken at each location. The 4 readings were taken while the device was sealed at the location, without removing the device and resealing. This data provides information about how the level of saturation will affect the permeability readings. The first reading was taken when only the fluid allowed to enter the pavement while filling the device is present in the layer. The remaining readings are taken when the flow from the previous tests are within the layer. With each test, more fluid has entered the pavement, thus achieving a higher level of saturation. When the pavement was unsaturated, there was a suction force acting within the voids "pulling" the water through the voids. As the layer becomes saturated, this force is removed. It is expected that with a higher level of saturation, a lower coefficient of permeability is observed.

The data obtained from the field testing follows the expected pattern. As the layer became more saturated, the permeability coefficient became lower. The largest change permeability was generally between the first and second readings. This was when the pavement was almost dry and a significant amount of fluid has entered the pavement layer. There was generally a smaller change in permeability between the second to fourth tests. This would suggest that an acceptable level of saturation has been met to give consistent results. The data for each location is given below in Figures 4.6 to 4.14.

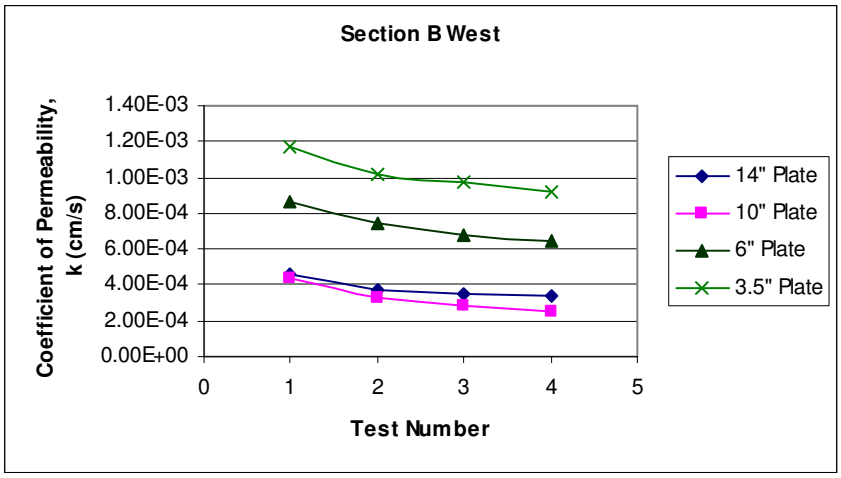

Figure 4.6 – Coefficient of Permeability Section B, West

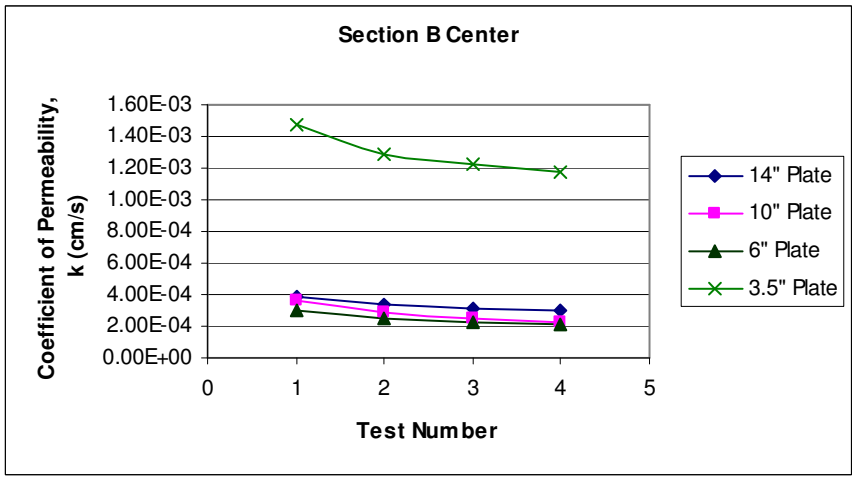

Figure 4.7 – Coefficient of Permeability Section B, Center

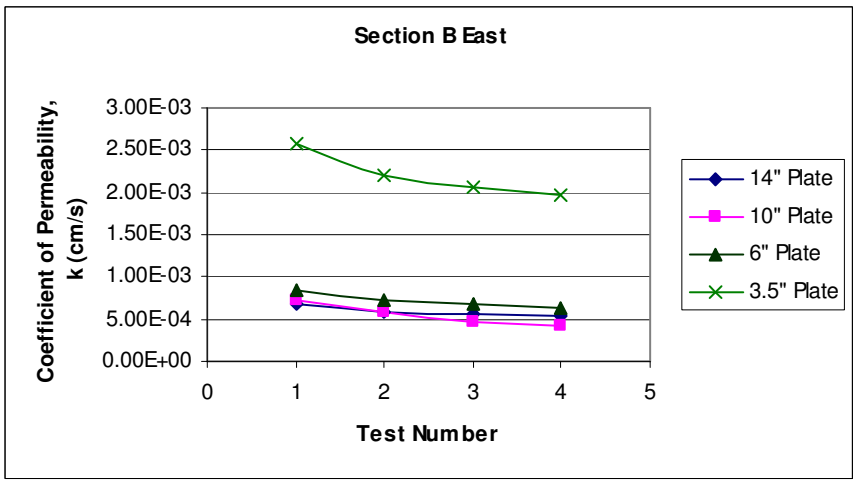

Figure 4.8 – Coefficient of Permeability Section B, East

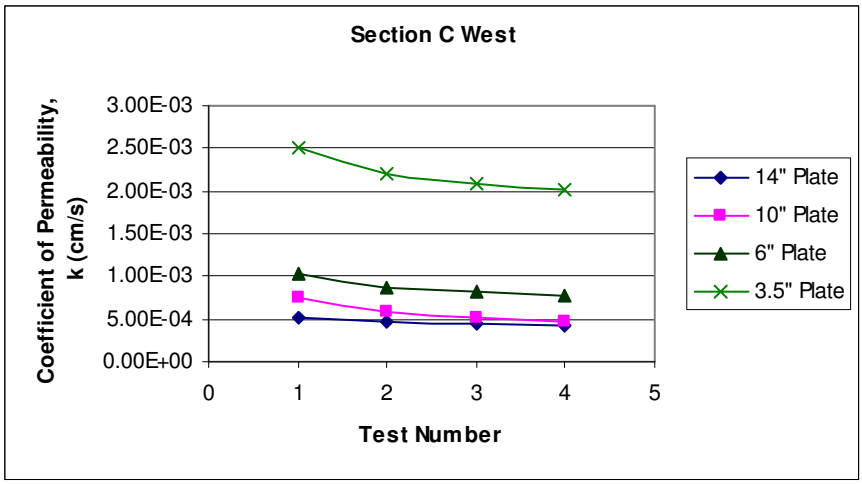

Figure 4.9 – Coefficient of Permeability Section C, West

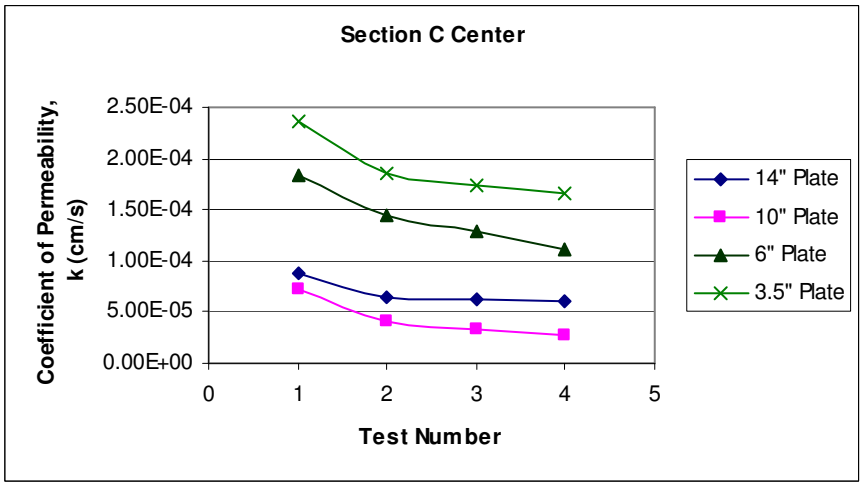

Figure 4.10 – Coefficient of Permeability Section C, Center

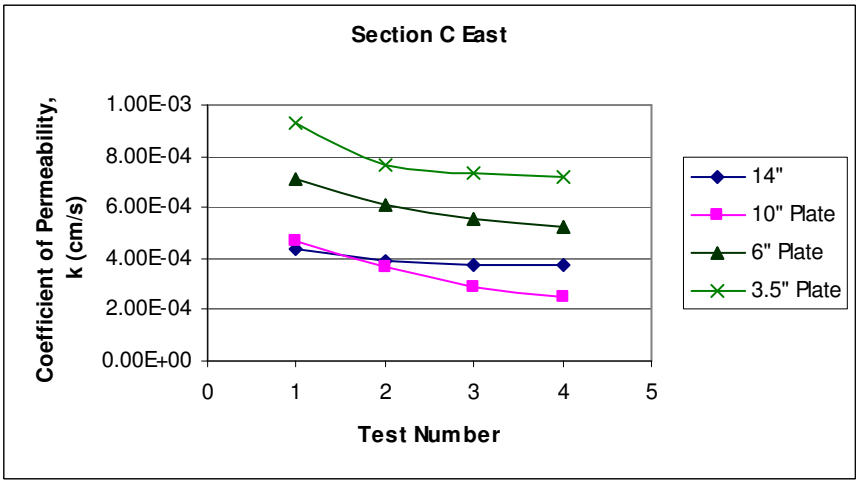

Figure 4.11 – Coefficient of Permeability Section C, East

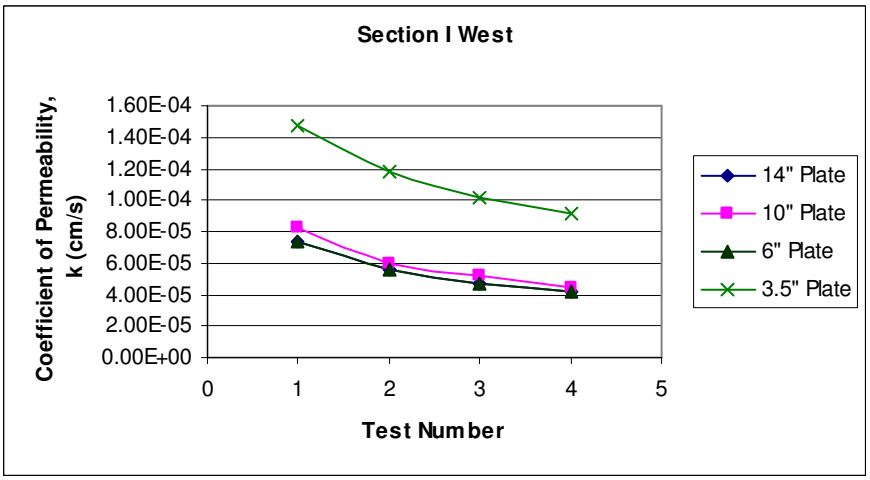

Figure 4.12 – Coefficient of Permeability Section I, West

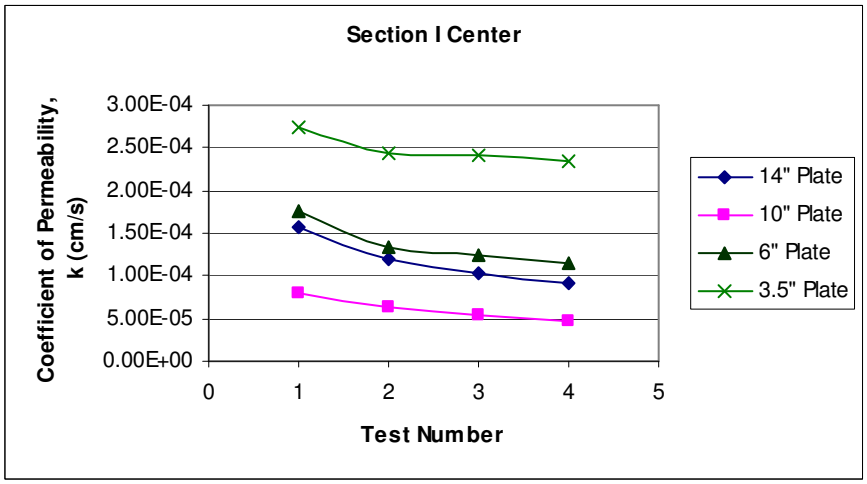

Figure 4.13 – Coefficient of Permeability Section I, Center

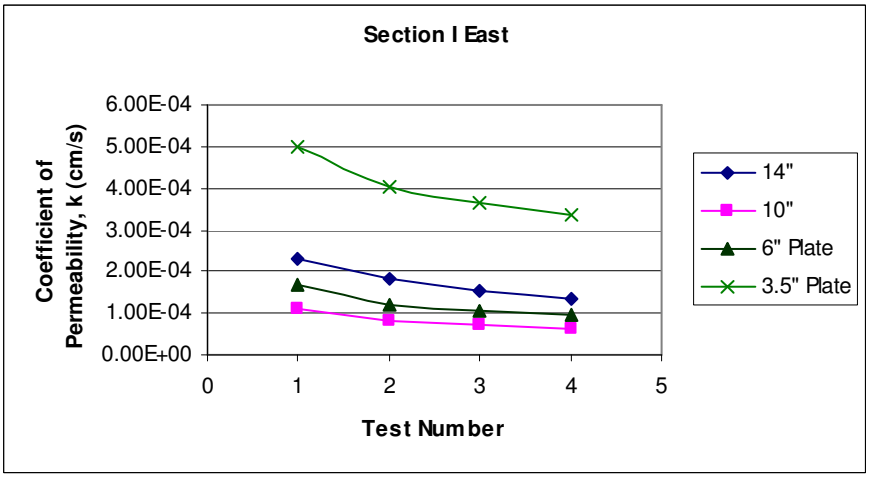

Figure 4.14 – Coefficient of Permeability Section I, East

The data shows that the effect of saturation on the field test was fairly small on overall permeability after the first test. Between the first and fourth test, the average ratio of permeability values is 1.58. This was somewhat significant, but this was the most extreme case when the first value was taken when the pavement was completely dry. Between the second and fourth tests, the average permeability ratio was 1.24. For this type of data, this ratio was small. The data values are small in magnitude, and there was the potential for human error in reading the head levels. The average ratio between the third and fourth tests was 1.10. This shows a very small difference between readings. In order to establish an average value of permeability, the second through fourth readings could be used for an accurate estimation.

4.3.2 Effect of Water-Pavement Contact Area

An average value of permeability was found for each location and the corresponding water-pavement contact area was established by using the second through fourth permeability measurements. The general trend shows that the 3.5 inch diameter contact area yields the highest permeability measurements. This was due to the greater influence of horizontal permeability which was generally larger than the vertical permeability in HMA. The horizontal discharge area was computed by multiplying the circumference by the layer thickness. The vertical discharge section was calculated by finding the area of the contact area circle. This case has a 1.7 times larger exposure to the horizontal discharge section than the vertical discharge section. The relationship of horizontal and vertical discharge area for a 1.5 inch layer thickness is shown in Figure 4.15.

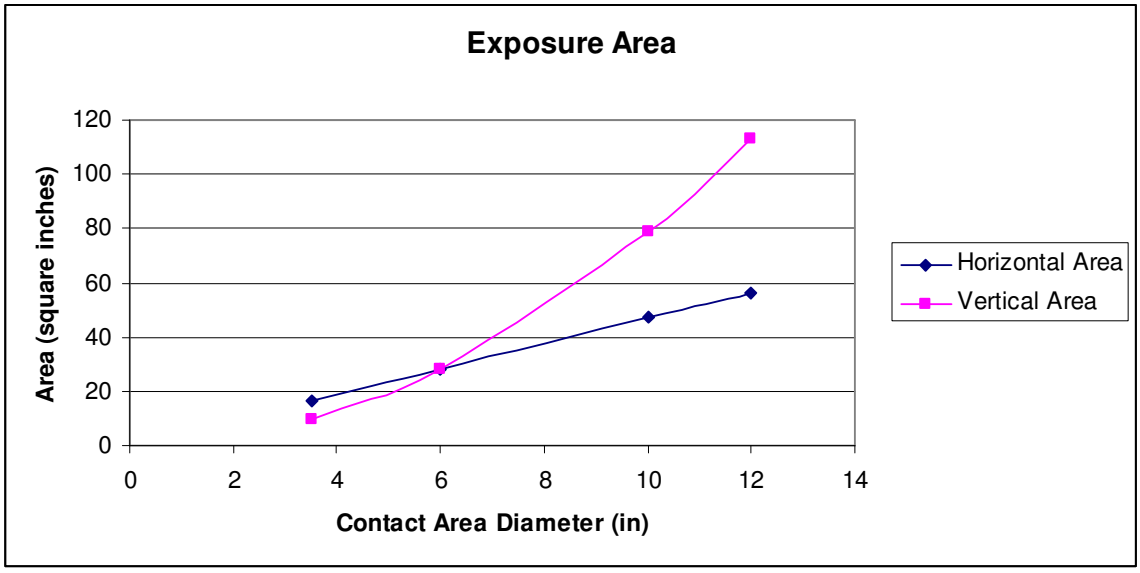

Figure 4.15 – Vertical and Horizontal Exposure Area for Contact Area Diameter

The general trend is Section B shows that permeability with the 3.5 inch contact area was the highest value, then the values somewhat level off as the contact area increases. This is due to the influence of the vertical discharge section becoming larger than the horizontal discharge section. The average permeability values for section B can be found in Figure 4.16.

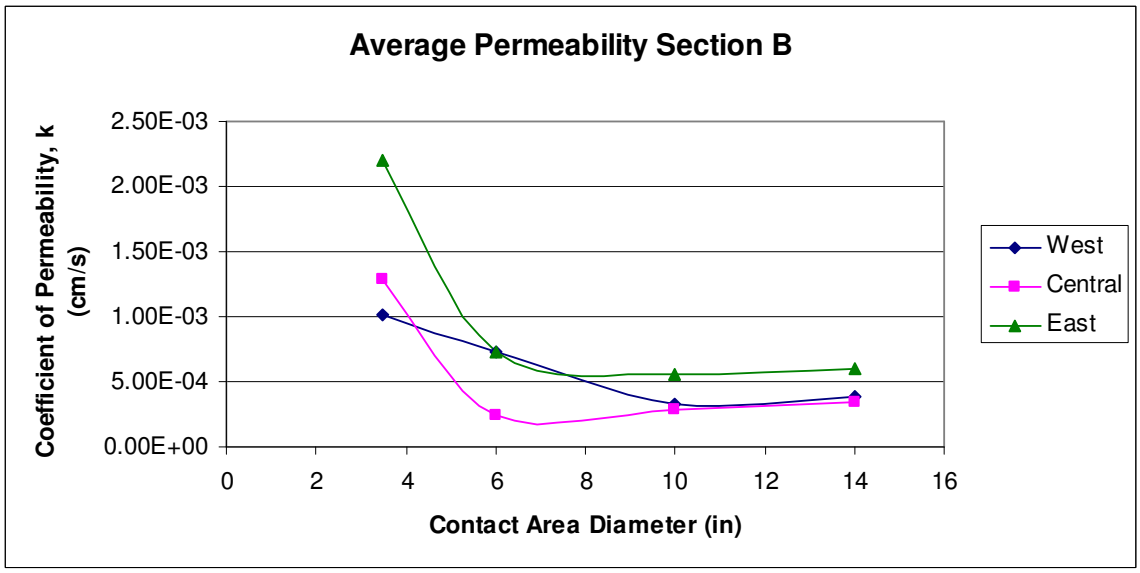

Figure 4.16 – Average Permeability, Section B

The data from Section C is somewhat similar to the data in Section B. The 3.5 inch contact area was the largest value for each location. The West section has a more dramatic difference between the 3.5 and 6 inch contact areas. The Central and East section have a flatter curve, showing that there isn't as large of a difference between the contact areas. The average permeability values for section C can be found in Figure 4.17.

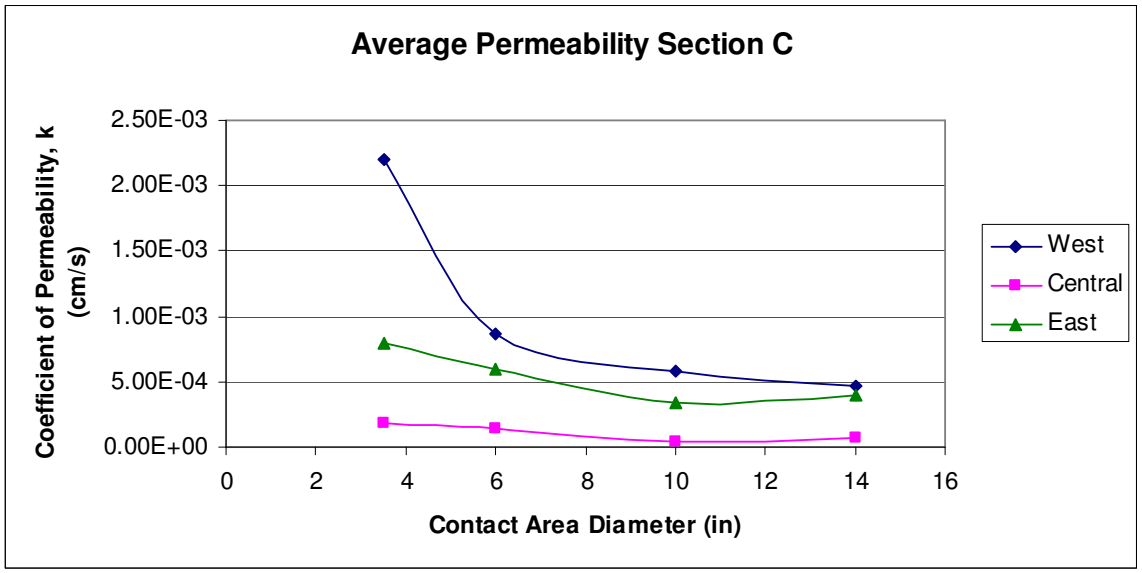

Figure 4.17 – Average Permeability, Section C

The data in Section I show more variability than the previous sections. In the East and Central Sections, the 3.5 inch contact area has similar results to previous sections. Although for these locations, the permeability increased when moving from 10 to 14 inch contact areas. The West Section shows a lower permeability value for the 3.5 inch contact area when compared to the 6 inch contact area. The average permeability values for section I can be found in Figure 4.18.

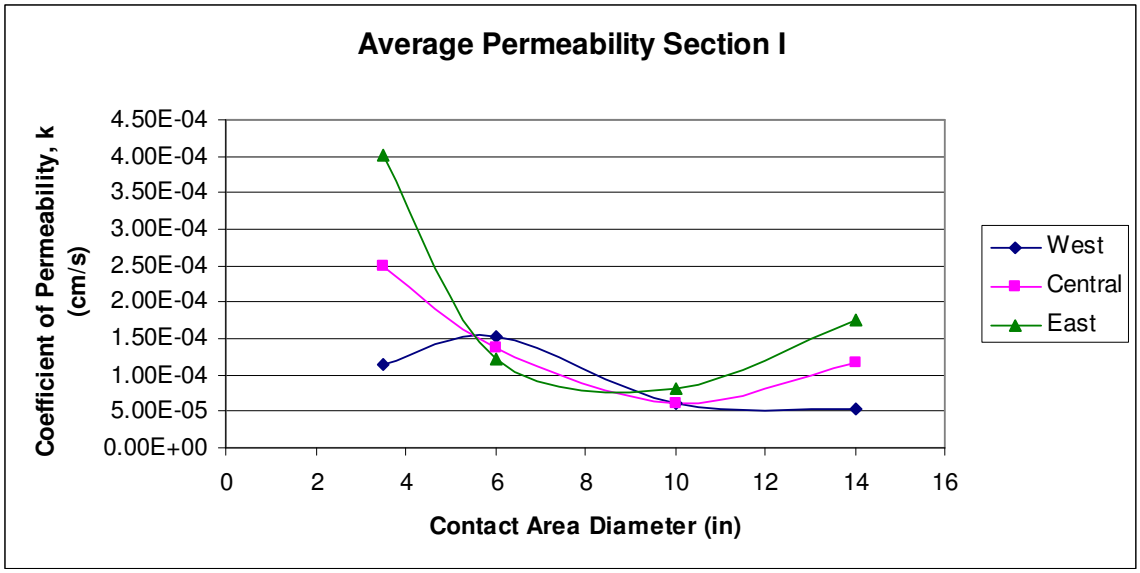

Figure 4.18 – Average Permeability, Section I

The variability within the sections can be described by the varying condition of the pavement and the testing location. The pavement sections that were used for testing have been in service for multiple years. Distresses such as bottom up cracking could have been present at the testing locations, thus increasing permeability by exposing larger voids. Also, the testing locations were very similar but not exactly the same. Roadside markers were used to identify the testing location because no marking could be placed within the lane. Since the tests were run in the center of the lane, human error in placement of the device can affect the results.

4.3.2.1 Fischer's LSD by Section

Pairwise comparisons were made between each of the different contact areas used for the tests at the given locations. The data was compared with values calculated in the entire section (West, Center, East). The results of the Minitab output show that 44 of the 54 comparisons (81%) were significantly different. The individual comparisons are shown in table 4.2. The comparisons are summarized in Tables 4.3 and 4.4. The 3.5 inch plate was shown to be significantly different than the other tests except with the 6 inch contact area in Section C, Center location. When comparing the 6 inch plate to the 10 and

14 in plates, 14 of the 18 comparisons (88%) were shown to be significantly different. This would suggest that there is still significant variation between these two contact areas. Finally, comparing the 10 in plate to the 14 in plate, 4 of the 9 comparisons (44%) were shown to be significantly different from each other. This suggests that the data obtained from the 10 in plate is somewhat comparable to the data from the 14 in plate.

Table 4.2 – Fischer's Pairwise Comparisons, Section Data

BW	**3.5**	**6**	**10**	**CW**	**3.5**	**6**	**10**	**IW**	**3.5**	**6**	**10**
6	Y			**6**	Y			**6**	Y		
10	Y	Y		**10**	Y	Y		**10**	Y	Y	
14	Y	Y	N	**14**	Y	Y	Y	**14**	Y	Y	N
BC	**3.5**	**6**	**10**	**CC**	**3.5**	**6**	**10**	**IC**	**3.5**	**6**	**10**
6	Y			**6**	N			**6**	Y		
10	Y	N		**10**	Y	Y		**10**	Y	Y	
14	Y	N	N	**14**	Y	N	N	**14**	Y	N	Y
BE	**3.5**	**6**	**10**	**CE**	**3.5**	**6**	**10**	**IE**	**3.5**	**6**	**10**
6	Y			**6**	Y			**6**	Y		
10	Y	Y		**10**	Y	Y		**10**	Y	Y	
14	Y	Y	N	**14**	Y	Y	Y	**14**	Y	Y	Y

*Y - Significantly Different N - Not Significantly Different

Table 4.3 – Number (Percentage) of Significantly Different Comparisons by Section, Section Data

B	**3.5**	**6**	**10**	**C**	**3.5**	**6**	**10**	**I**	**3.5**	**6**	**10**
6	3 (1)			**6**	2 (.67)			**6**	3 (1)		
10	3 (1)	2 (.67)		**10**	3 (1)	3 (1)		**10**	3 (1)	3 (1)	
14	3 (1)	2 (.67)	0 (0)	**14**	3 (1)	2 (.67)	2 (.67)	**14**	3 (1)	2 (.67)	2 (.67)

Table 4.4 – Total Number (Percentage) of Significantly Different Comparisons, Section Data

	3.5	**6**	**10**
6	8 (.89)		
10	9 (1)	8 (.89)	
14	9 (1)	6 (.67)	4 (.44)

4.3.2.2 *Fischer's LSD by Individual Location*

The data was analyzed individually by location by performing pairwise comparisons of the permeability values. The results of the Minitab output show that 44 of the 54 comparisons (81%) were significantly different. The individual comparisons are

shown in table 4.5. The comparisons are summarized in Tables 4.6 and 4.7. The 3.5 inch plate was shown to always be significantly different than the other tests. When comparing the 6 inch plate to the 10 and 14 in plates, 14 of the 18 comparisons (78%) were shown to be significantly different. This would suggest that there is still significant variation between these two contact areas. Finally, comparing the 10 in plate to the 14 in plate, 3 of the 9 comparisons (33%) were shown to be significantly different from each other. This suggests that the data obtained from the 10 in plate is comparable to the data from the 14 in plate.

Table 4.5 –Fisher's Pairwise Comparisons, Location Data

BW	**3.5**	**6**	**10**	**CW**	**3.5**	**6**	**10**	**IW**	**3.5**	**6**	**10**
6	Y			**6**	Y			**6**	Y		
10	Y	Y		**10**	Y	Y		**10**	Y	Y	
14	Y	Y	N	**14**	Y	Y	N	**14**	Y	Y	N
BC	**3.5**	**6**	**10**	**CC**	**3.5**	**6**	**10**	**IC**	**3.5**	**6**	**10**
6	Y			**6**	Y			**6**	Y		
10	Y	N		**10**	Y	Y		**10**	Y	Y	
14	Y	Y	N	**14**	Y	Y	N	**14**	Y	Y	Y
BE	**3.5**	**6**	**10**	**CE**	**3.5**	**6**	**10**	**IE**	**3.5**	**6**	**10**
6	Y			**6**	Y			**6**	Y		
10	Y	Y		**10**	Y	Y		**10**	Y	N	
14	Y	N	N	**14**	Y	Y	Y	**14**	Y	Y	Y

* Y – Significantly Different N – Not Significantly Different

Table 4.6 – Number (Percentage) of Significantly Different Comparisons by Section, Location Data

B	**3.5**	**6**	**10**	**C**	**3.5**	**6**	**10**	**I**	**3.5**	**6**	**10**
6	3 (1)			**6**	3 (1)			**6**	3 (1)		
10	3 (1)	2 (.67)		**10**	3 (1)	3 (1)		**10**	3 (1)	2 (.67)	
14	3 (1)	2 (.67)	0 (0)	**14**	3 (1)	3 (1)	1 (.33)	**14**	3 (1)	2 (.67)	2 (.67)

Table 4.7 – Total Number (Percentage) of Significantly Different Comparisons, Location Data

	3.5	**6**	**10**
6	9 (1)		
10	9 (1)	7 (.78)	
14	9 (1)	7 (.78)	3 (.33)

4.3.2.3 Combined Analysis

When the data from the two statistical tests are combined, a general trend can be found. With increasing contact area diameter, the significance on the permeability values decreases. The comparison with the 3.5 inch contact area was significantly different 94% of the scenarios. Comparisons between the 6 inch with both the 10 and 14 inch contact areas show a decreasing amount of significantly different values with 83% and 72% respectively. The comparison between the 10 and 14 inch contact areas were significantly different 39% of the time.

Table 4.8 – Combined Number (Percentage) of Significantly Different Comparisons by Section

B	**3.5**	**6**	**10**	**C**	**3.5**	**6**	**10**	**I**	**3.5**	**6**	**10**
6	6 (1)			**6**	5 (.83)			**6**	6 (1)		
10	6 (1)	4 (.67)		**10**	6 (1)	6 (1)		**10**	6 (1)	5 (.83)	
14	6 (1)	4 (.67)	0 (0)	**14**	6 (1)	5 (.83)	3 (.5)	**14**	6 (1)	4 (.67)	4 (.67)

Table 4.9 – Combined Total Number (Percentage) of Significantly Different Comparisons

	3.5	**6**	**10**
6	17 (.94)		
10	18 (1)	15 (.83)	
14	18 (1)	13 (.72)	7 (.39)

4.4 Finite Element Analysis

A finite element analysis was conducted to simulate field permeability testing. Phase^2 6.0 developed by Rocscience was the software package used for this analysis. This program is an elasto-plastic stress analysis program that includes groundwater seepage analysis. A pavement layer with the same thickness as the layer tested in the field was modeled with a permeable lower boundary and an impermeable lower boundary. A parametric study was done using 3 values for total permeability, 3 values for the ratio of horizontal to vertical permeability, and 4 applied pressure length that correspond to the contact areas used in field testing.

4.4.1 Permeable Lower Boundary

The permeable lower boundary represents a HMA surface layer that allows fluid flow to the lower layers. A discharge line from the top to the bottom of the layer located at the edge of the applied pressure section measures the horizontal flow that exits the specimens cross sectional area. The vertical flow is measured by a discharge line at the bottom of the layer directly under the applied pressure head section. The flows were measured to determine the influence of the horizontal flow during field permeability testing. The ratio of vertical flow to horizontal flow was used to determine this influence. The results of the simulations can be found in Figures 4.19 to 4.21.

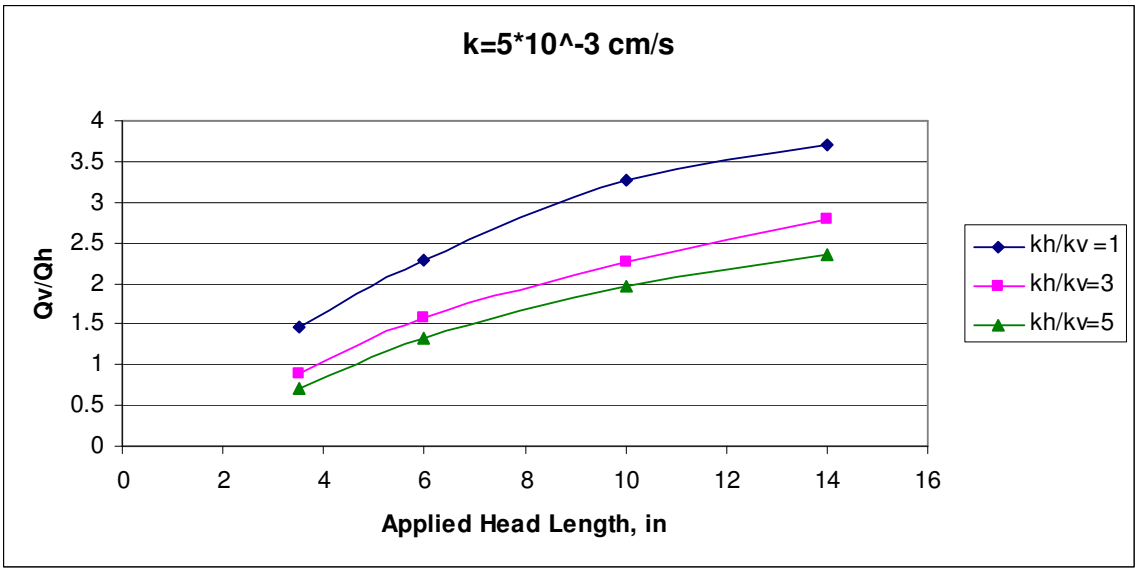

Figure 4.19 – Ratio of Horizontal to Vertical Flow (Permeable), k = $5x10^{-3}$ cm/s

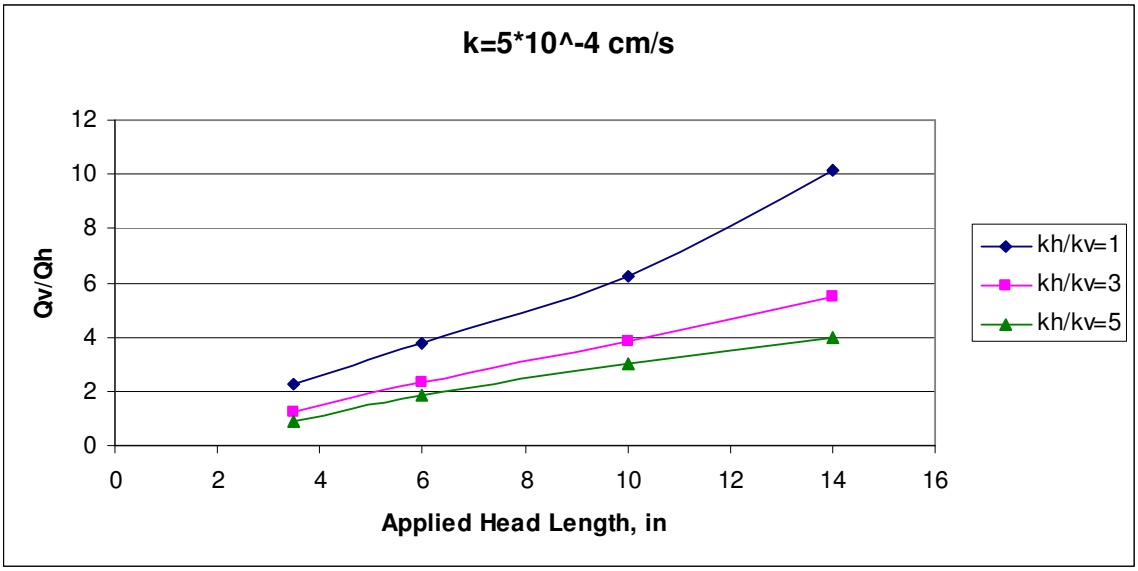

Figure 4.20 – Ratio of Horizontal to Vertical Flow (Permeable), k = $5x10^{-4}$ cm/s

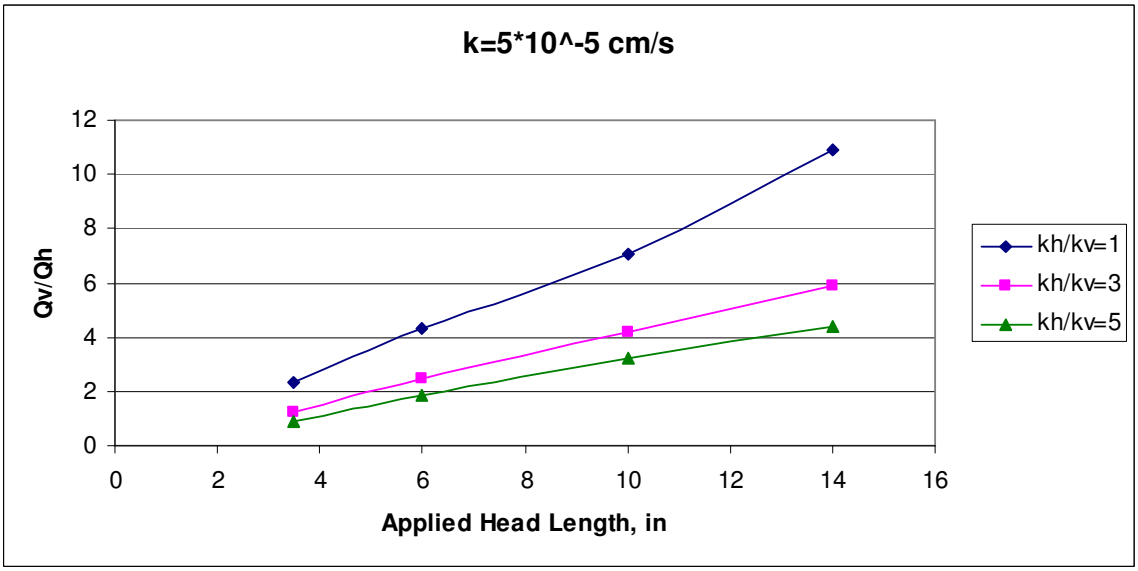

Figure 4.21 – Ratio of Horizontal to Vertical Flow (Permeable), k = $5x10^{-5}$ cm/s

The data shows that the vertical flow was larger than the horizontal flow. This was because the applied pressure was in the vertical direction and the length of the discharge section is larger in the area of vertical flow. The significance of the horizontal flow decreases as the applied pressure head length increases. With a smaller applied head length, the horizontal flow section was similar in size to the vertical flow section. This

creates a more even distribution of flow between the horizontal and vertical flows. As the vertical applied head length increases, the majority of the flow moves vertically through the layer before it reaches the area outside of the specimen (head length). This point was well visualized by analyzing flow lines within the structure. Figure 4.22 to 4.24 show the flow lines through the surface layer.

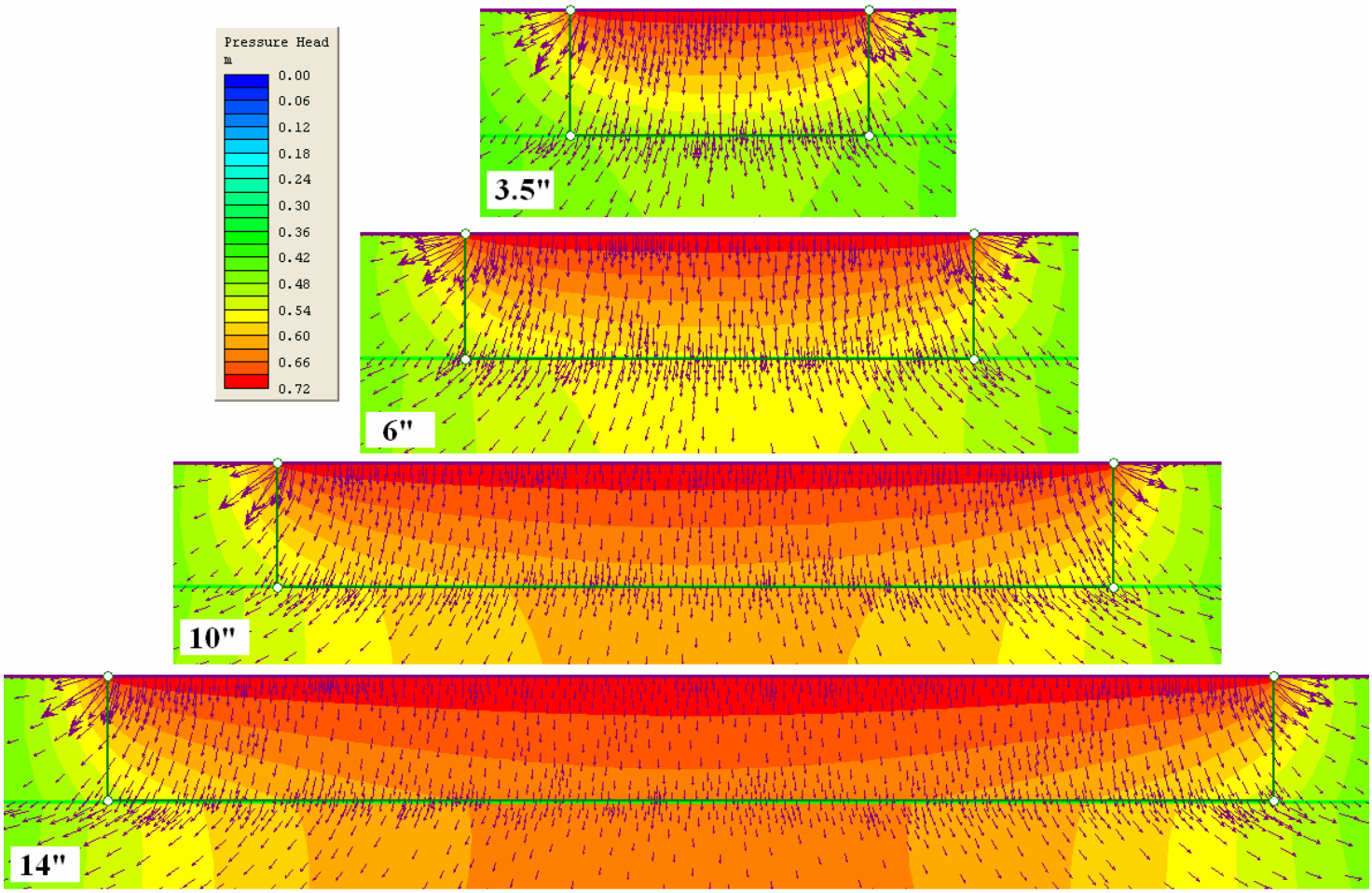

Figure 4.22 – Flow Lines/Pressure Head (Permeable) for $k_h/k_v = 1$, $k = 5x10^{-3}$ cm/s

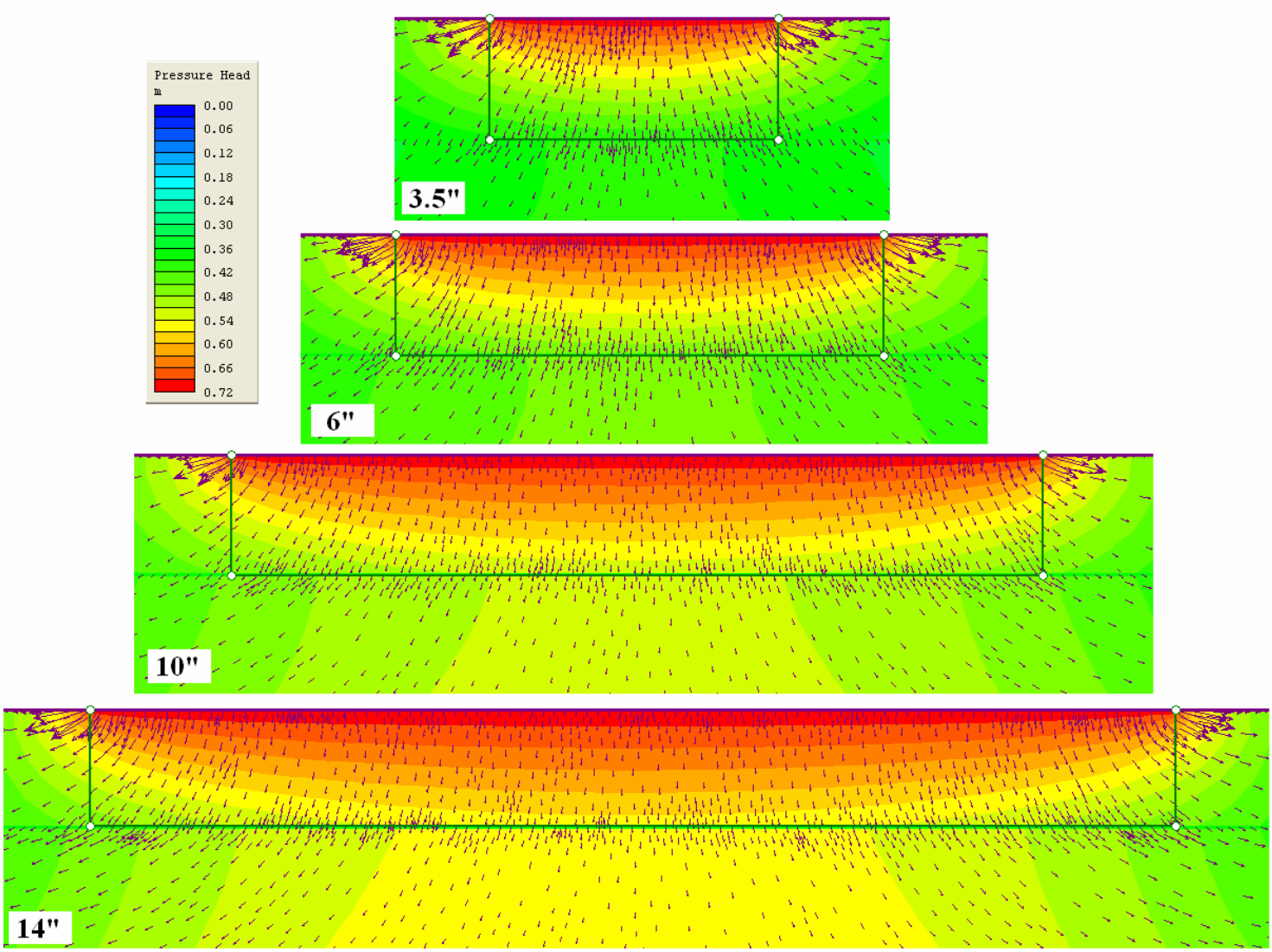

Figure 4.23 – Flow Lines/Pressure Head (Permeable) for $k_h/k_v = 3$, $k = 5x10^{-3}$ cm/s

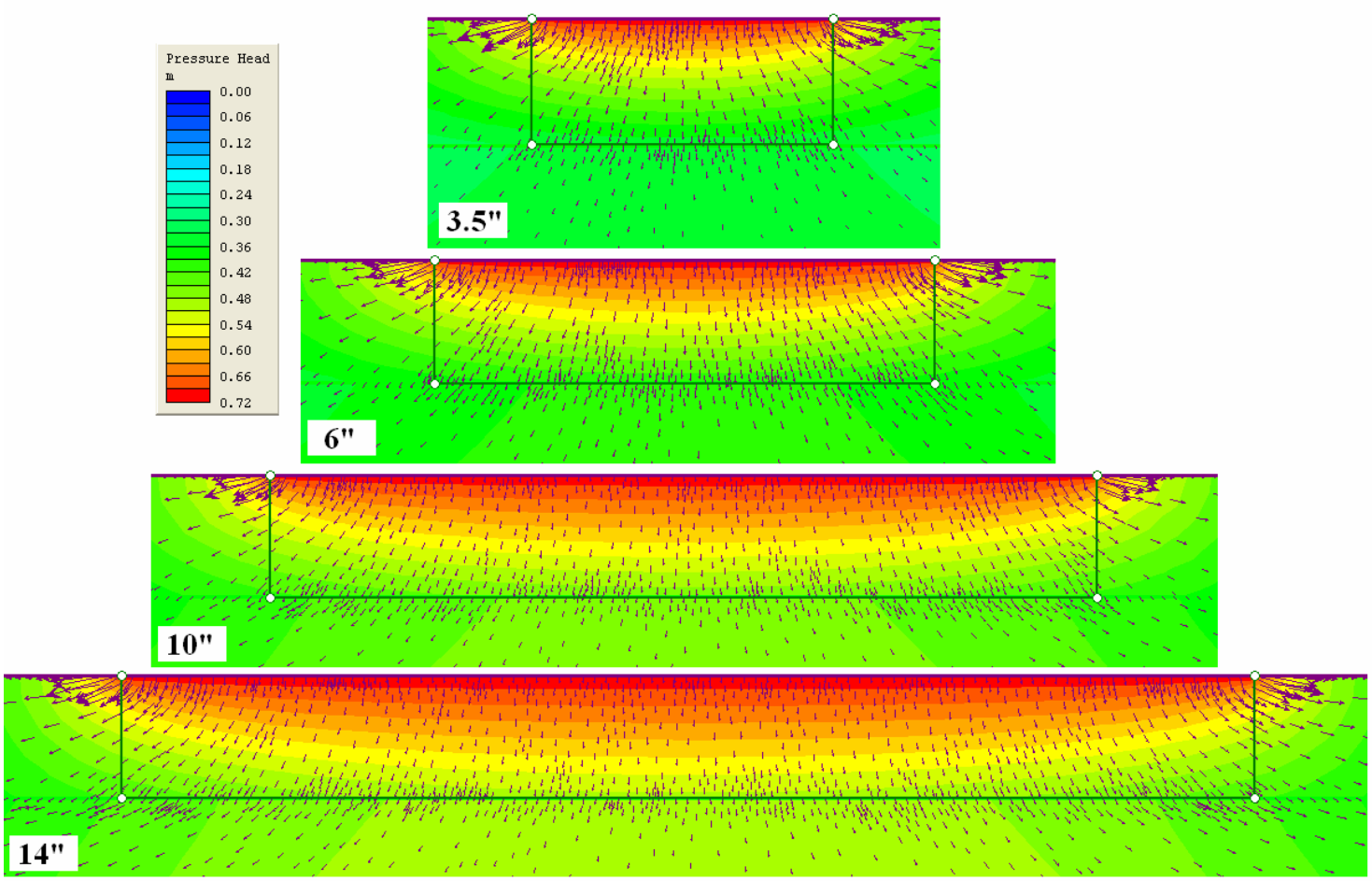

Figure 4.24 – Flow Lines/Pressure Head (Permeable) for $k_h/k_v = 5$, $k = 5x10^{-3}$ cm/s

This data correlates well with the data obtained from the field permeameter. The permeability was largest with the 3.5 inch diameter contact area. Since the influence of horizontal permeability is greatest with this area, and the horizontal permeability was generally larger than vertical permeability, this would yield the largest permeability values. As the contact area increased, the influence of horizontal permeability decreased. Since the vertical permeability was lower than the horizontal, the permeability values calculated were lower.

As the ratio of horizontal to vertical permeability increases, the effect of the horizontal flow rate also increases. With a greater opportunity to flow in the horizontal direction, the flow will increase and distribute more fluid outside of the specimen area.

Due to the increased flow due to the added flow in the horizontal direction, the measured permeability using the field testing method will be larger when the horizontal

flow has a large influence. As the vertical permeability becomes more influential, the measured permeability will be closer to the actual permeability of the material. The total flow out of the sample area was taken from the finite element model and entered into Darcy's Law constant head method to determine the permeability that would be found from the field test. As the applied pressure head length increased, the Darcy's law permeability approached the actual vertical permeability of the material. The Darcy's law permeability was larger than the actual permeability in ever case except the 14 inch applied pressure length with the horizontal permeability equal to the vertical permeability for an overall permeability of $5x10^{-3}$ cm/s. Using a 3.5 inch contact area will yield much higher vertical permeability readings compared to the actual vertical permeability of the material. These results correlate well with the results from field permeability testing. The comparison of the Darcy's Law vertical permeability (kd) to actual vertical permeability (kv) can be found in Figures 4.25 to 4.28.

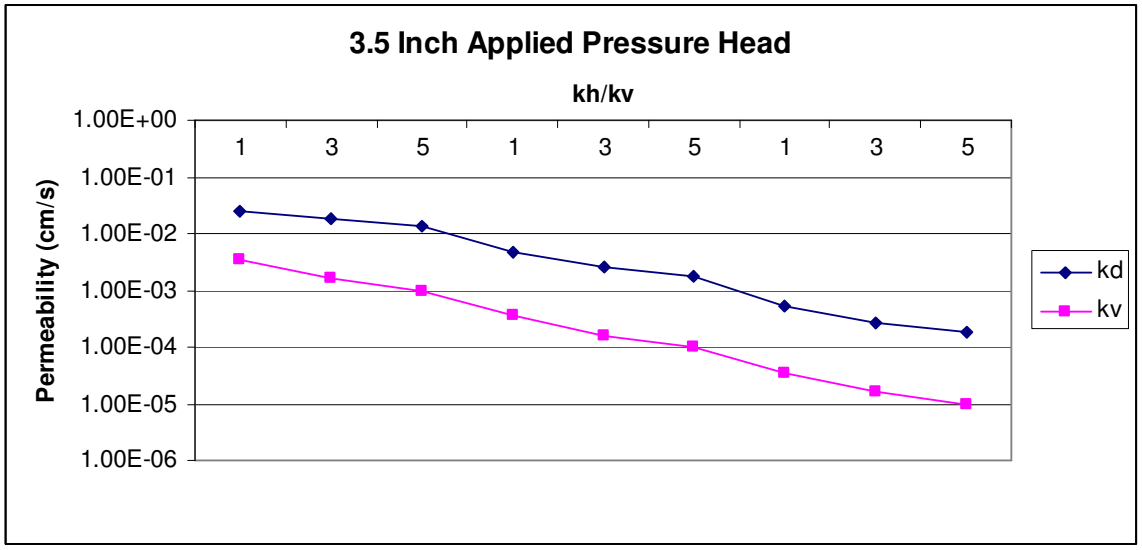

Figure 4.25 – Comparison of Darcy's and Actual Vertical Permeability, 3.5 Inch Applied Pressure Head, Permeable Lower Boundary

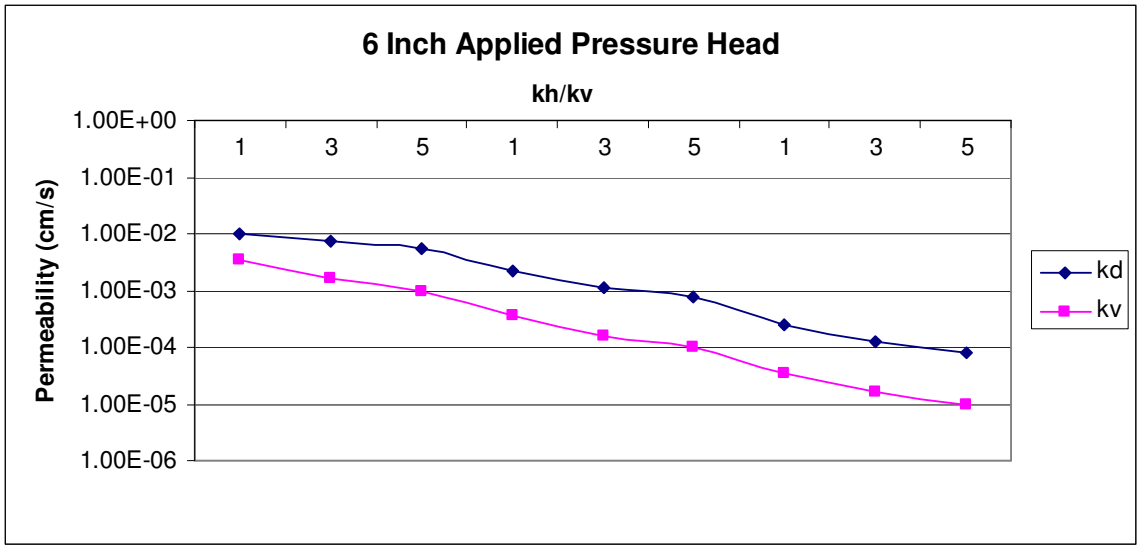

Figure 4.26 – Comparison of Darcy's and Actual Vertical Permeability, 6 Inch Applied Pressure Head, Permeable Lower Boundary

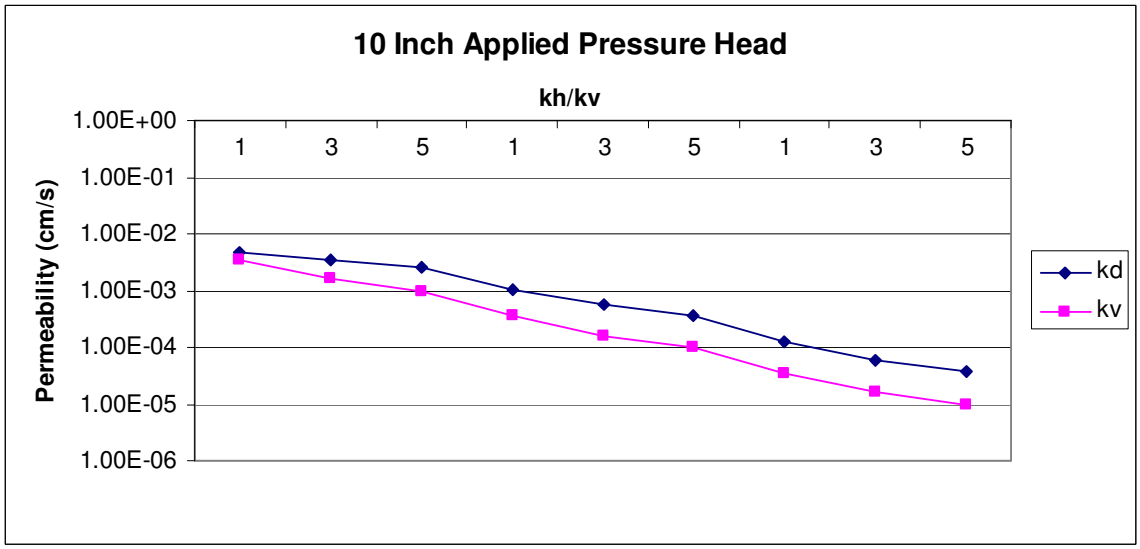

Figure 4.27 – Comparison of Darcy's and Actual Vertical Permeability, 10 Inch Applied Pressure Head, Permeable Lower Boundary

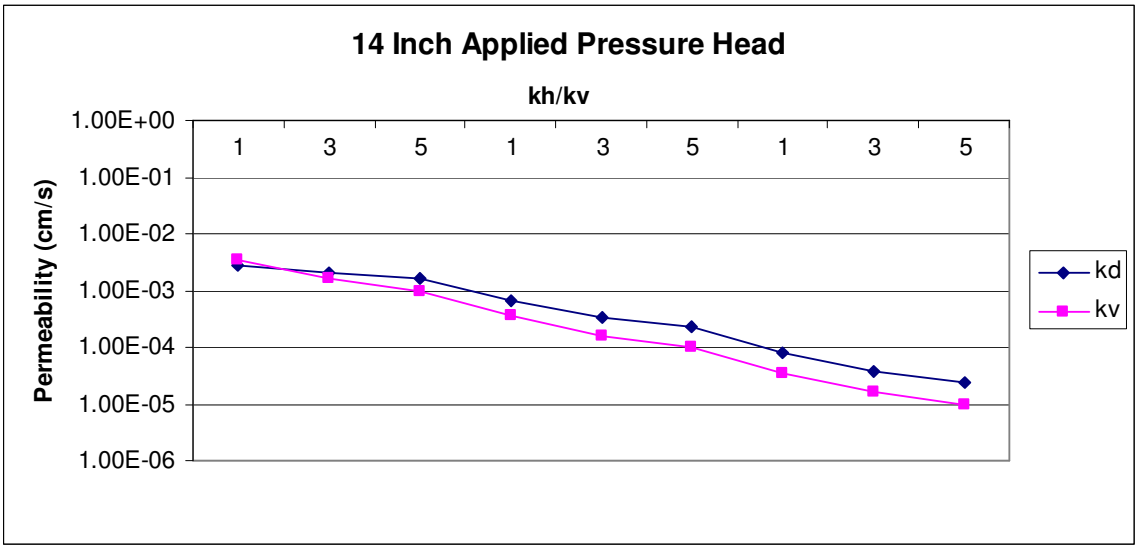

Figure 4.28 – Comparison of Darcy's and Actual Vertical Permeability, 14 Inch Applied Pressure Head, Permeable Lower Boundary

4.4.2 Impermeable Lower Boundary

The impermeable lower boundary condition was used to simulate a evenly applied tack coat that was used to bond the base layer to the surface layer. Under these circumstances, there would be no flow from the bottom of the surface layer. The only flow would be within the surface layer and out of the surface. This situation would most likely be encountered during newly placed pavements when the tack coat was freshly applied. The tack coat would deteriorate over time creating permeable sections between layers. The vertical and horizontal flow rates were observed at the center of the surface layer. This was necessary due to the fact that there is no vertical flow at the lower boundary of the layer. The results from this analysis are given in Figures 4.29 to 4.31.

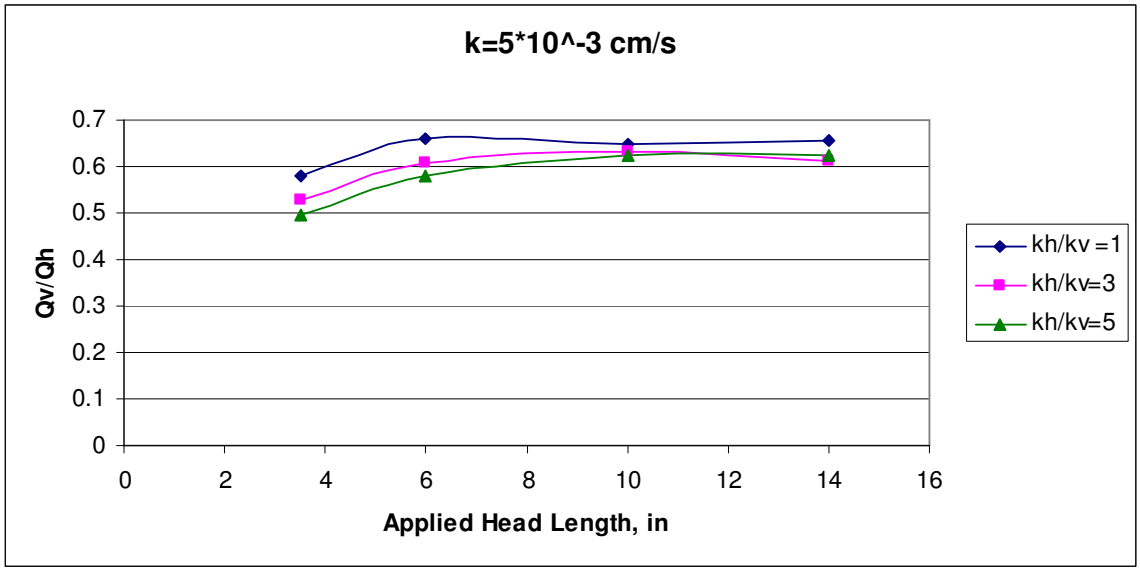

Figure 4.29 – Ratio of Horizontal to Vertical Flow (Impermeable), k = $5x10^{-3}$ cm/s

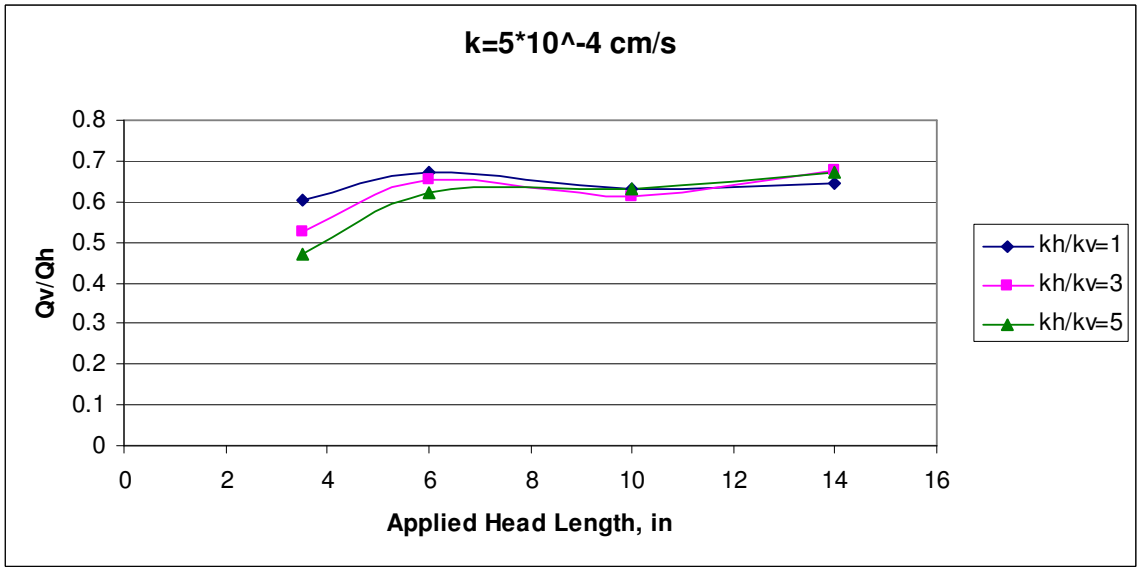

Figure 4.30 – Ratio of Horizontal to Vertical Flow (Impermeable), k = $5x10^{-4}$ cm/s

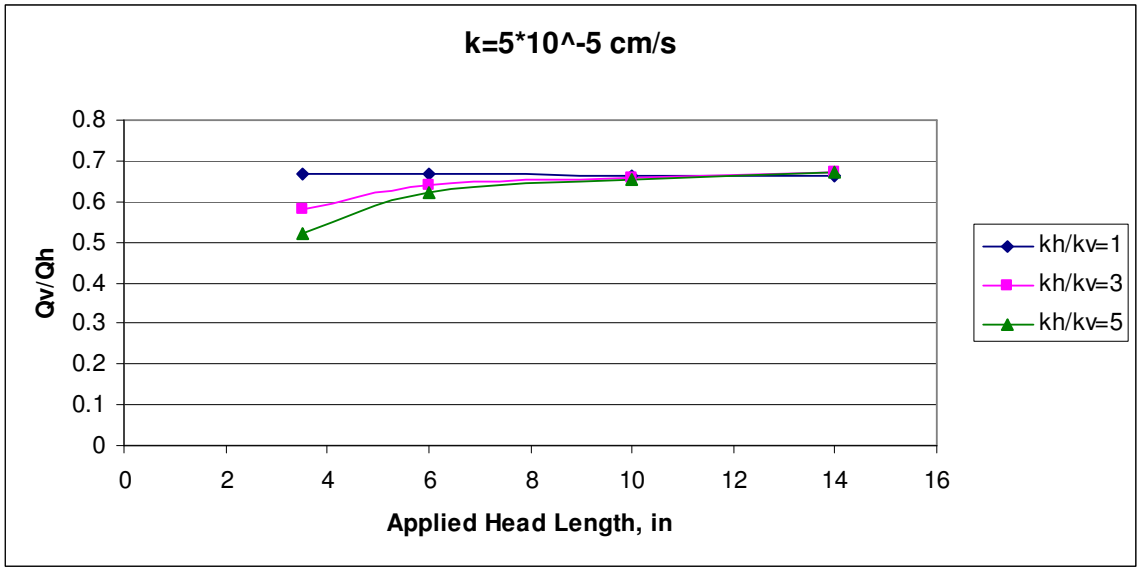

Figure 4.31 – Ratio of Horizontal to Vertical Flow (Impermeable), k = $5x10^{-5}$ cm/s

The data shows that the significance of the horizontal flow decreases as the applied pressure head length increases from 3.5 inches to 6 inches. As the length increases from 6 to 10 and 14 inches, the ratio of vertical to horizontal flow is somewhat variable. This is due to the inability of the layer to drain from the lower boundary. The only drainage is at the surface outside of the testing device. The flow lines for these scenarios are given in Figures 4.32 to 4.34.

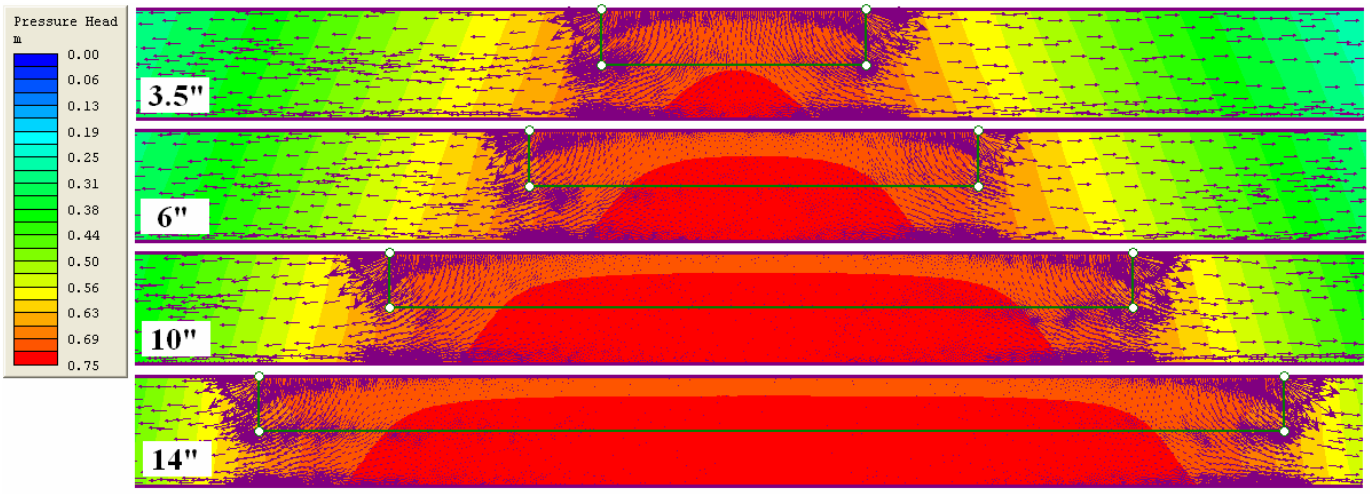

Figure 4.32 – Flow Lines/Pressure Head (Impermeable) for k_h/k_v = 1, k = $5x10^{-3}$ cm/s

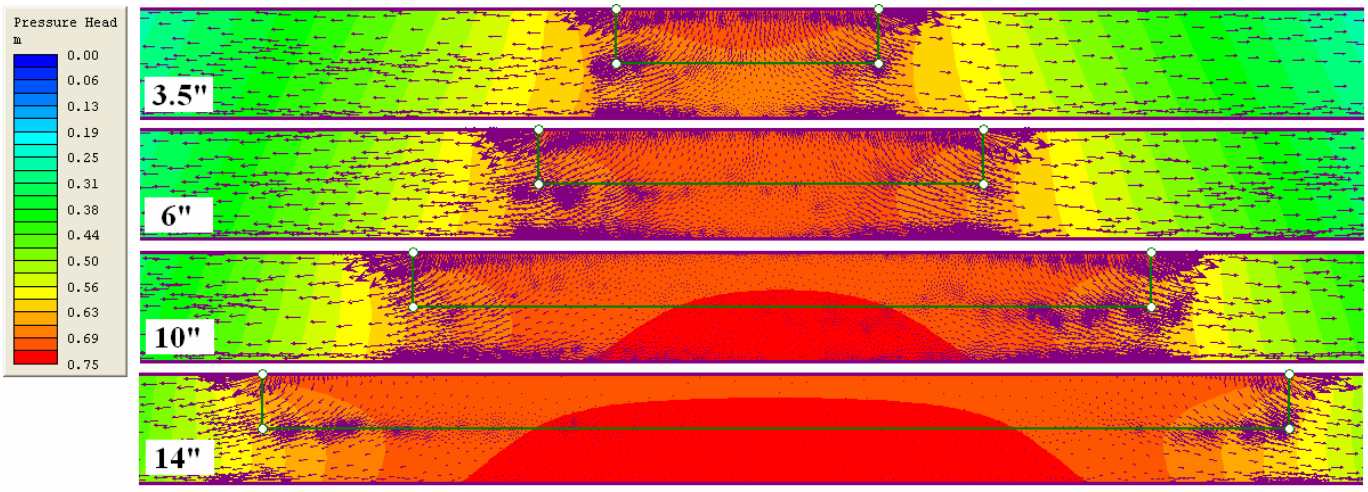

Figure 4.33 – Flow Lines/Pressure Head (Impermeable) for $k_h/k_v = 3$, $k = 5x10^{-3}$ cm/s

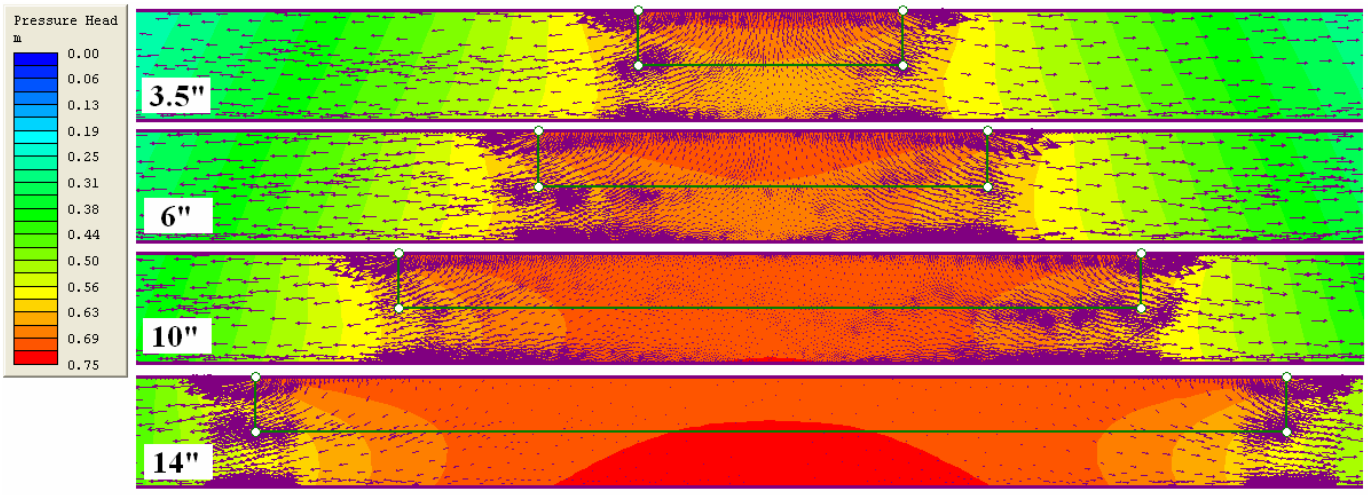

Figure 4.34 – Flow Lines/Pressure Head (Impermeable) for $k_h/k_v = 5$, $k = 5x10^{-3}$ cm/s

The flow at the center of the layer shows that the ratio vertical to horizontal flow is between 1 and 1.4. Since the fluid has no path vertically, the flow is shifted to completely horizontal when it moves outside the specimen area. The largest flow is near the surface at the edge of the applied pressure head. This is the location where the highest pressure gradient can be found because it has the shortest distance from the applied pressure to the surface discharge location.

Generally as the ratio of horizontal to vertical permeability increased, the influence of horizontal flow also increased. The results are similar for the three values of

total permeability. This was expected due to the flow being isolated within a single layer of the same permeability. The flows decreased proportionally to the decrease in total permeability.

This data also correlates fairly well with the data obtained in field testing. The influence of horizontal permeability is largest with a 3.5 inch applied pressure head, which would yield the largest permeability. This scenario can be easily identified in the field by the presence of water discharging at the surface of the pavement. This was not the case during field testing.

The flow outside the specimen was completely horizontal because of the impermeable lower boundary. The flow rate at the boundary of the specimen was used to calculate the permeability using Darcy's Law constant head method. This value was then compared to the actual vertical permeability of the material. The Darcy's Law value was always larger than the actual permeability for the 3.5 inch applied pressure head length. The ratio is variable for the 6 inch length depending on the horizontal to vertical permeability ratio. For the 10 and 14 inch length the Darcy's Law permeability is equal to or lower than the actual permeability value. The comparison of the Darcy's Law vertical permeability (kd) to actual vertical permeability (kv) can be found in Figures 4.35 to 4.38.

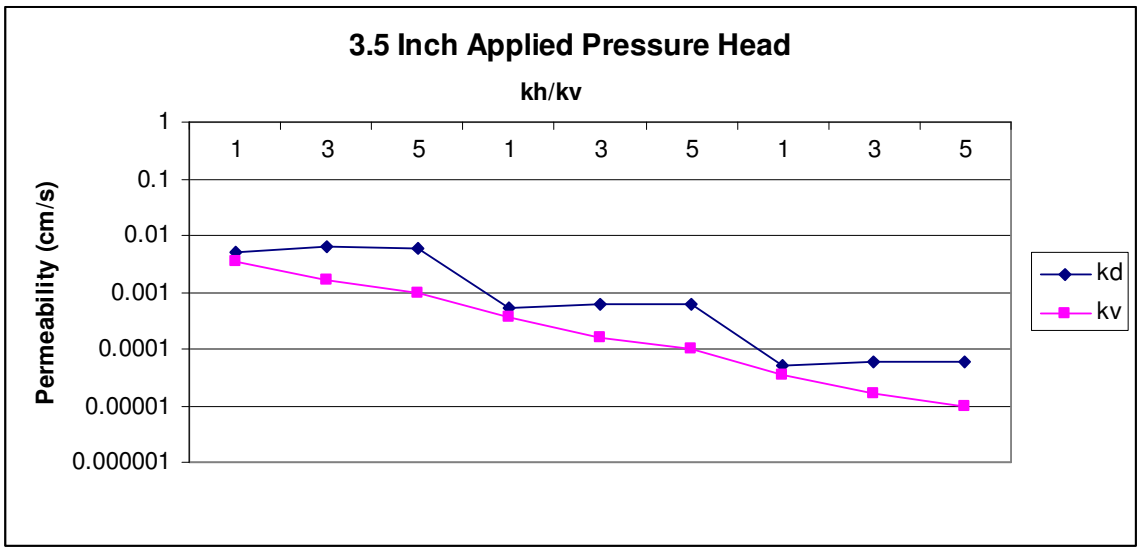

Figure 4.35 – Comparison of Darcy's and Actual Vertical Permeability, 3.5 Inch Applied Pressure Head, Impermeable Lower Boundary

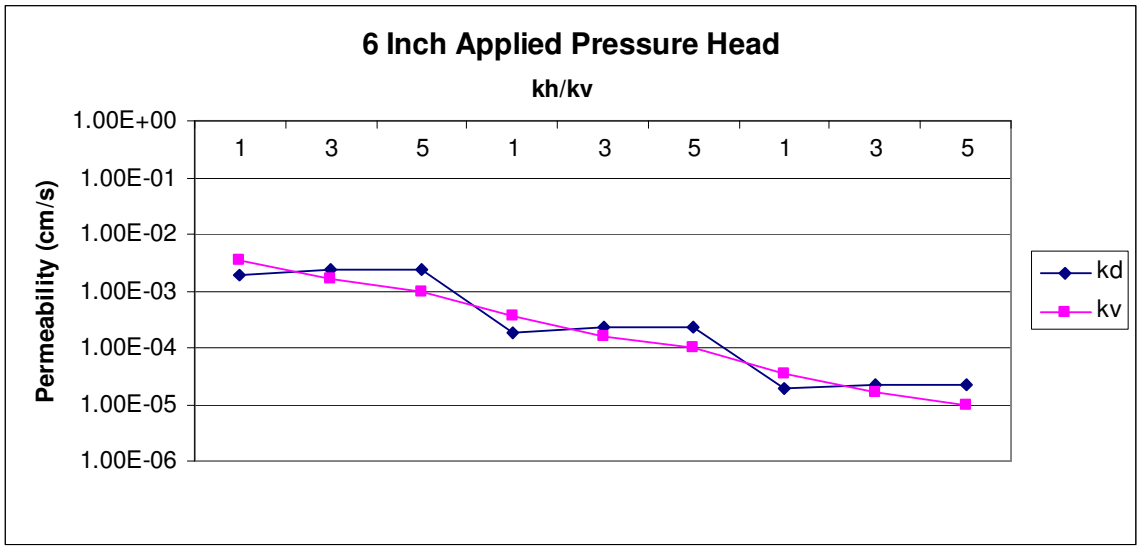

Figure 4.36 – Comparison of Darcy's and Actual Vertical Permeability, 6 Inch Applied Pressure Head, Impermeable Lower Boundary

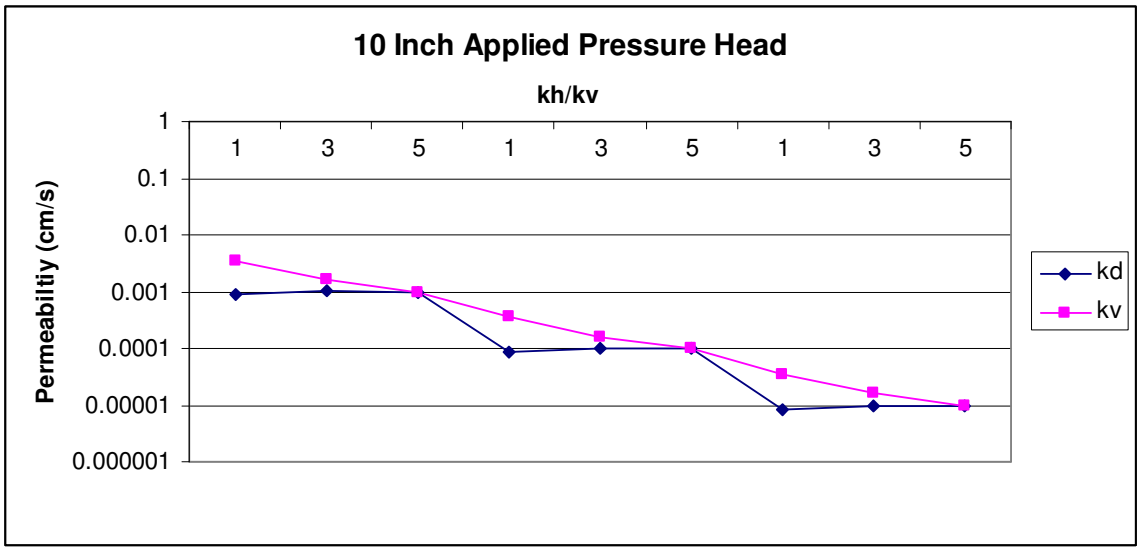

Figure 4.37 – Comparison of Darcy's and Actual Vertical Permeability, 10 Inch Applied Pressure Head, Impermeable Lower Boundary

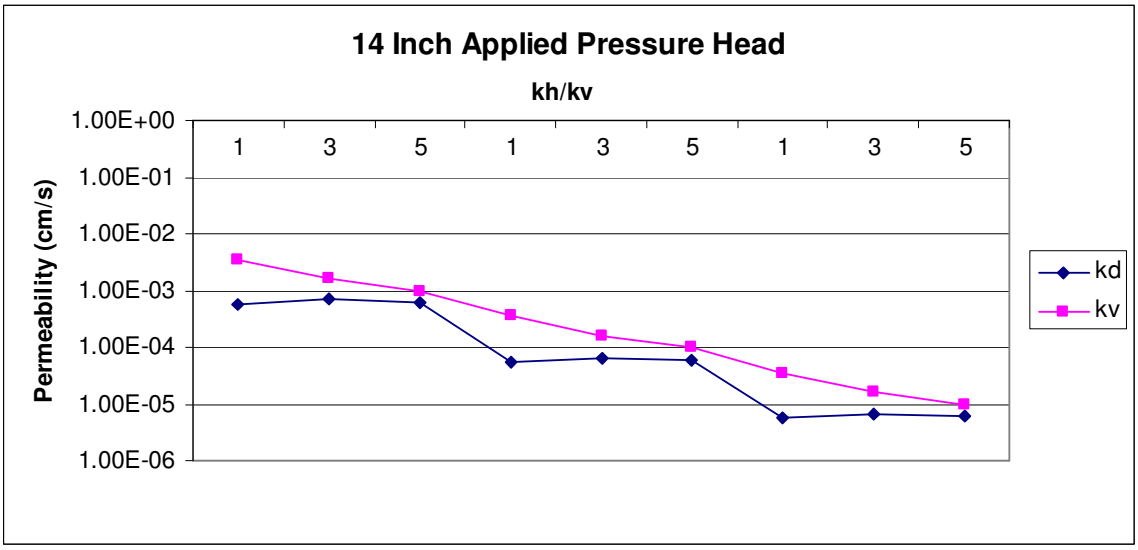

Figure 4.38 – Comparison of Darcy's and Actual Vertical Permeability, 14 Inch Applied Pressure Head, Impermeable Lower Boundary

In rain conditions there is a small distributed head over the surface of the pavement. With this small head level, there was almost no flow throughout the layer. This would trap in moisture until it evaporated or can drain through the soil at the edge of the pavement. This illustrates the need for adequate drainage design within the pavement to allow for fluid to flow into the lower layers and be removed from the structure. An impermeable lower surface layer would not allow this drainage and would accelerate the deterioration in this layer. This scenario is shown in Figure 4.39. A 0.5 inch pressure head was applied to the length of the pavement section. The horizontal flow was shown to be extremely small, thus trapping the rain water in the surface layer.

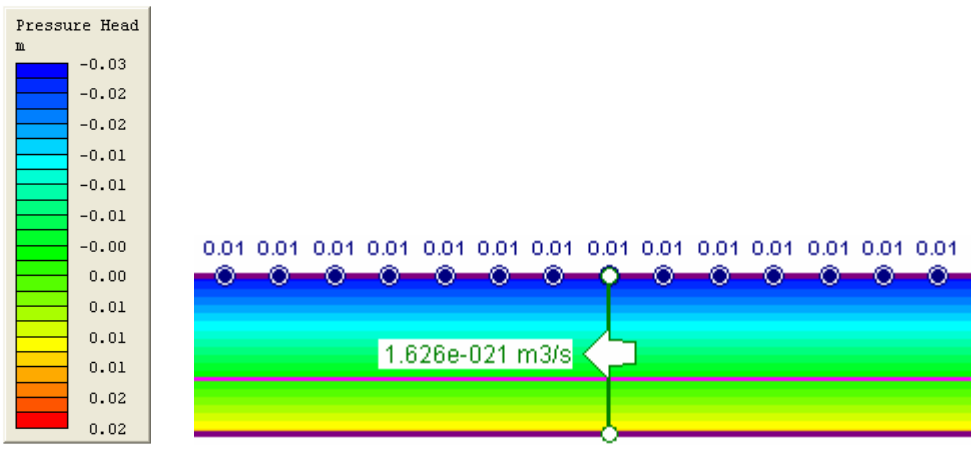

Figure 4.39 – Flow and Head Values under Rain Conditions

Chapter 5
Conclusions and Recommendations

5.1 Conclusions

The results of the lab tests for anisotropic properties in lab specimens were similar results to previous studies. The specimens used for this study can be prepared in the majority of Department of Transportation materials laboratories. The testing device was inexpensive and simple to use. The testing can be completed by a technician with minimal training. The vertical permeability device is already in use by many DOTs and the addition of the horizontal testing apparatus would be inexpensive. The coupling of the two devices can provide important data on the permeability of HMA and be used for indicating durability along with density measurements.

Field testing with the improved field permeameter provided an easy and consistent seal with the pavement. The use of multiple base plates with different water-pavement contact areas provided data on the influence of horizontal and vertical permeability on field calculations. When the contact area is smaller, the horizontal permeability is more significant than when there is a larger contact area. The permeability values for the 3.5” diameter contact area were significantly larger then the readings with the larger contact areas. The statistical analysis suggests that the permeability values are similar between the 10” and 14” contact areas.

A 14” diameter water-pavement contact area for field permeability testing is recommended. Darcy’s law assumes a one-dimensional flow, and by using this contact area, the influence of horizontal flow is minimized. This test will provide more accurate data in field permeability because the analysis is more appropriate. Directional permeability can then be investigated in the laboratory to be correlated with the field results.

Finally, the field data was validated using a finite element analysis. This analysis confirmed that the horizontal flow has a larger effect on the field test with a contact area of 3.5”. The results then vary depending on the lower boundary condition of the surface

layer. For the permeable lower boundary, the trend continues that shows vertical permeability becoming more influential as the applied pressure head length increases. The majority of the flow was from the surface layer to the base layer within the specimen area. The impermeable boundary conditions shows similar ratios of vertical to horizontal flow rates for the 6", 10" and 14" applied pressure lengths. The flow pattern is primarily horizontal because the only path for the water to flow was to the surface of the HMA layer. This condition can be identified by the observance of this surface discharge.

5.2 Limitations

There are some limitations to this study. The sample sizes for both the field and lab tests were limited. The field test sampled three sections of pavement and the lab test was run on 10 samples. This was useful to establish general trends, but a larger sample size would further validate the results and provide more information in predicting trends.

The field test was run on one nominal maximum aggregate size. There are a range of NMAS currently used in construction. The 9.5mm NMAS has been shown to be similar to 12.5mm mixes in permeability characteristics. The majority of the mixes today use these sized but there are other specialty mixes, intermediate and base layers that use a different size.

Directional permeability data cannot presently be obtained in the field. The current technique of using the falling head method with Darcy's Law concentrates on one dimensional flow. Directional data must still be obtained by using laboratory testing.

In laboratory samples, the distribution of voids is highly variable throughout the sample. The voids structure directly controls the permeability of the sample. This will create some variability in the permeability values for the lab testing due to different air void contents throughout the sample.

5.3 Recommendations for Further Study

I would recommend testing a variety of sections with the improved field permeameter to further validate the results and provide a stronger relationship between

the contact areas. The tests would include mixes with a NMAS of 12.5mm, 19mm, and 25mm, along with SMA and OGFC mixes. The lab tests should be utilized on a larger sample size along with using the aforementioned mixes. I believe that with a larger data set, valuable data can be found to relate the anisotropic properties of HMA with the measured permeability values.

Improvement on the field permeameter could yield a test that would provide both horizontal and vertical permeability results. The test would use the 3.5" contact area to obtain a steady state permeability value that would include both vertical and horizontal flow. Next, the 14" contact area would be established without removing the device from the pavement and the steady state permeability value would be found for the vertical direction. The vertical permeability could be separated from the permeability containing both directional flows to find the horizontal permeability.

Further studies into the effects of the flow between layers should be conducted. Fluid flows through the surface layer to the intermediate or base layers during the field permeability tests. Currently, this effect the interface is considered a free flow condition thus having no effect on the permeability of the surface layer. There could be an effect on the surface layer permeability related to the permeability of the lower layers.

The effect of sample thickness in both field and laboratory tests needs additional study. The percent of interconnected voids appears to increase as a sample's thickness decreases. This yields larger permeability values for samples with a smaller thickness. Also, the effects of air voids distribution within a laboratory compacted sample on lab permeability testing should be investigated. Studies have shown that the center of the sample is compacted to a higher density than the outside of the sample. This is due to the friction between the mold and asphalt concrete prohibiting the proper alignment of aggregates.

References

Allen, D. L., Schultz, D. B. Jr., and Fleckenstein, L. J. Jr. (2001). *Development and Proposed Implementation of a Field Permeability Test for Asphalt Concrete.* Research Report KTC-01-19/SPR216-00-1F. Kentucky Transportation Center. Lexington, KY.

Al-Omari, A. (2004). *Analysis of HMA Permeability Through Microstructure Characterization and Simulation of Fluid Flow in X-Ray CT Images.* Ph. D Dissertation. Texas A & M University. College Station, TX.

Choubane, B., Page, G.C., and Musselman, J.A. (1998). *Investigation of Water Permeability of Coarse Graded Superpave Pavements*. Journal of the Association of Asphalt Paving Technologists. Volume 67.

Cooley, L. A. Jr. (1999). *Permeability of SuperPave Mixtures: Evaluation of Field Permeameters.* National Center for Asphalt Technology. Auburn, AL. NCAT Report 99-1.

Cooley, L. A. Jr, Brown, and E. R., Maghsoodloo, S. (2001). *Development of Critical Field Permeability and Pavement Density Values for Coarse-Graded SuperPave Pavements.* National Center for Asphalt Technology. Auburn, AL. NCAT Report 01-03.

Cooley, L A. Jr., Prowell, B. D., and Brown, E. R.. (2002). *Issues Pertaining to the Permeability Characteristics of Coarse-Graded SuperPave Mixes.* National Center for Asphalt Technology. Auburn, AL. NCAT Report 02-06.

CoreLok Operator's Guide. InstroTek Incorporation.

Gogula, A., Hossain, M., Romanoschi, S., and Glenn, A.F. (2003). *Correlation Between the Laboratory and Field Permeability Values for the SuperPave Pavements.* Kansas State University. Manhattan, KS.

Hainin, M. R., Cooley, L. A. Jr., and Prowell, B. D. (2003). *An Investigation of Factors Influencing Permeability of SuperPave Mixes.* Transportation Research Board. National Center for Asphalt Technology. Auburn, AL.

Kanitpong, K., Bahia, H. U., Benson, C. H., and Wang, X. (2003). *Measuring and Predicting Hyraulic Conductivity (Permeability) of Compacted Asphalt Mixtures in the Laboratory.* Transportation Research Board. Washington, D.C.

Kovacs, G. *Developments in water Science*. (1981). Elsevier Scientific Publishing Co., Amsterdam, Netherlands, and Akademiai Kaido Publishing House of the Hungarian Academy of sciences, Budapest. 30, 241-243, 261.

Kutay, M. E., Aydilek, A. H., Masad, E., and Harman, T. (2006) "Computational and Experimental Evaluation of Hydraulic Conductivity Anisotropy in Hot-Mix Asphalt," *International Journal of Pavement Engineering.*

Mallick, R.B., L.A. Cooley, Jr., and M. Teto. (1999). *Evaluation of Permeability of Superpave Mixes in Maine.* Final Report. Technical Report ME-001.

Mallick, R. B., Cooley, L. A. Jr., Teto, M. R., and Bradbury, R. L. (2001). *Development of a Simple Test for Evaluation of In-Place Permeability of Asphalt Mixes.* Worcester Polytechnic Institute. Worcester, MA.

Mallick, R. B., Cooley, L. A. Jr., Teto, M. R., Bradbury, R. L., and Peabody, D. (2003). *An Evaluation of Factors Affecting Permeability of SuperPave Designed Pavements.* NCAT report 03-02. National Center for Asphalt Technology. Auburn, AL.

Masad, E., Al-Omari, A., and Lytton, R. (2006). *A Simple Method for Predicting Laboratory and Field Permeability of Hot Mix Asphalt.* Transportation Research Record. Vol. 1970. 55-63.

Masad, E., Birgisson, B., Al-Omari, A., and Cooley, A. (2004). *Analytical Derivation of Permeability and Numerical Simulation of Fluid Flow in Hot-Mix Asphalt.* Journal of Materials in Civil Engineering. 487-496.

Maupin, Jr., G. W. (2005). *Asphalt Permeability Testing Between Laboratories.* VTRC Report 05-R24. Virginia Transportation Research Council. Charlottesville, VA.

Maupin, Jr., G. W. (2000). *Investigation of Test Methods, Pavements, and Laboratory Design Related to Aspahlt Permeability.* Virginia Transportation Research Council. Charlottesville, VA.

Mohammad, L. N., Herath, A., Huang, B. (2003). *Evaluation of Permeability of SuperPave Asphalt Mixtures.* Transportation Research Board. Louisiana Transportation Research Center. Baton Rouge, LA.

Wisconsin Department of Transportation. (2004). *Effect of Pavement Thickness on SuperPave Mix Permeability and Density.* Highway Research Study 0092-02-14.

VITA

Christopher H. Harris received a Bachelor of Science degree in Civil Engineering from Virginia Polytechnic Institute and State University in Blacksburg, Virginia in December 2005. In January 2006, he entered the Masters of Science program in Civil Engineering at Virginia Polytechnic Institute and State University. He successfully defended his thesis on November 14, 2008.

Appendix A

Florida Method of Test for Measurement of Water Permeability of Compacted Asphalt Paving Mixtures

Florida Method of Test
For

MEASUREMENT OF WATER PERMEABILITY OF COMPACTED ASPHALT PAVING MIXTURES

Designation: FM 5-565

1. SCOPE

1.1 This test method covers the laboratory determination of the water conductivity of a compacted asphalt paving mixture sample. The measurement provides an indication of water permeability of that sample as compared to those of other asphalt samples tested in the same manner.

1.2 The procedure uses either laboratory compacted cylindrical specimens or field core samples obtained from existing pavements.

1.3 The values stated in metric (SI) units are to be regarded as standard. Values given in parenthesis are for information and reference purposes only.

1.4 *This standard does not purport to address all of the safety problems associated with its use. It is the responsibility of the user of this standard to establish appropriate safety, and health practices and determine the applicability of regulatory limitations prior to use.*

2. APPLICABLE DOCUMENTS

2.1 AASHTO Standards:
M 231 Weights and Balances Used in the Testing of Highway Materials.

2.2 Florida Test Methods
FM 1-T 166Bulk Specific Gravity of Compacted Bituminous Mixtures.

3. SUMMARY OF TEST METHOD

3.1 A falling head permeability test apparatus, as shown in Figure 1, is used to determine the rate of flow of water through the specimen. Water in a graduated cylinder is allowed to flow through a saturated asphalt sample and the interval of time taken to reach a known change in head is recorded. The coefficient of permeability of the asphalt sample is then determined based on Darcy's law.

4. SIGNIFICANCE AND USE

4.1 This test method provides a means for determining water conductivity of water-saturated asphalt samples. It applies to one-dimensional, laminar flow of water. It is assumed that Darcy's law is valid.

5. APPARATUS

5.1 *Permeameter* - See Figure 1. The device shall be meet the following requirements:

a)A calibrated cylinder of 31.75 ± 0.5 mm (1.25 ± 0.02 in.) inner diameter graduated in millimeters capable of dispensing 500 ml of water.

b) A sealing tube using a flexible latex membrane 0.635 mm (0.025 in) thick and capable of confining asphalt concrete specimens up to 152.4 mm (6.0 in.) in diameter and 80 mm (3.15 in.) in height.

c)An upper cap assembly for supporting the graduated cylinder and expanding an o-ring against the sealing tube. The opening in the uppercap shall have the same diameter as the inner diameter of the calibrated cylinder mentioned previously in 5.1 a. The underside of the upper cap assembly should be tapered at an angle of 10 ± 1° (see Figure 1).

d) A lower pedestal plate for supporting the asphalt concrete specimen and expanding an o-ring against the sealing tube. The opening in the plate should have a minimum diameter of 18 mm (0.71 in.). The top side of the lower cap should be tapered at an angle of 10 ± 1° (see Figure 1).

e)O-rings of sufficient diameter and thickness for maintaining a seal against the sealing tube.

f) A frame and clamp assembly for supplying a compressive force to the upper cap assembly and lower pedestal necessary to expand the o-rings.

g) An air pump capable of applying 103.42 kPa (15 psi) pressure and capable of applying vacuum to evacuate the air from the sealing tube / membrane cavity.

h) A pressure gauge with range 0 to 103.42 kPa (0 to 15 psi) with +/- 2% accuracy.

i) Quick connects and pressure line for inflating and evacuating the sealing tube / membrane cavity.

j) An outlet pipe with a minimum inside diameter of 18 mm (0.71 in.) with shutoff valve for draining water.

NOTE 1: A device manufactured by Karol Warner Soil Testing Systems has been found to meet the above specifications.

5.2 *Water* - A continuous supply of clean, non-aerated water, preferably supplied by flexible hose from water source to top of graduated cylinder.

5.3 *Thermometer* - A mercury or thermocouple device capable of measuring the temperature of water to the nearest 0.1°C (0.2°F).

5.4 *Beaker* - A 600 ml beaker or equivalent container to be used while measuring the temperature of a water sample.

5.5 *Timer* - A stop watch or other timing device graduated in divisions of 0.1 s or less and accurate to within 0.05% when tested over intervals of not less than 15 min.

5.6 *Measuring Device* - A device used to measure the dimensions of the specimen, capable of measuring to the nearest 0.5 mm or better.

5.7 *Saw* - Equipment for wet cutting the specimen to the desired thickness. Dry cut type saws are not to be used.

5.8 *Sealing Agent* - Petroleum jelly.

5.9 *Spatula* - Used for applying the petroleum jelly to the sides of laboratory compacted specimens.

5.10 *Fan* - An electric fan for drying the wet cut asphalt specimen.

5.11 *Container* - A five gallon bucket or equivalent container for soaking the specimens prior to testing.

6. PREPARATION OF TEST SAMPLES

6.1 Saw cut the field core or the laboratory compacted specimen to the desired test sample thickness. The thickness shall be as close to the actual or desired in-place thickness as possible. For both field cores and laboratory compacted specimens, both the top and bottom faces shall be trimmed.

6.2 Wash the test sample thoroughly with water to remove any loose, fine material resulting from saw cutting.

6.3 Determine the bulk specific gravity of the specimen, if necessary. Use Method B of FM 1-T 166.

6.4 Measure and record, to the nearest 0.5 mm (0.02 in.) or better, the height and diameter of the sample at three different locations. The three height measurements shall not vary by more than 5 mm (0.2 in.). The diameter of the specimen shall not be less than 144 mm (5.67 in.).

NOTE 2: During the permeability test, the sample will need to reach a saturated state as defined in 7.8. As an aid in saturating the sample, and if time permits, place it in the container described in 5.11 and fill with a sufficient quantity of water to completely cover the sample. Let the sample soak for a period of one to two hours.

6.5 For laboratory compacted specimens it is necessary to apply a thin layer of petroleum jelly to the sides of the specimen. This will fill the large void pockets around the sides of the specimen which are not representative of the level of compaction of the interior of the specimen. If the sample is wet, wipe the sides with a towel to remove any free standing water. Use a spatula or similar device and apply the petroleum jelly to the sides of the specimen only.

7. TEST PROCEDURE

7.1 Evacuate the air from the sealing tube / membrane cavity.

NOTE 3: Complete evacuation of the air is aided by pinching the membrane and slightly pulling it away from the hose barb fitting as the pump is stroked.

7.2 Place the specimen on top of the lower pedestal plate and center it.

7.3 Place the sealing tube over the specimen and lower pedestal plate making sure that the sealing tube is oriented so that the hose barb fitting will be located between the o-rings on the upper cap and lower pedestal.

7.4 Insert the upper cap assembly into the sealing tube and let it rest on the top of the asphalt concrete specimen.

NOTE 4: Insertion of the upper cap assembly is aided if the graduated cylinder is already inserted into the upper cap assembly. The graduated cylinder can then be used as a handle.

7.5 Install the two clamp assemblies onto the permeameter frame and evenly tighten each one, applying a moderate pressure to the upper cap assembly. This action seals the o-rings against the membrane and sealing tube.

7.6 Inflate the membrane to 68.9 ± 3.4 kPa (10 ± 0.5 psi). Maintain this pressure throughout the test.

7.7 Fill the graduated cylinder with water approximately half way and rock the permeameter back, forth ,and sideways enough to dislodge any trapped air from the upper cavity.

7.8 Fill the graduated cylinder to a level above the upper timing mark, see Figure 1. Start the timing device when the bottom of the meniscus of the water reaches the upper timing mark. Stop the timing device when the bottom of the meniscus reaches the lower timing mark. Record the time to the nearest second. Perform this test three times and check for saturation. While checking for saturation, do not allow the remaining water in the graduated cylinder to run out, as this will allow air to re-enter the specimen. Saturation is defined as the repeatability of the time to run 500 ml of water through the specimen. A specimen will be considered saturated when the % difference between the first and third test is ≤ 4.0%. Therefore, a minimum of three tests will be required for each asphalt concrete specimen except as stated in Note 6. Saturation of the specimen may require many test runs prior to achieving the ≤ 4.0% requirement. One technique that aids in achieving saturation is to nearly fill the graduated cylinder with water and adjust the water inflow so that it equals the outflow. Allow the water to run in this manner for five or ten minutes and then begin the timed testing. If more than three test runs are required, which is typically the case, then the ≤ 4.0% requirement shall apply to the last three testing times measured.

NOTE 5: If after the third run, the test run time is greater than ten minutes, then the tester can use judgement and consider ending the test, using the lowest time recorded in the permeability calculation.

NOTE 6: If the test time is approaching thirty minutes during the first test run without the water level reaching the lower timing mark, then the tester may mark the water level at thirty minutes and record this mark and time. Run the test one more time and record the mark and time. Use the mark and time which will result in the highest permeability value.

7.9 Obtain a sample of water in a beaker or other suitable container and determine the temperature to the nearest 0.1 °C (0.2 °F).

7.10 After the saturation has been achieved and the final time and mark recorded, then release the pressure from the container and evacuate the sealing tube / membrane cavity. Remove the clamp assemblies, upper cap, and specimen. If petroleum jelly was used on the specimen, wipe off any excess left on the latex membrane.

8. CALCULATIONS

8.1 The coefficient of permeability, k, is determined using the following equation:

$$k = \frac{aL}{At} \ln(h_1 / h_2) * t_c$$

Where: k = coefficient of permeability, cm/s;
a = inside cross-sectional area of the buret, cm^2;
L = average thickness of the test specimen, cm;
A = average cross-sectional area of the test specimen, cm^2;
t = elapsed time between h_1 and h_2, s;
h_1 = initial head across the test specimen, cm;
h_2 = final head across the test specimen, cm.
t_c = temperature correction for viscosity of water; see Tables 1 and 2. A temperature of 20°C (68°F) is used as the standard.

8.2 h_1 and h_2 are the dimensions shown in Figure 1.

NOTE 7: It is beneficial to determine a set of constant dimensional values for a particular permeameter. The dimensions from the underside of the top cap assembly to the lower timing mark and from the underside of the top cap assembly to the upper timing mark are constants. Add the average specimen thickness to these two dimensions and h_1 and h_2 are determined. If the test is stopped at a mark other than the 0 ml lower mark, then add the difference to the h_2 value to arrive at the new h_2 value for this sample. It is helpful to create a spreadsheet that will calculate these values and permeability values automatically.

8.3 For each sample, the coefficient of permeability is computed based on the time and lower mark recorded in 7.8. The result is reported in whole units x 10^{-5} cm/s.

Table 1 - Temperature Correction for Viscosity of Water, Celsius

°C	0.0	0.1	0.2	0.3	0.4	0.5	0.6	0.7	0.8	0.9
10	1.30	1.30	1.29	1.29	1.29	1.28	1.28	1.27	1.27	1.27
11	1.26	1.26	1.26	1.25	1.25	1.25	1.24	1.24	1.24	1.23
12	1.23	1.23	1.22	1.22	1.22	1.21	1.21	1.21	1.20	1.20
13	1.20	1.19	1.19	1.19	1.18	1.18	1.18	1.17	1.17	1.17
14	1.16	1.16	1.16	1.16	1.15	1.15	1.15	1.14	1.14	1.14
15	1.13	1.13	1.13	1.13	1.12	1.12	1.12	1.11	1.11	1.11
16	1.10	1.10	1.10	1.10	1.09	1.09	1.09	1.09	1.08	1.08
17	1.08	1.07	1.07	1.07	1.07	1.06	1.06	1.06	1.06	1.05
18	1.05	1.05	1.05	1.04	1.04	1.04	1.03	1.03	1.03	1.03
19	1.02	1.02	1.02	1.02	1.01	1.01	1.01	1.01	1.00	1.00
20	1.00	1.00	1.00	0.99	0.99	0.99	0.99	0.98	0.98	0.98
21	0.98	0.97	0.97	0.97	0.97	0.96	0.96	0.96	0.96	0.96
22	0.95	0.95	0.95	0.95	0.94	0.94	0.94	0.94	0.94	0.93
23	0.93	0.93	0.93	0.93	0.92	0.92	0.92	0.92	0.91	0.91
24	0.91	0.91	0.91	0.90	0.90	0.90	0.90	0.90	0.89	0.89
25	0.89	0.89	0.89	0.88	0.88	0.88	0.88	0.88	0.87	0.87
26	0.87	0.87	0.87	0.87	0.86	0.86	0.86	0.86	0.86	0.85
27	0.85	0.85	0.85	0.85	0.84	0.84	0.84	0.84	0.84	0.84
28	0.83	0.83	0.83	0.83	0.83	0.83	0.82	0.82	0.82	0.82
29	0.82	0.81	0.81	0.81	0.81	0.81	0.81	0.80	0.80	0.80
30	0.80	0.80	0.80	0.79	0.79	0.79	0.79	0.79	0.79	0.78
31	0.78	0.78	0.78	0.78	0.78	0.78	0.77	0.77	0.77	0.77
32	0.77	0.77	0.76	0.76	0.76	0.76	0.76	0.76	0.76	0.75
33	0.75	0.75	0.75	0.75	0.75	0.74	0.74	0.74	0.74	0.74
34	0.74	0.74	0.73	0.73	0.73	0.73	0.73	0.73	0.73	0.72
35	0.72	0.72	0.72	0.72	0.72	0.72	0.71	0.71	0.71	0.71

Appendix B

Test Method for Determining In-Place Permeability

Test Method for Determining In-Place Permeability

1. **Scope**

1.1 This test method covers the in-place estimation of the water permeability of a compacted hot mix asphalt (HMA) pavement. The estimate provides an indication of water permeability of a pavement.

1.2 The values states in metric (SI) units are regarded as standard. Values given in parenthesis are for information and reference purposes only.

1.3 This standard does not purport to address all of the safety problems associated with its use. It is the responsibility of the user of this standard to establish appropriate safety and health practices and determine the applicability of regulatory limitations prior to use.

2. **Summary of Test Method**

2.1 A falling head permeability test is used to estimate the rate at which water flows into a compacted HMA pavement. Water from a graduated standpipe is allowed to flow into a compacted HMA pavement and the interval of time taken to reach a known change in head loss is recorded. The coefficient of permeability of a compacted HMA pavement is then estimated based on Darcy's Law.

3. **Significance and Use**

3.1 This test method provides a means of estimating water permeability of compacted HMA pavements. This estimation of water permeability is based upon assumptions that the sample thickness is equal to the immediately underlying HMA pavement course thickness; the area of the tested sample is equal to the area of the permeameter from which water is allowed to penetrate the HMA pavement; one-dimensional flow; and laminar flow of the water. It is assumed Darcy's Law is valid.

4. **Apparatus**

4.1 Field Permeameter – A field permeameter made to the dimensions and specifications shown in Figure 1.

4.2 Gasket – A gasket made of ethyl vinyl acetate (or similar, suitable, closed cell material) to be used for sealing the field permeameter to the pavement surface.

4.3 Weights – Cylindrical weights, a total of 120 lb, constructed to fit over the permeameter and rest on the permeameter base, to aid in sealing the gasket to the pavement surface.

4.4 Timing Device – A stopwatch or other timing device graduated in divisions of 1.0 seconds.

5. **Test Procedure**

5.1 Permeameter Setup

5.1.1 Ensure that both sides of the gasket are free of debris.

5.1.2 Place the gasket on the pavement surface over the desired testing location.

5.1.3 Place the permeameter on the gasket, ensuring the holes in each are properly aligned.

5.1.4 Place the cylindrical weights over the permeameter, letting them rest on the base flange of the permeameter.

5.2 Permeability Test

5.2.1 Fill the standpipe to just above the desired initial head.

Note 1: For most applications, enough water should be introduced to bring the water level to the top of the top tier standpipe.

5.2.2 When the water level has fallen to the desired initial head, start the timing device. (See Note 2) Stop the timing device when the water level within the standpipe reaches the desired head. (See Note 3) Record the initial head, final head, and time interval between the initial and final head.

Note 2: For relatively impermeable pavements, the water level will drop very slowly within the top tier standpipe. Therefore, the initial head should be taken within the top tier standpipe. For pavements of "medium" permeability, the water level will drop very quickly through the top tier standpipe. Therefore, the initial head should be taken within the middle tier standpipe. For very permeable pavements the water level will drop very quickly through the top and middle tier standpipes but slow down when it reaches the bottom tier standpipe. Therefore, the initial head should be taken in the bottom tier standpipe.

Note 3: The initial and final head determinations should be made within the same standpipe tier.

6. **Calculation**

6.1 The coefficient of permeability, k, is estimated using the following equation:

$$k = \frac{a L}{A \Delta t} * \ln (h_1 / h_2)$$

where: k = coefficient of permeability
a = area of stand pipe
L = length of sample

A = cross-sectional area of sample
Δt = time during which the change in head is measured
h_1 = water head at beginning of test
h_2 = water head at end of test

6.2 Report results for k to the nearest whole units, in cm/s, using scientific notation.

Appendix C

Lab Sample Mix Design

VIRGINIA DEPARTMENT OF TRANSPORTATION

MATERIALS DIVISION

STATEMENT OF ASPHALT CONCRETE OR CENTRAL-MIX AGGREGATE JOB-MIX FORMULA

Submit to the District Administrator, Virginia Department of Transportation. Approval must be received by the contractor from the Materials Division before work is begun. This job-mix design is approved for all projects of the Department for the type of mix and the calendar year shown below.

Contractor Design Mix No. 2025-2005-31 Design Lab No. S-1

Date 1/2/2007 Job Mix ID No. _____ Calendar Yr. 2007 TSR Test No. 82%

Type Mix / Size Aggregate SM-9.5D (144

Producer Name & Plant Location Adams Construction Co., Blacksburg Phone 540-552-3799

Materials					Kind	Source
Approval Phase	A	B*	C			
Aggregate	45	45		%	#8	Salem Stone, Sylvatus, VA
Aggregate				%		
Rap	15	15		%	Processed	Adams Construction Co., Roanoke, VA
Sand	15	15		%	Concrete Sand	Wyth Sand Co., Wythville, VA
Screening	25	25		%	#10	Salem Stone, Sylvatus, VA
Lime				%		
Asphalt Cement	5.7	5.7			PG 70-22	Associated Asphalt, Roanoke, VA
Asphalt Prime/Tack						
Additives:	0.5	0.5			Adhere HP+	Arr-Maz Products, Winter Haven, FL

Job-Mix Sieves	Total % Passing		Tolerance % + or -	Acceptance Range Average of 4 Test(s)		End of Year Average	Design/Spec. Range
	Lab JMF	Production JMF					
Approval Phase	A	B*		A	B	C	
1/2"	100	100	0	100	100		100
3/8"	90	90	4	86-94	86-94		90-100
#4	57	57	4	53-61	53-61		80 Max
#8	38	38	4	34-42	34-42		38-67
#200	6	6	1	5-7	5-7		2-10
Asphalt (%)	5.7	5.7	.3	5.4-6.0	5.4-6.0		

Lay Down Temperatures	250-350 °F(°C)	Muffle Furnace Correction Factor:	0.62
		Field Correction Factor ($G_{se} - G_{sb}$):	0.20
Lab Compaction Temperatures	284-293 °F (°C)	Pill Weight:	4850
		SMA Mixes	

		VCA_{DRC}:	
Producer Technician's Certification Number	M. Wallace	G_{CA}:	

MATERIALS DIVISION USE ONLY

Remarks	VMA=15.3, VFA=80, Ni=87.3, F/A=1.10, {be=5.43, Gse=2.702, Perm=100						
Nominal Max. Size Aggregate		Application Rates:	Min.	lb/yd^2 (kg/m^2)	Max.	lb/yd^2 (kg/m^2)	
Mix Properties at the Job-Mix Asphalt Content:	Compacted Unit Weight	148.9 lb/ft^3 (kg/m^3)	VTM:	3.5	$G_{mm:}$	2.473	
Checked By: J.A. Henderson 1/11/2007							
Approved tentatively subject to the production of material meeting all other applicable requirements of the specification. * Note: Part B 'Production JMF' and corresponding Material percentages will be filled out by the DME upon receipt of the additional requirements of the HMA producer within the first three lots under Section 502.01(b)							

Copies: State Materials Engineer District Materials Engineer Project Inspector Sub-Contractor and/or Producer	Approvals	☒	Part A:	R.P. Bryant	Date:	1/10/06
		X	Part B:	D.C. Landreth	Date:	1/11/2007
		☐	Part C:		Date:	

Appendix D

Mintab Output

One-way Analysis of Variance

```
Analysis of Variance for BW
Source     DF        SS        MS        F        P
Plate       3 0.0000009 0.0000003   172.71    0.000
Error       8 0.0000000 0.0000000
Total      11 0.0000009
                                  Individual 95% CIs For Mean
                                  Based on Pooled StDev
Level       N      Mean     StDev  -+---------+---------+---------+-----
 3.5        3  9.71E-04  4.84E-05                              (-*-)
 6.0        3  6.92E-04  4.99E-05                   (--*-)
10.0        3  2.87E-04  4.21E-05  (-*--)
14.0        3  3.55E-04  1.97E-05     (-*-)
                                  -+---------+---------+---------+-----
Pooled StDev = 4.18E-05           0.00025   0.00050   0.00075   0.00100

Fisher's pairwise comparisons

    Family error rate = 0.176
Individual error rate = 0.0500

Critical value = 2.306

Intervals for (column level mean) - (row level mean)

                3.5         6.0        10.0

     6.0  0.00020114
          0.00035864

    10.0  0.00060574  0.00032585
          0.00076324  0.00048335

    14.0  0.00053774  0.00025785 -0.00014675
          0.00069524  0.00041535  0.00001075
```

One-way Analysis of Variance

```
Analysis of Variance for BC
Source     DF        SS        MS        F        P
Plate       3 0.0000021 0.0000007   549.32    0.000
Error       8 0.0000000 0.0000000
Total      11 0.0000021
                                  Individual 95% CIs For Mean
                                  Based on Pooled StDev
Level       N      Mean     StDev  ----+---------+---------+---------+--
 3.5        3  1.23E-03  5.70E-05                                    (-*-)
 6.0        3  2.32E-04  2.18E-05  (-*)
10.0        3  2.56E-04  3.34E-05   (-*)
14.0        3  3.19E-04  1.51E-05     (-*)
                                  ----+---------+---------+---------+--
Pooled StDev = 3.56E-05             0.00030   0.00060   0.00090   0.00120

Fisher's pairwise comparisons

    Family error rate = 0.176
Individual error rate = 0.0500

Critical value = 2.306

Intervals for (column level mean) - (row level mean)

                3.5         6.0        10.0

     6.0  0.00093029
          0.00106432

    10.0  0.00090647 -0.00009083
          0.00104050  0.00004320

    14.0  0.00084371 -0.00015359 -0.00012978
          0.00097774 -0.00001956  0.00000426
```

One-way Analysis of Variance

```
Analysis of Variance for BE
Source     DF        SS        MS        F        P
Plate       3 0.0000051 0.0000017   283.28    0.000
Error       8 0.0000000 0.0000000
Total      11 0.0000051
                                  Individual 95% CIs For Mean
                                  Based on Pooled StDev
Level       N      Mean     StDev  ---+---------+---------+---------+---
 3.5        3  2.08E-03  1.11E-04                                  (--*-)
 6.0        3  6.80E-04  5.76E-05       (-*-)
10.0        3  5.02E-04  8.62E-05   (-*-)
14.0        3  5.66E-04  2.70E-05    (-*-)
                                  ---+---------+---------+---------+---
Pooled StDev = 7.73E-05            0.00050   0.00100   0.00150   0.00200

Fisher's pairwise comparisons

    Family error rate = 0.176
Individual error rate = 0.0500

Critical value = 2.306

Intervals for (column level mean) - (row level mean)

                3.5         6.0        10.0

     6.0   0.0012523
           0.0015434

    10.0   0.0014301   0.0000322
           0.0017211   0.0003232

    14.0   0.0013654  -0.0000325  -0.0002102
           0.0016564   0.0002586   0.0000808
```

One-way Analysis of Variance

```
Analysis of Variance for CW
Source     DF        SS        MS        F        P
Plate       3 0.0000053 0.0000018   545.55    0.000
Error       8 0.0000000 0.0000000
Total      11 0.0000053
                                  Individual 95% CIs For Mean
                                  Based on Pooled StDev
Level       N      Mean     StDev  ---+---------+---------+---------+---
 3.5        3  2.10E-03  8.91E-05                                    (-*)
 6.0        3  8.20E-04  4.50E-05          (*-)
10.0        3  5.28E-04  5.17E-05    (-*)
14.0        3  4.46E-04  1.77E-05  (-*)
                                  ---+---------+---------+---------+---
Pooled StDev = 5.69E-05            0.00050   0.00100   0.00150   0.00200

Fisher's pairwise comparisons

    Family error rate = 0.176
Individual error rate = 0.0500

Critical value = 2.306

Intervals for (column level mean) - (row level mean)

                3.5         6.0        10.0

     6.0   0.0011719
           0.0013863

    10.0   0.0014640   0.0001849
           0.0016783   0.0003992

    14.0   0.0015460   0.0002669  -0.0000252
           0.0017603   0.0004812   0.0001892
```

One-way Analysis of Variance

```
Analysis of Variance for CC
Source     DF        SS        MS        F        P
Plate       3 0.0000000 0.0000000   115.04    0.000
Error       8 0.0000000 0.0000000
Total      11 0.0000000
                                  Individual 95% CIs For Mean
                                  Based on Pooled StDev
Level       N      Mean     StDev  -------+---------+---------+---------
 3.5        3  1.75E-04  9.41E-06                              (--*--)
 6.0        3  1.28E-04  1.67E-05                    (--*-)
10.0        3  3.33E-05  7.04E-06   (--*-)
14.0        3  6.27E-05  2.86E-06         (--*-)
                                  -------+---------+---------+---------
Pooled StDev = 1.03E-05                0.000050  0.000100  0.000150

Fisher's pairwise comparisons

    Family error rate = 0.176
Individual error rate = 0.0500

Critical value = 2.306

Intervals for (column level mean) - (row level mean)

                3.5         6.0        10.0

     6.0  0.00002739
          0.00006620

    10.0  0.00012210  0.00007531
          0.00016092  0.00011412

    14.0  0.00009273  0.00004594 -0.00004878
          0.00013155  0.00008475 -0.00000996
```

One-way Analysis of Variance

```
Analysis of Variance for CE
Source     DF        SS        MS        F        P
Plate       3 0.0000003 0.0000001    80.47    0.000
Error       8 0.0000000 0.0000000
Total      11 0.0000004
                                  Individual 95% CIs For Mean
                                  Based on Pooled StDev
Level       N      Mean     StDev  ----+---------+---------+---------+--
 3.5        3  7.42E-04  2.24E-05                                (--*---)
 6.0        3  5.62E-04  4.42E-05                       (--*---)
10.0        3  3.03E-04  5.67E-05   (--*---)
14.0        3  3.79E-04  9.32E-06        (--*---)
                                  ----+---------+---------+---------+--
Pooled StDev = 3.80E-05             0.00030   0.00045   0.00060   0.00075

Fisher's pairwise comparisons

    Family error rate = 0.176
Individual error rate = 0.0500

Critical value = 2.306

Intervals for (column level mean) - (row level mean)

                3.5         6.0        10.0

     6.0  0.00010907
          0.00025200

    10.0  0.00036804  0.00018751
          0.00051097  0.00033044

    14.0  0.00029151  0.00011097 -0.00014800
          0.00043444  0.00025390 -0.00000507
```

One-way Analysis of Variance

```
Analysis of Variance for IW
Source     DF        SS        MS        F        P
Plate       3 0.0000000 0.0000000    53.19    0.000
Error       8 0.0000000 0.0000000
Total      11 0.0000000
                                  Individual 95% CIs For Mean
                                  Based on Pooled StDev
Level       N      Mean     StDev  -+---------+---------+---------+-----
 3.5        3  1.04E-04  1.31E-05                   (---*---)
 6.0        3  1.38E-04  1.22E-05                             (---*---)
10.0        3  5.21E-05  7.36E-06    (---*---)
14.0        3  4.80E-05  6.58E-06   (---*---)
                                  -+---------+---------+---------+-----
Pooled StDev = 1.02E-05          0.000035  0.000070  0.000105  0.000140

Fisher's pairwise comparisons

    Family error rate = 0.176
Individual error rate = 0.0500

Critical value = 2.306

Intervals for (column level mean) - (row level mean)

                3.5         6.0        10.0

     6.0 -0.00005324
         -0.00001472

    10.0  0.00003228  0.00006627
          0.00007080  0.00010478

    14.0  0.00003635  0.00007033 -0.00001519
          0.00007487  0.00010885  0.00002333
```

One-way Analysis of Variance

```
Analysis of Variance for IC
Source     DF        SS        MS        F        P
Plate       3 0.0000001 0.0000000   177.51    0.000
Error       8 0.0000000 0.0000000
Total      11 0.0000001
                                  Individual 95% CIs For Mean
                                  Based on Pooled StDev
Level       N      Mean     StDev  ----+---------+---------+---------+--
 3.5        3  2.40E-04  5.49E-06                                  (-*-)
 6.0        3  1.24E-04  1.05E-05             (--*-)
10.0        3  5.53E-05  8.29E-06   (-*-)
14.0        3  1.04E-04  1.44E-05          (-*--)
                                  ----+---------+---------+---------+--
Pooled StDev = 1.02E-05             0.000060  0.000120  0.000180  0.000240

Fisher's pairwise comparisons

    Family error rate = 0.176
Individual error rate = 0.0500

Critical value = 2.306

Intervals for (column level mean) - (row level mean)

                3.5         6.0        10.0

     6.0  0.00009698
          0.00013533

    10.0  0.00016570  0.00004954
          0.00020406  0.00008790

    14.0  0.00011682  0.00000066 -0.00006806
          0.00015518  0.00003902 -0.00002970
```

One-way Analysis of Variance

```
Analysis of Variance for IE
Source     DF        SS        MS        F        P
Plate       3 0.0000002 0.0000001   112.01    0.000
Error       8 0.0000000 0.0000000
Total      11 0.0000002
                                  Individual 95% CIs For Mean
                                  Based on Pooled StDev
Level       N      Mean     StDev  ------+---------+---------+---------+
 3.5        3  3.69E-04  3.38E-05                                (--*--)
 6.0        3  1.08E-04  1.14E-05      (--*--)
10.0        3  7.14E-05  1.06E-05  (--*--)
14.0        3  1.56E-04  2.26E-05           (--*--)
                                  ------+---------+---------+---------+
Pooled StDev = 2.18E-05               0.00010   0.00020   0.00030   0.00040

Fisher's pairwise comparisons

    Family error rate = 0.176
Individual error rate = 0.0500

Critical value = 2.306

Intervals for (column level mean) - (row level mean)

                3.5         6.0        10.0

     6.0  0.00021959
          0.00030160

    10.0  0.00025648 -0.00000412
          0.00033848  0.00007789

    14.0  0.00017160 -0.00008900 -0.00012588
          0.00025360 -0.00000699 -0.00004388
```

One-way Analysis of Variance

```
Analysis of Variance for B
Source     DF        SS        MS        F        P
C1         11 0.0000095 0.0000009   287.21    0.000
Error      24 0.0000001 0.0000000
Total      35 0.0000095

                                  Individual 95% CIs For Mean
                                  Based on Pooled StDev
Level       N      Mean     StDev  --------+---------+---------+--------
C10         3  2.56E-04  3.34E-05   (*)
C14         3  3.19E-04  1.51E-05    (*)
C3.5        3  1.23E-03  5.70E-05                  (*-)
C6          3  2.32E-04  2.18E-05   (*)
E10         3  5.02E-04  8.62E-05      (*)
E14         3  5.66E-04  2.70E-05       (*-)
E3.5        3  2.08E-03  1.11E-04                                  (*)
E6          3  6.80E-04  5.76E-05         (*)
W10         3  2.87E-04  4.21E-05    (*)
W14         3  3.55E-04  1.97E-05     (*)
W3.5        3  9.71E-04  4.84E-05              (*)
W6          3  6.92E-04  4.99E-05         (-*)
                                  --------+---------+---------+--------
Pooled StDev = 5.47E-05                 0.00060   0.00120   0.00180

Fisher's pairwise comparisons

    Family error rate = 0.650
Individual error rate = 0.0500

Critical value = 2.064

Intervals for (column level mean) - (row level mean)

                C10         C14        C3.5          C6         E10         E14

    C14   -0.0001550
           0.0000295

    C3.5  -0.0010657  -0.0010030
          -0.0008812  -0.0008185

    C6    -0.0000684  -0.0000057   0.0009051
           0.0001161   0.0001788   0.0010896

    E10   -0.0003382  -0.0002754   0.0006353  -0.0003620
          -0.0001537  -0.0000909   0.0008198  -0.0001775

    E14   -0.0004028  -0.0003401   0.0005706  -0.0004267  -0.0001569
          -0.0002184  -0.0001556   0.0007551  -0.0002422   0.0000276

    E3.5  -0.0019137  -0.0018510  -0.0009403  -0.0019376  -0.0016678  -0.0016031
          -0.0017292  -0.0016665  -0.0007558  -0.0017531  -0.0014833  -0.0014186

    E6    -0.0005159  -0.0004531   0.0004576  -0.0005397  -0.0002700  -0.0002053
          -0.0003314  -0.0002686   0.0006421  -0.0003552  -0.0000855  -0.0000208

    W10   -0.0001234  -0.0000606   0.0008501  -0.0001472   0.0001225   0.0001872
           0.0000611   0.0001239   0.0010346   0.0000373   0.0003070   0.0003717

    W14   -0.0001914  -0.0001286   0.0007821  -0.0002152   0.0000545   0.0001192
          -0.0000069   0.0000559   0.0009666  -0.0000307   0.0002390   0.0003037

    W3.5  -0.0008079  -0.0007451   0.0001656  -0.0008317  -0.0005620  -0.0004973
          -0.0006234  -0.0005606   0.0003501  -0.0006472  -0.0003775  -0.0003128

    W6    -0.0005280  -0.0004652   0.0004455  -0.0005518  -0.0002821  -0.0002174
          -0.0003435  -0.0002807   0.0006300  -0.0003673  -0.0000976  -0.0000329
```

```
              E3.5          E6         W10         W14        W3.5

E6      0.0013056
        0.0014901

W10     0.0016981   0.0003003
        0.0018826   0.0004848

W14     0.0016301   0.0002323  -0.0001602
        0.0018146   0.0004168   0.0000242

W3.5    0.0010136  -0.0003842  -0.0007767  -0.0007087
        0.0011981  -0.0001997  -0.0005922  -0.0005242

W6      0.0012935  -0.0001043  -0.0004968  -0.0004288   0.0001876
        0.0014780   0.0000802  -0.0003124  -0.0002444   0.0003721
```

One-way Analysis of Variance

```
Analysis of Variance for C
Source     DF        SS        MS        F        P
C1         11 0.0000103 0.0000009   585.58    0.000
Error      24 0.0000000 0.0000000
Total      35 0.0000103
                                  Individual 95% CIs For Mean
                                  Based on Pooled StDev
Level       N      Mean     StDev  -+---------+---------+---------+-----
C10         3  3.33E-05  7.04E-06   (*
C14         3  6.27E-05  2.86E-06   (*)
C3.5        3  1.75E-04  9.41E-06     (*)
C6          3  1.28E-04  1.67E-05    (*)
E10         3  3.03E-04  5.67E-05       (*)
E14         3  3.79E-04  9.32E-06         *)
E3.5        3  7.42E-04  2.24E-05               *)
E6          3  5.62E-04  4.42E-05            *)
W10         3  5.28E-04  5.17E-05           (*)
W14         3  4.46E-04  1.77E-05          *)
W3.5        3  2.10E-03  8.91E-05                                     (*)
W6          3  8.20E-04  4.50E-05                (*
                                  -+---------+---------+---------+-----
Pooled StDev = 3.99E-05          0.00000   0.00060   0.00120   0.00180

Fisher's pairwise comparisons

    Family error rate = 0.650
Individual error rate = 0.0500

Critical value = 2.064
```

Intervals for (column level mean) - (row level mean)

	C10	C14	C3.5	C6	E10	E14
C14	-0.0000967 0.0000379					
C3.5	-0.0002088 -0.0000742	-0.0001795 -0.0000448				
C6	-0.0001620 -0.0000274	-0.0001327 0.0000020	-0.0000205 0.0001141			
E10	-0.0003367 -0.0002021	-0.0003073 -0.0001727	-0.0001952 -0.0000606	-0.0002420 -0.0001074		
E14	-0.0004133 -0.0002786	-0.0003839 -0.0002493	-0.0002717 -0.0001371	-0.0003185 -0.0001839	-0.0001439 -0.0000092	
E3.5	-0.0007762 -0.0006416	-0.0007469 -0.0006122	-0.0006347 -0.0005001	-0.0006815 -0.0005469	-0.0005068 -0.0003722	-0.0004303 -0.0002957
E6	-0.0005957 -0.0004611	-0.0005663 -0.0004317	-0.0004542 -0.0003196	-0.0005010 -0.0003663	-0.0003263 -0.0001917	-0.0002498 -0.0001151
W10	-0.0005619 -0.0004273	-0.0005325 -0.0003979	-0.0004204 -0.0002857	-0.0004672 -0.0003325	-0.0002925 -0.0001579	-0.0002159 -0.0000813
W14	-0.0004799 -0.0003453	-0.0004505 -0.0003159	-0.0003384 -0.0002038	-0.0003852 -0.0002506	-0.0002105 -0.0000759	-0.0001340 0.0000007
W3.5	-0.0021330 -0.0019984	-0.0021037 -0.0019690	-0.0019915 -0.0018569	-0.0020383 -0.0019037	-0.0018636 -0.0017290	-0.0017871 -0.0016525
W6	-0.0008540 -0.0007193	-0.0008246 -0.0006900	-0.0007124 -0.0005778	-0.0007592 -0.0006246	-0.0005846 -0.0004499	-0.0005080 -0.0003734

	E3.5	E6	W10	W14	W3.5
E6	0.0001132 0.0002478				
W10	0.0001470 0.0002817	-0.0000335 0.0001011			
W14	0.0002290 0.0003636	0.0000485 0.0001831	0.0000147 0.0001493		
W3.5	-0.0014241 -0.0012895	-0.0016047 -0.0014700	-0.0016385 -0.0015038	-0.0017205 -0.0015858	
W6	-0.0001450 -0.0000104	-0.0003256 -0.0001909	-0.0003594 -0.0002248	-0.0004414 -0.0003067	0.0012118 0.0013464

One-way Analysis of Variance

```
Analysis of Variance for I
Source     DF        SS        MS        F        P
C1         11 0.0000003 0.0000000   112.20    0.000
Error      24 0.0000000 0.0000000
Total      35 0.0000003
                                  Individual 95% CIs For Mean
                                  Based on Pooled StDev
Level       N      Mean     StDev  -------+---------+---------+---------
C10         3  5.53E-05  8.29E-06   (-*)
C14         3  1.04E-04  1.44E-05        (*-)
C3.5        3  2.40E-04  5.49E-06                    (-*-)
C6          3  1.24E-04  1.05E-05          (*-)
E10         3  7.14E-05  1.06E-05    (-*-)
E14         3  1.56E-04  2.26E-05             (-*)
E3.5        3  3.69E-04  3.38E-05                                   (-*-)
E6          3  1.08E-04  1.14E-05        (-*-)
W10         3  5.21E-05  7.36E-06  (-*-)
W14         3  4.80E-05  6.58E-06  (-*-)
W3.5        3  1.04E-04  1.31E-05        (*-)
W6          3  1.38E-04  1.22E-05           (-*-)
                                  -------+---------+---------+---------
Pooled StDev = 1.51E-05                0.00010   0.00020   0.00030

Fisher's pairwise comparisons

    Family error rate = 0.650
Individual error rate = 0.0500

Critical value = 2.064

Intervals for (column level mean) - (row level mean)

                C10         C14         C3.5          C6         E10         E14

    C14  -0.00007430
         -0.00002346

    C3.5 -0.00021030 -0.00016142
         -0.00015946 -0.00011058

    C6   -0.00009414 -0.00004526  0.00009073
         -0.00004330  0.00000558  0.00014158

    E10  -0.00004153  0.00000735  0.00014334  0.00002719
          0.00000931  0.00005819  0.00019419  0.00007803

    E14  -0.00012641 -0.00007754  0.00005846 -0.00005769 -0.00011030
         -0.00007557 -0.00002669  0.00010931 -0.00000685 -0.00005946

    E3.5 -0.00033901 -0.00029014 -0.00015414 -0.00027029 -0.00032290 -0.00023802
         -0.00028817 -0.00023929 -0.00010329 -0.00021945 -0.00027206 -0.00018718

    E6   -0.00007842 -0.00002954  0.00010646 -0.00000970 -0.00006230  0.00002258
         -0.00002758  0.00002130  0.00015730  0.00004115 -0.00001146  0.00007342

    W10  -0.00002225  0.00002663  0.00016263  0.00004647 -0.00000614  0.00007874
          0.00002859  0.00007747  0.00021347  0.00009731  0.00004470  0.00012958

    W14  -0.00001818  0.00003070  0.00016669  0.00005054 -0.00000207  0.00008281
          0.00003266  0.00008154  0.00021754  0.00010138  0.00004877  0.00013365

    W3.5 -0.00007379 -0.00002491  0.00011109 -0.00000507 -0.00005768  0.00002720
         -0.00002295  0.00002593  0.00016193  0.00004577 -0.00000684  0.00007804

    W6   -0.00010778 -0.00005890  0.00007710 -0.00003905 -0.00009166 -0.00000678
         -0.00005693 -0.00000805  0.00012794  0.00001179 -0.00004082  0.00004406
```

	E3.5	E6	W10	W14	W3.5
E6	0.00023518				
	0.00028602				
W10	0.00029134	0.00003074			
	0.00034218	0.00008159			
W14	0.00029541	0.00003481	-0.00002135		
	0.00034625	0.00008565	0.00002949		
W3.5	0.00023980	-0.00002080	-0.00007696	-0.00008103	
	0.00029064	0.00003005	-0.00002612	-0.00003019	
W6	0.00020582	-0.00005478	-0.00011094	-0.00011501	-0.00005940
	0.00025666	-0.00000394	-0.00006010	-0.00006417	-0.00000856